A MECHANICAL ANALOGY AND GRAPHICAL METHOD FOR EXPLAINING NEGATIVE TRANSCONDUCTANCE IN CROSSED ELECTROSTATIC AND MAGNETIC FIELDS

by

Ray Kinslow

Thesis submitted to the Graduate Faculty of the
Virginia Polytechnic Institute
in candidacy for the degree of

MASTER OF SCIENCE

in

Applied Mechanics

APPROVED:

Director of Graduate Studies

Dean of Engineering

APPROVED:

Head of the Department

Major Professor

August 29, 1952

Blacksburg, Virginia

TABLE OF CONTENTS

I. List of Figures 3

II. List of Symbols 6

III. Introduction 9
Purpose of the Study. 9
Transconductance in Vacuum Tubes. 9
The Discovery of Negative Transconductance in Crossed Fields 10
Some Probable Applications of the Effect. 10

IV. The Investigation 15
Actual Tube Characteristics 15
Assumptions 21
Laws of Motion of Charged Particles 35
A Mechanical Analogy for Determining Electron Motion in Crossed Fields. 43
Application of the Gyroscope Analogy. 51
A Graphical Method for Determining Electron Trajectories. 58
Maximum Displacement in Uniform Fields. 62
Potential Distribution in Electron Tube 68
Theoretical Tube Characteristics 72

V. Conclusions. 91

VI. Acknowledgments. 95

VII. Bibliography. 96

VIII. Vita. 98

I

LIST OF FIGURES

Figure Number	Title	Page
1	Plate-Current Surface for a Type 45 Electron Tube in the Presence of a Magnetic Field	11
2	Applications of Negative Transconductance Electron Tube	13
3	Electron Tube in Magnetic Field	16
4	Construction of Type 45 Electron Tube	17
5	Circuit for Determining Tube Characteristics	18
6	Plate Current-Grid Voltage Characteristics (Normal Conditions)	19
7	Plate Current-Grid Voltage Characteristics for Various Values of Filament Potential	20
8	Plate Current-Plate Voltage Characteristics for Various Values of B	22
9	Plate Current-Magnetic Field Intensity Relations for Various Values of Plate Voltage	23
10	Transconductance-Grid Voltage Relations	24
11	Plate Current-Grid Voltage Characteristics in Magnetic Field for Various Values of Plate Voltage	25
12	Plate Current-Grid Voltage Characteristics for Various Values of B	26
13	Oscillograph of Plate Current-Grid Voltage Characteristics for Various Values of B	27
14	Oscillograph of Plate Current-Grid Voltage Characteristics for Various Values of Filament Potential and Constant B	28
15	Plate Current-Grid Voltage Characteristics with Reduced Filament Potential (Both with and without Magnetic Field)	29

16	Plate Current-Grid Voltage Characteristics of Type 101-A Electron Tube for Various Values of Filament Potential	30
17	Velocity Distribution of Electrons Resulting from Thermonic Emission	32
18	Photograph Showing Ionization in Type 101-A Electron Tube in the Presence of a Magnetic Field	34
19	Helical Path of Electron in Magnetic Field	38
20	Coordinates Used in Gyroscope Analogy	44
21	Gyroscope and Model of Electron Tube	52
22	Photograph Showing Various Speeds of Gyroscope	54
23	Theoretical Characteristic Curve Based on Gyroscope Analogy	56
24	Photograph Showing the Gyroscope at 1550 Revolutions per Minute	57
25	Nomograph for Finding Instantaneous Radius of Curvature of Electron Path	61
26	Templet for Determining $1/\varepsilon_N$	63
27	Graphical Method of Determining Electron Path	64
28	Maximum Displacement of Electron in y-Direction When Initial Velocity is Zero	66
29	Rolling Surfaces Which Generate Trochoidal Motion	67
30	Graphical Determination of Maximum Displacement of Electron in y-Direction	69
31	Grid for Determining Potential Distribution by Relaxation Method	71
32	Potential Distribution in Electron Tube with Grid Potential of -30 Volts	73

33	Potential Distribution in Electron Tube with Grid Potential of -20 Volts	74
34	Potential Distribution in Electron Tube with Grid Potential of -15 Volts	75
35	Potential Distribution in Electron Tube with Grid Potential of -10 Volts	76
36	Potential Distribution in Electron Tube with Grid Potential of -5 Volts	77
37	Potential Distribution in Electron Tube with Grid Potential of 0 Volts	78
38	Potential Distribution in Electron Tube with Grid Potential of +5 Volts	79
39	Potential Distribution in Electron Tube with Grid Potential of +10 Volts	80
40	Potential Distribution in Electron Tube with Grid Potential of +20 Volts	81
41	Potential Distribution in Electron Tube with Grid Potential of +30 Volts	82
42	Electron Trajectories with Zero Grid Potential	84
43	Electron Trajectories with Grid Potential of -10 Volts	85
44	Percentage of Electrons Reaching the Plate of the Tube	86
45	Theoretical Characteristic Curve with Normal Filament Potential	89
46	Theoretical Characteristic Curve with Reduced Filament Potential	90
47	Comparison of Actual and Theoretical Characteristic Curves	93

II

LIST OF SYMBOLS

a	a constant
A	a constant
b	a constant
B	magnetic flux density
B_x, B_y, B_z	components of magnetic flux density
c	velocity of light
C, C_1, C_2	constants
e	charge of an electron
e_b	plate voltage of electron tube
e_c	control grid voltage
E	electric potential
$\mathcal{E}$	electric field intensity
$\mathcal{E}_N$	normal electric field intensity
$\mathcal{E}_x$, $\mathcal{E}_y$, $\mathcal{E}_z$	components of electric field intensity
F	force
F_x, F_y, F_z	components of force
F_{NE}	normal force due to electrostatic field
g_m	transconductance of vacuum tube
i_b	plate current of electron tube
I_x, I_y, I_z	moments of inertia relative to coordinate axes
K	curvature
K_E	curvature due to electric field
K_M	curvature due to magnetic field
L	length

m	mass of particle in motion
m_o	mass of particle at rest
q	unit charge
R	radius
R_E	instantaneous radius curvature due to an electric field
R_M	instantaneous radius curvature due to a magnetic field
R_O	residual at point 0
s	distance
t	time
t_1	period
T	kinetic energy
v	velocity
v_o	initial velocity
v_x, v_y, v_z	components of velocity
v_{ox}, v_{oy}, v_{oz}	components of initial velocity
v_{xy}	projection of velocity vector on x-y plane
v_R	radial component of velocity
v_T	tangential component of velocity
x, y, z	rectangular axes fixed in space
X, Y, Z	rectangular axes relative to a body and moving with it
α	angle measured from x-axis
Δ	an increment
θ, ϕ, ψ	Eulerian angles
ν	magnetic pole strength
ρ	polar distance

ω	angular velocity
$\omega_x, \omega_y, \omega_z$	components of angular velocity relative to fixed axes
$\omega_X, \omega_Y, \omega_Z$	components of angular velocity relative to moving axes

III

INTRODUCTION

Purpose of the Study

Numerous electronic devices utilize crossed electric and magnetic fields, but only the very simplest of cases may be analyzed by analytical methods. The purpose of this study is to demonstrate the use of a mechanical analogy and graphical methods in the solution of the more complex problems of this type. Specifically, these methods were employed to explain the phenomena of negative transconductance in crossed fields. To the best of the writer's knowledge, the graphical method derived in this study is the first method, other than that of conformal mapping, which enables one to plot the path of electrons in crossed fields, and the first attempt to apply a mechanical analogy to such fields in vacuum tubes consisting of more than two elements.

Transconductance in Vacuum Tubes

The transconductance (or mutual conductance) g_m, of an electron tube is defined as the rate of change of plate current with respect to a change in grid voltage. If the grid voltage is changed by the amount Δe_c, the resulting change in plate current, Δi_b, is given by the relation,

$$\Delta i_b = g_m \Delta e_c$$

Therefore,

$$g_m = \lim_{e_c \to 0} \left[\frac{\Delta i_b}{\Delta e_c} \right]_{e_b \text{ constant}} = \frac{\partial i_b}{\partial e_c}$$

where e_b is the plate voltage of the tube.

There are at least two instances in which tubes exhibit negative transconductance.[1] One case is that of a beam-power tube. The plate current can be made to decrease as the control-grid voltage increases provided that the space current is high enough so that a virtual cathode forms between the screen-grid and the plate. A negative transconductance also exists between the suppressor-grid and the screen-grid in a pentode tube.

The Discovery of Negative Transconductance in Crossed Fields

During the development of an electronic flux meter for the Atomic Energy Commission,[2] it was noticed that under certain conditions of crossed fields it was possible to cause the tube to exhibit a region of negative transconductance,[3] that is, when operating in certain critical regions of grid bias, it was possible to produce a decrease in plate current with a positive increase in grid voltage. Figure 1 shows the plate-current surface under such conditions. Studies made at that time offered no explanation of the phenomenon. A search of literature was made by the patent office of the Atomic Energy Commission which reported that there was no record of this effect having been observed previous to that time. On July 13, 1949, this material was declassified and permission was given to continue the study. In 1950, the writer was awarded a grant by the Tennessee Academy of Science and the American Association for the Advancement of Science to aid in the continuation of this research.

Some Probable Applications of the Effect

Dynatron Oscillator.[4] It was at once realized that a tube having a region of negative transconductance could be used as a

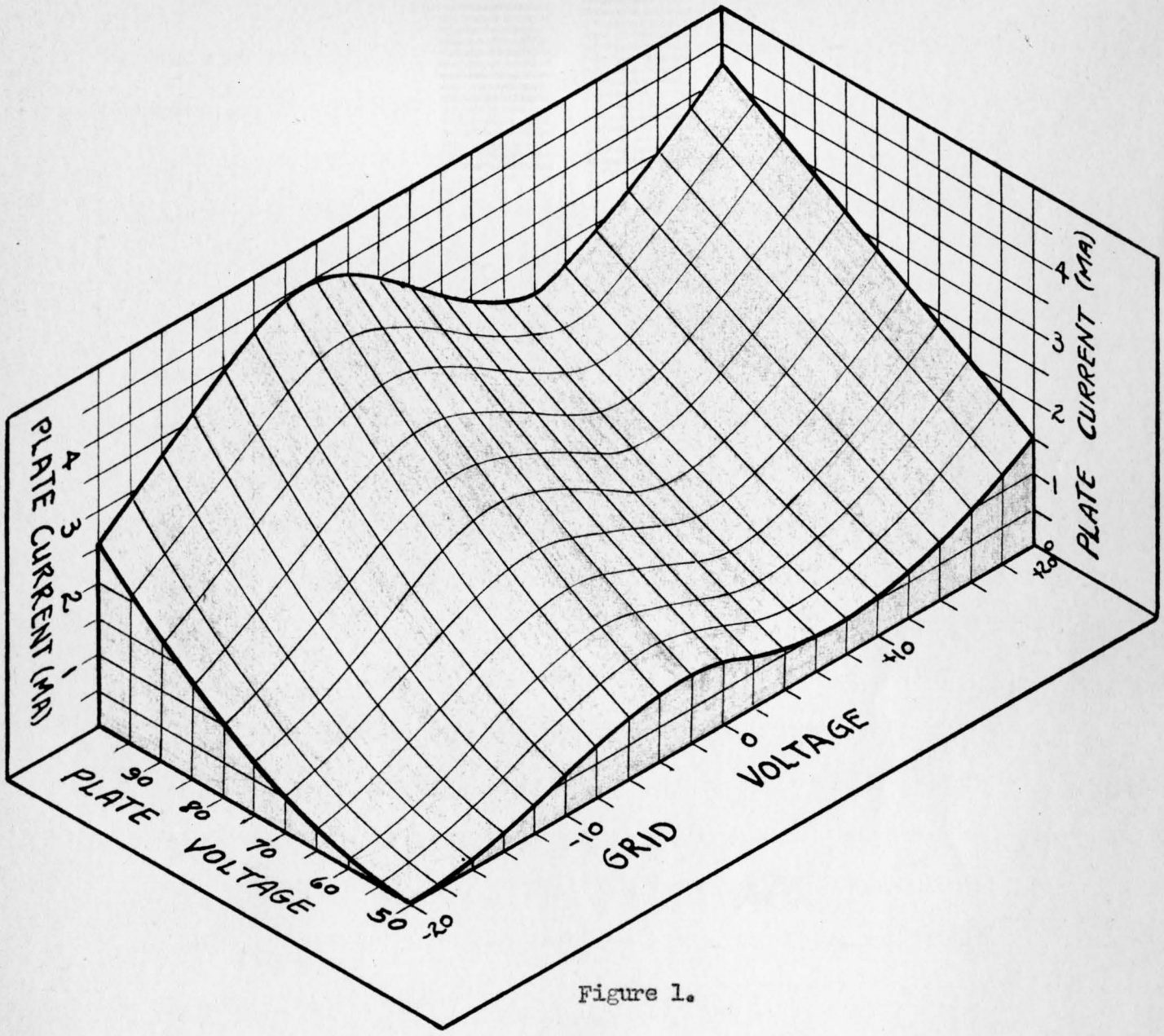

Figure 1.

PLATE-CURRENT SURFACE FOR A TYPE 45 ELECTRON TUBE IN THE PRESENCE OF A MAGNETIC FIELD

stable oscillator. Most tubes in the past have depended for their operation upon secondary emission effects. It is believed that this tube will be superior to those which have been used because there is no dependence upon unstable secondary emission.

Frequency Tripler. The transfer characteristic curve is of such a shape that it may be approximately represented by the equation

$$i_b = 4b(e_c/a)^3 - 3b(e_c/a)$$

if the axes are shifted so that the origin of the coordinate axes are as shown in Figure 2a. If an input signal, $e_c = a \sin \omega t$, is placed on the grid, the output will be

$$i_b = 4b(\sin^3 \omega t) - 3b(\sin \omega t) = - b \sin 3\omega t.$$

The tube may, therefore, be used as a frequency tripler provided that it is not necessary to maintain a perfect wave form.

Frequency Doubler. The ideal transfer characteristic curve for a frequency doubler would have the equation

$$i_b = b\left[1 - 2(e_c/a)^2\right]$$

since an input signal of $e_c = a \cos \omega t$ would produce an output of

$$i_b = b(1 - 2\cos^2 \omega t) = - b \cos 2\omega t.$$

The portion of the characteristic curve between points A and B in Figure 2b very closely approximates this equation.

Phase Shifter. As a portion of the characteristic curve is approximately a straight line having the equation $i_b = - (b/a)\, e_c$ an input signal of $e_c = a \sin \omega t$ would result in an output of

$$i_b = - b \sin \omega t = b \sin (\Pi/2 + \omega t)$$

Figure 2c.

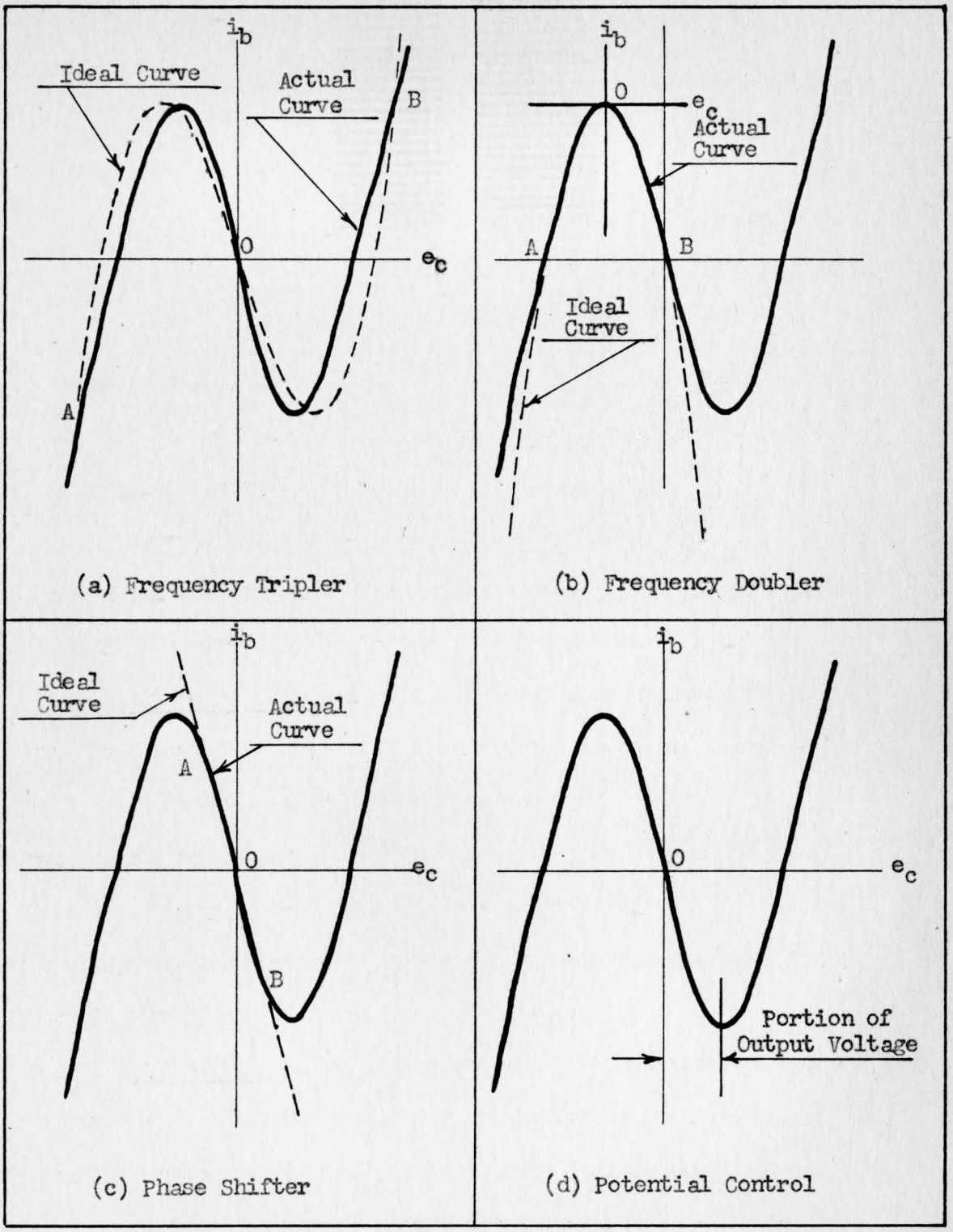

Figure 2.

APPLICATIONS OF NEGATIVE TRANSCONDUCTANCE ELECTRON TUBE

Voltage Regulator. The degree of regulation of a voltage regulator is a function of the transconductance of one of the tubes in the circuit.[5] If a resistance having a value equal to the reciprocal of the slope of the transfer characteristic curve at its inflection point is placed in the cathode circuit of the tube, the effective characteristic curve will have a region of infinite slope.[6] If a negative transconductance tube is so used in the regulator circuit, the theoretical regulation would be infinite as long as it is possible to operate on that portion of the curve.

Potential Control. The tube may be used to trip a relay or similar device when a DC voltage drops below or increases above certain limits. A portion of the output voltage is used to provide grid bias as shown in Figure 2d. The significant fact is that the plate current of the tube increases with either an increase or decrease in output supply voltage.

IV

THE INVESTIGATION

Actual Tube Characteristics

A type 45 power amplifier triode electron tube[7] placed in the magnetic field generated by an electromagnet, as shown in Figure 3, was used in this investigation of negative transconductance in magnetic fields. Figure 4 shows the construction and dimensions of the elements of this tube. Other tubes having different geometrical configurations were used only in checking various theories of operation.

Figure 5 is a schematic diagram showing the circuit used in determining tube characteristics. The cathode-ray oscilloscope is connected so that the pattern on the screen is a graph of the transfer characteristics of the tube.

The normal transfer characteristics of a type 45 tube are shown in Figure 6. These curves show the variations of plate current with grid voltage for various plate voltages, the slope of which represents the transconductance of the tube, which is always of positive value. Figure 7 shows the tube characteristics for various values of filament voltage.

The tube was placed between the poles of an electromagnet with the plates of the tube parallel to the direction of the magnetic field and the grid was connected to the annode ($e_c = 0$). As the strength of the magnetic field was increased, there was a decrease in plate current accompanied by an increase in grid current.

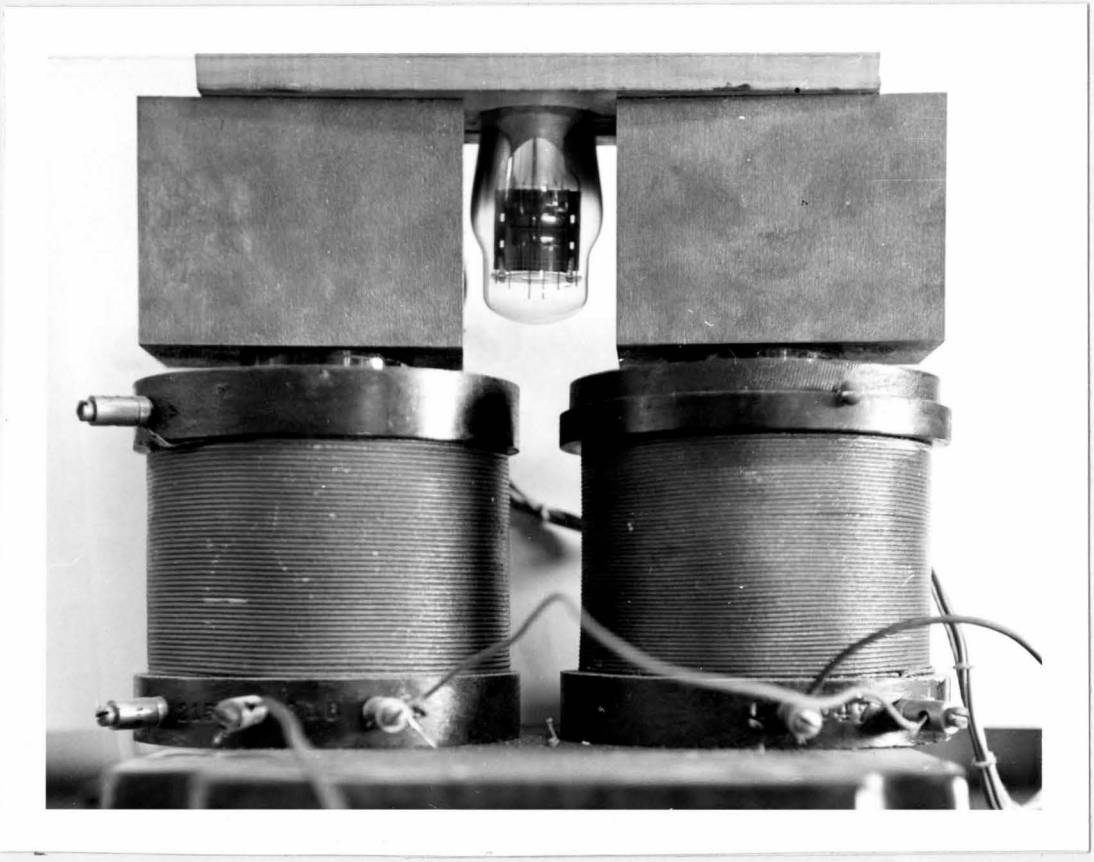

Figure 3.

ELECTRON TUBE IN MAGNETIC FIELD

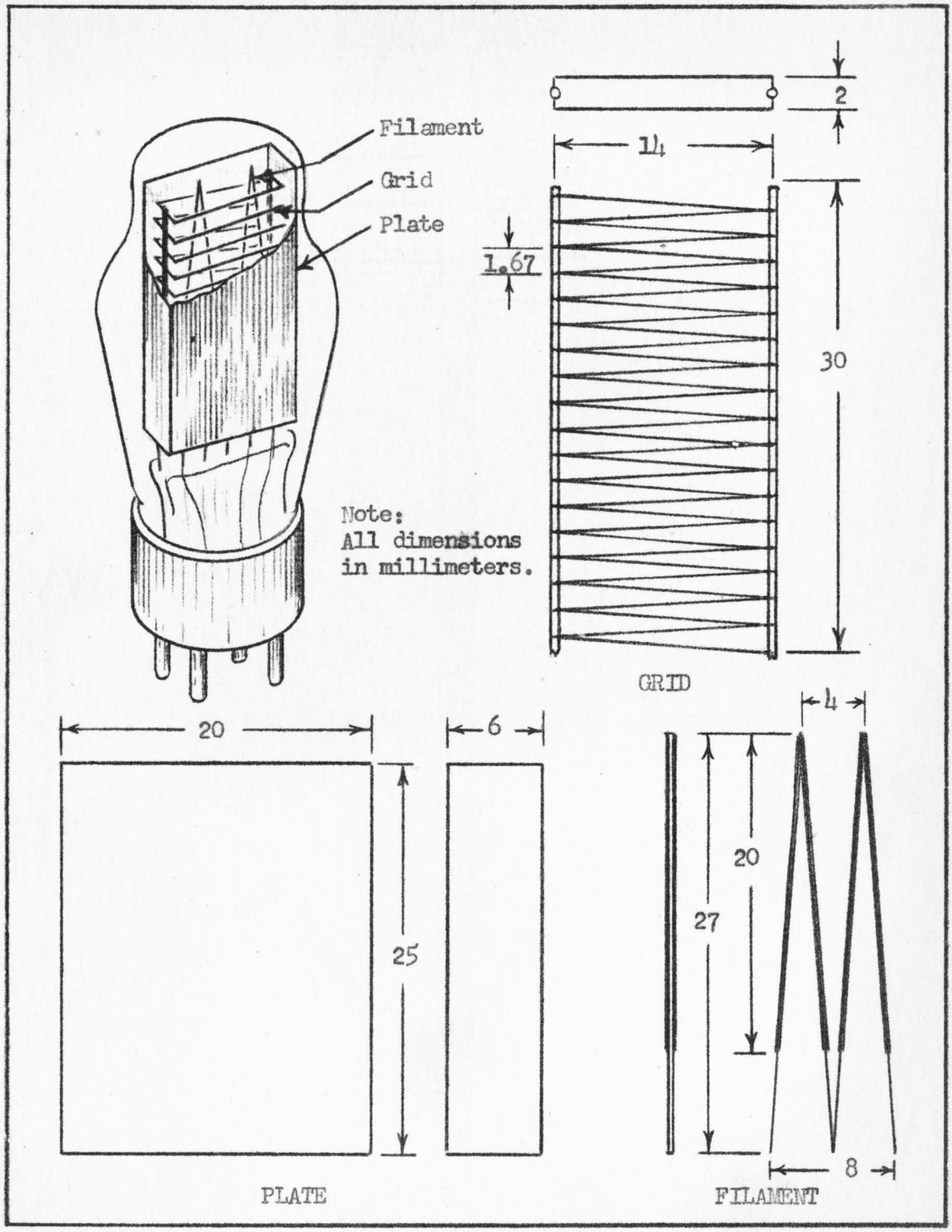

Figure 4.
CONSTRUCTION OF TYPE 45 ELECTRON TUBE

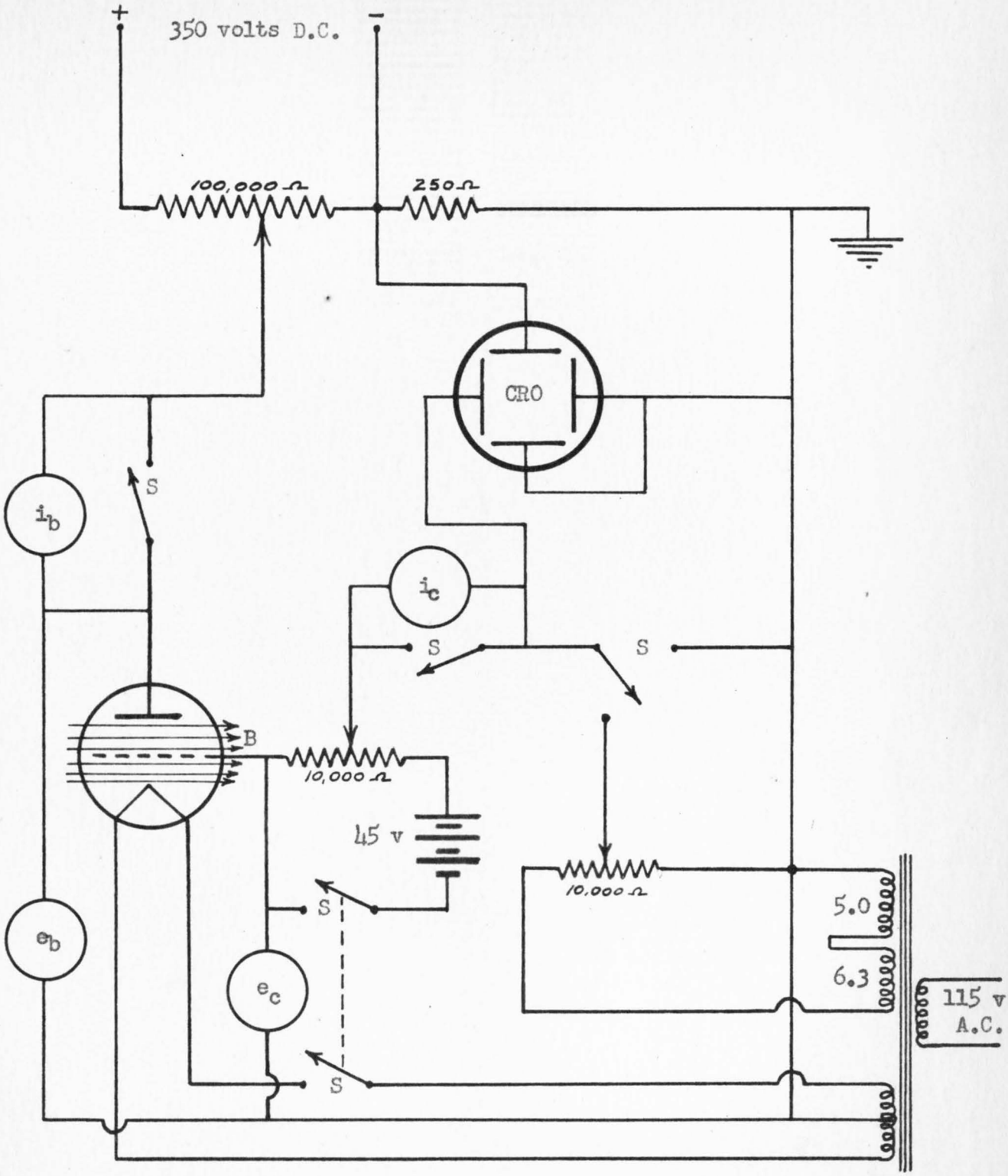

Figure 5.

CIRCUIT FOR DETERMINING TUBE CHARACTERISTICS

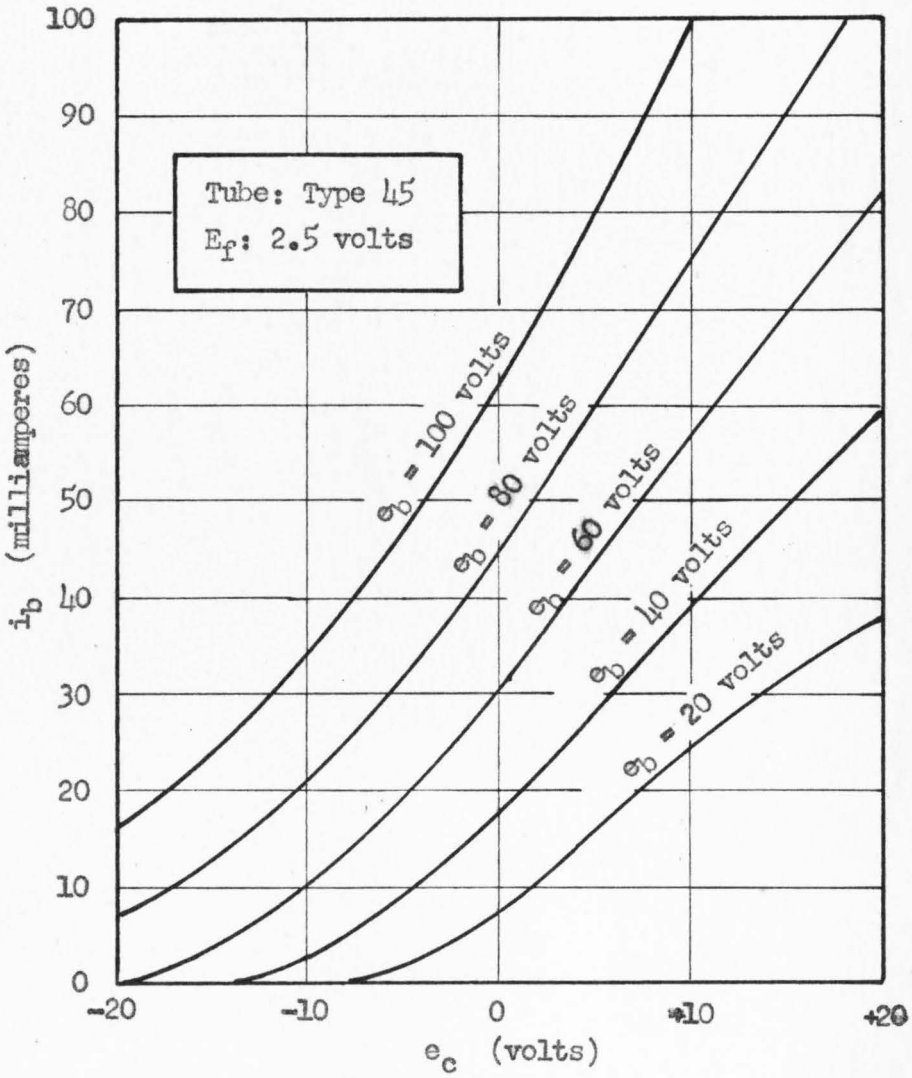

Figure 6.

PLATE CURRENT-GRID VOLTAGE CHARACTERISTICS (NORMAL CONDITIONS)

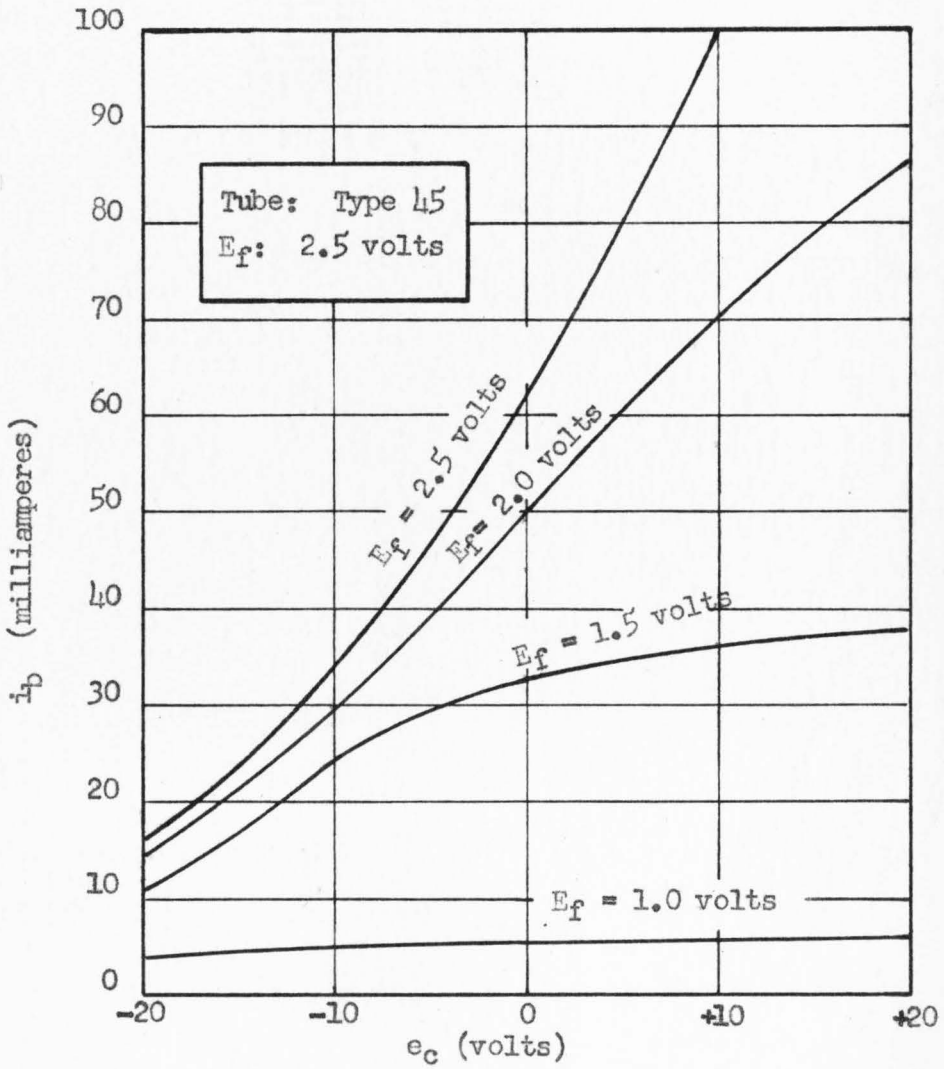

Figure 7.

PLATE CURRENT-GRID VOLTAGE CHARACTERISTICS FOR VARIOUS VALUES OF FILAMENT POTENTIAL

These variations for different values of plate voltages are shown in Figures 8 and 9.

With constant magnetic field strength (approximately 0.05 webers per square meter) and plate potential (100 volts), the grid potential was varied (from -20 to +20 volts). Figure 10 shows the variation in plate current. The values of transconductance is also shown in this figure. Plate current-grid potential relations are shown in Figure 11 for plate potentials of 50, 75, and 100 volts. Figure 12 shows the characteristic curves for various magnetic field strengths and a plate potential of 50 volts. Figure 13 is an oscillogram of these tube characteristics for a constant plate potential and various magnetic fields. Figure 14 shows the effect of varying the filament voltage with a constant plate potential and magnetic field. Figure 15 shows the tube characteristics, both with and without magnet, when the filament potential is reduced to 1.0 volts. Figure 16 gives the characteristics of a type 101-A electron tube with a constant plate potential and magnetic field but with various filament potentials.

Assumptions

In order to formulate a theory as to the reason for the region of negative transconductance, it is necessary to make some basic assumptions. The assumptions made are as follows:

1. The initial velocities of electrons leaving the filament are essentially zero.
2. Relativistic variation of mass of the electrons may be neglected.

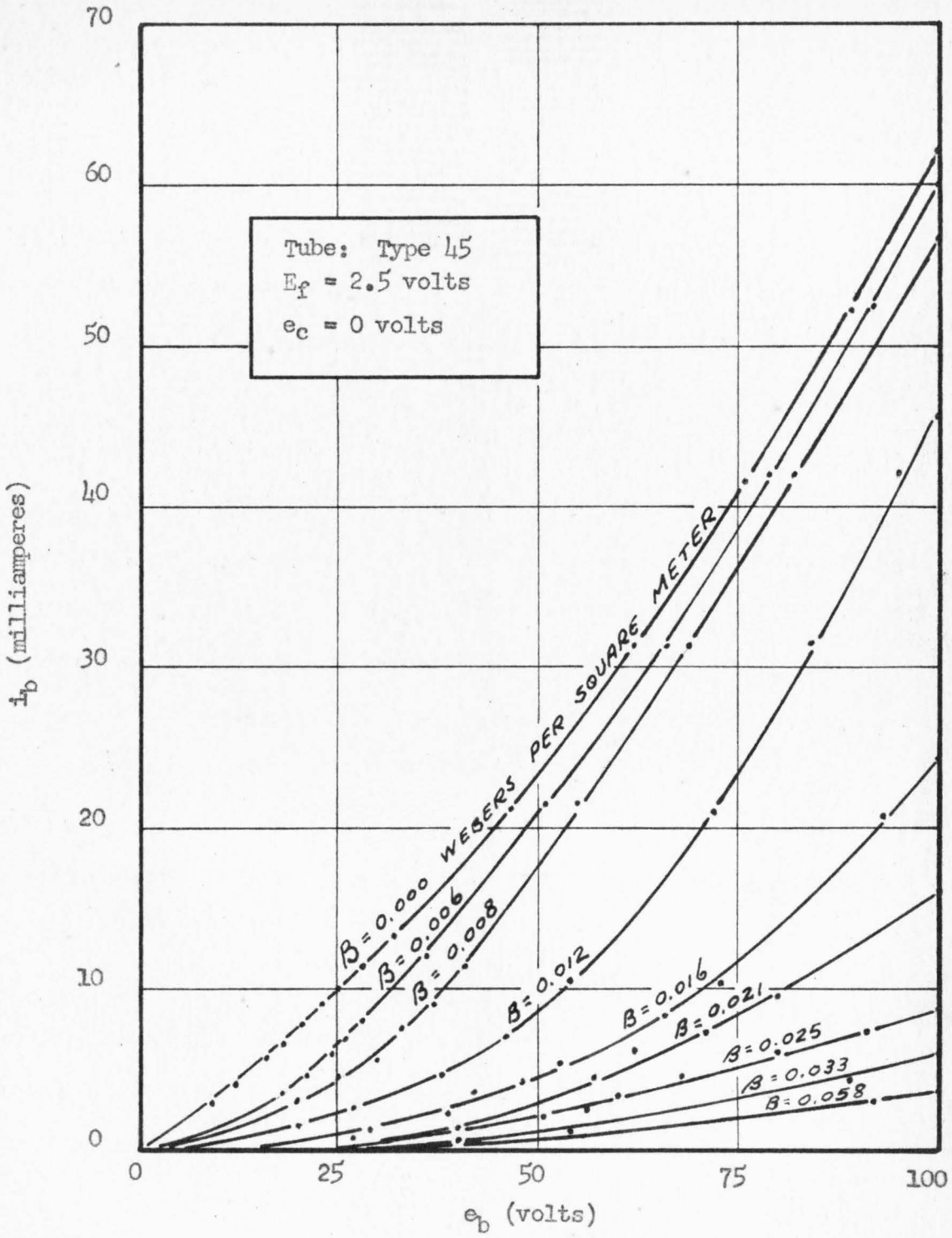

Figure 8.

PLATE CURRENT-PLATE VOLTAGE CHARACTERISTICS

FOR VARIOUS VALUES OF B

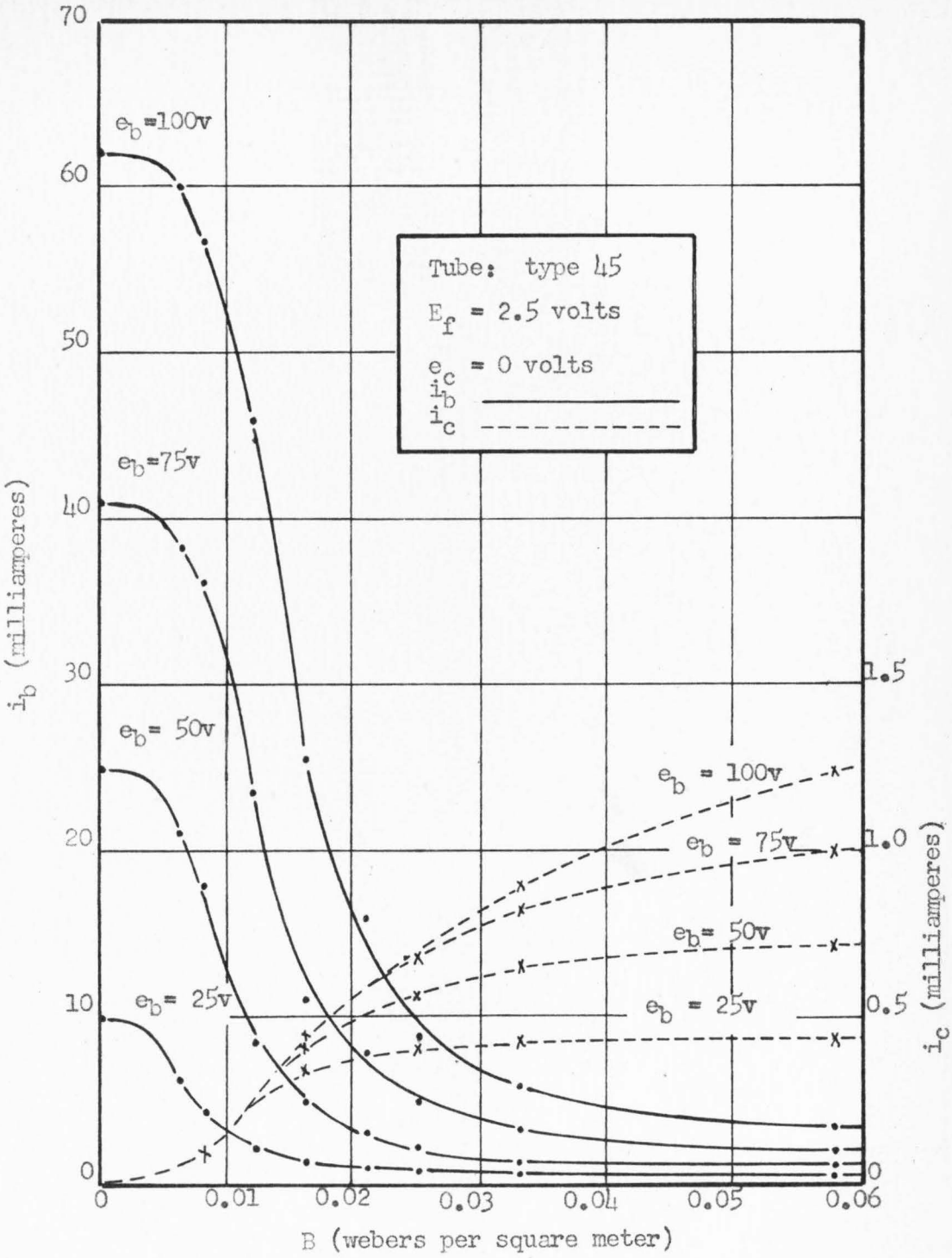

Figure 9.

PLATE CURRENT-MAGNETIC FIELD INTENSITY RELATIONS
FOR VARIOUS VALUES OF PLATE VOLTAGE

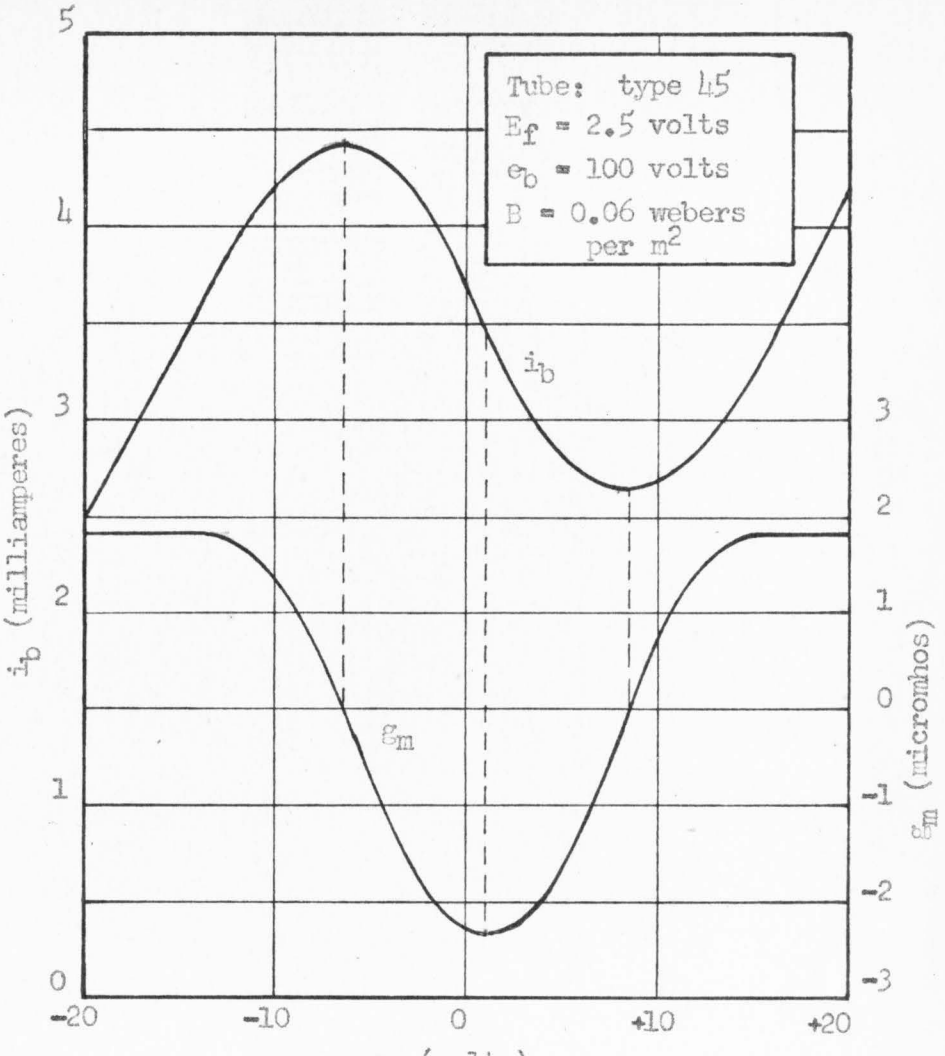

Figure 10.

TRANSCONDUCTANCE-GRID VOLTAGE RELATIONS

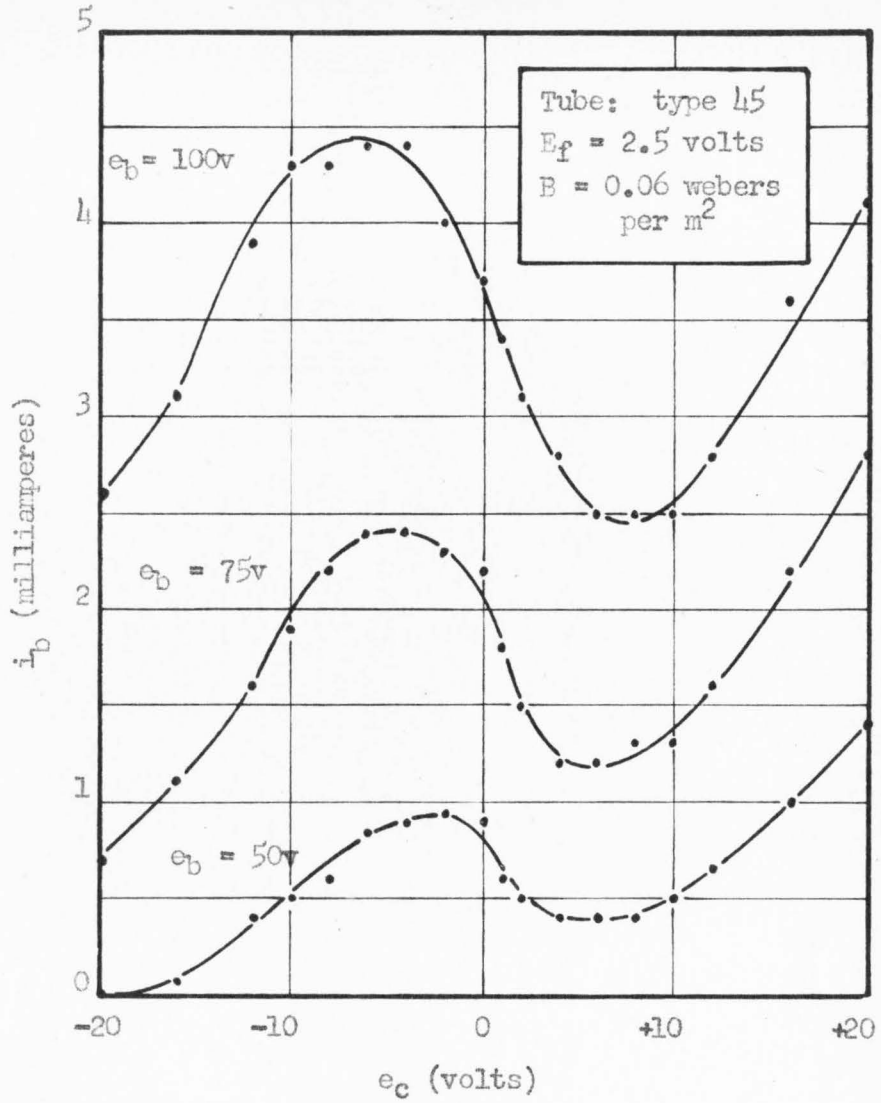

Figure 11.

PLATE CURRENT-GRID VOLTAGE CHARACTERISTICS
IN MAGNETIC FIELD FOR VARIOUS VALUES OF PLATE VOLTAGE

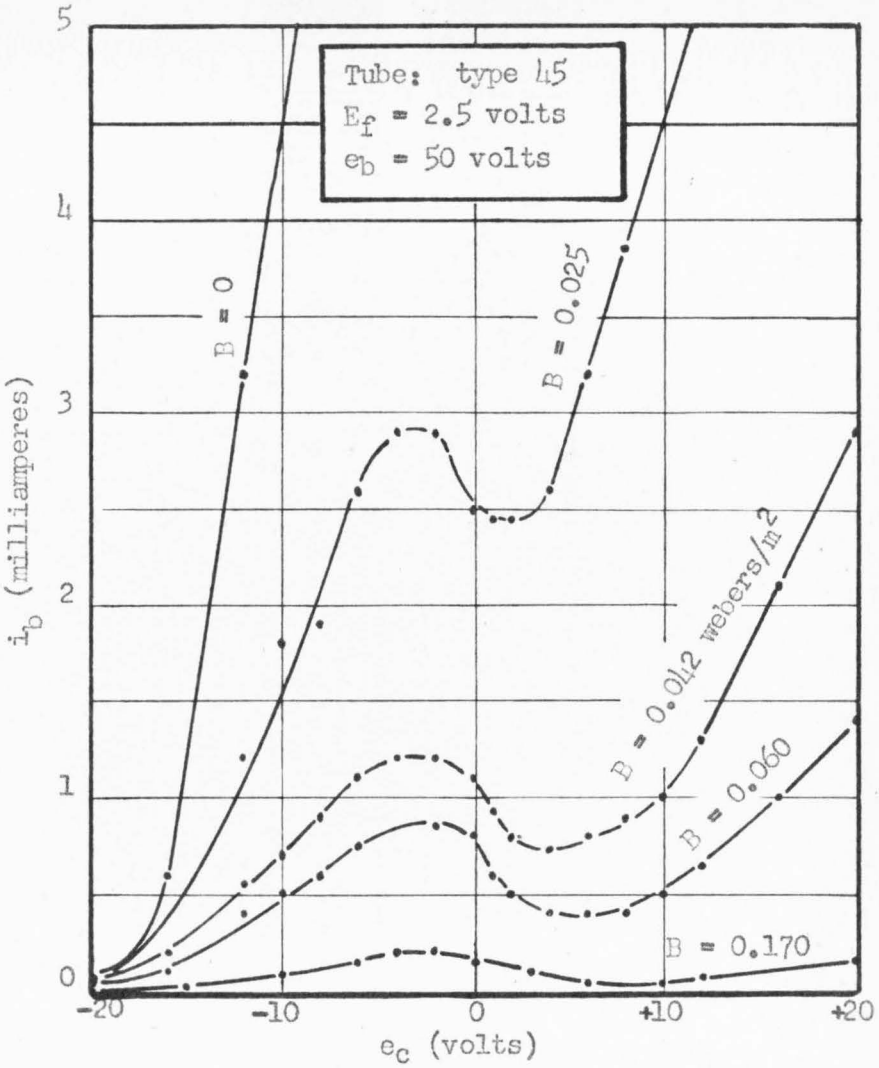

Figure 12.

PLATE CURRENT-GRID VOLTAGE CHARACTERISTICS
FOR VARIOUS VALUES OF B

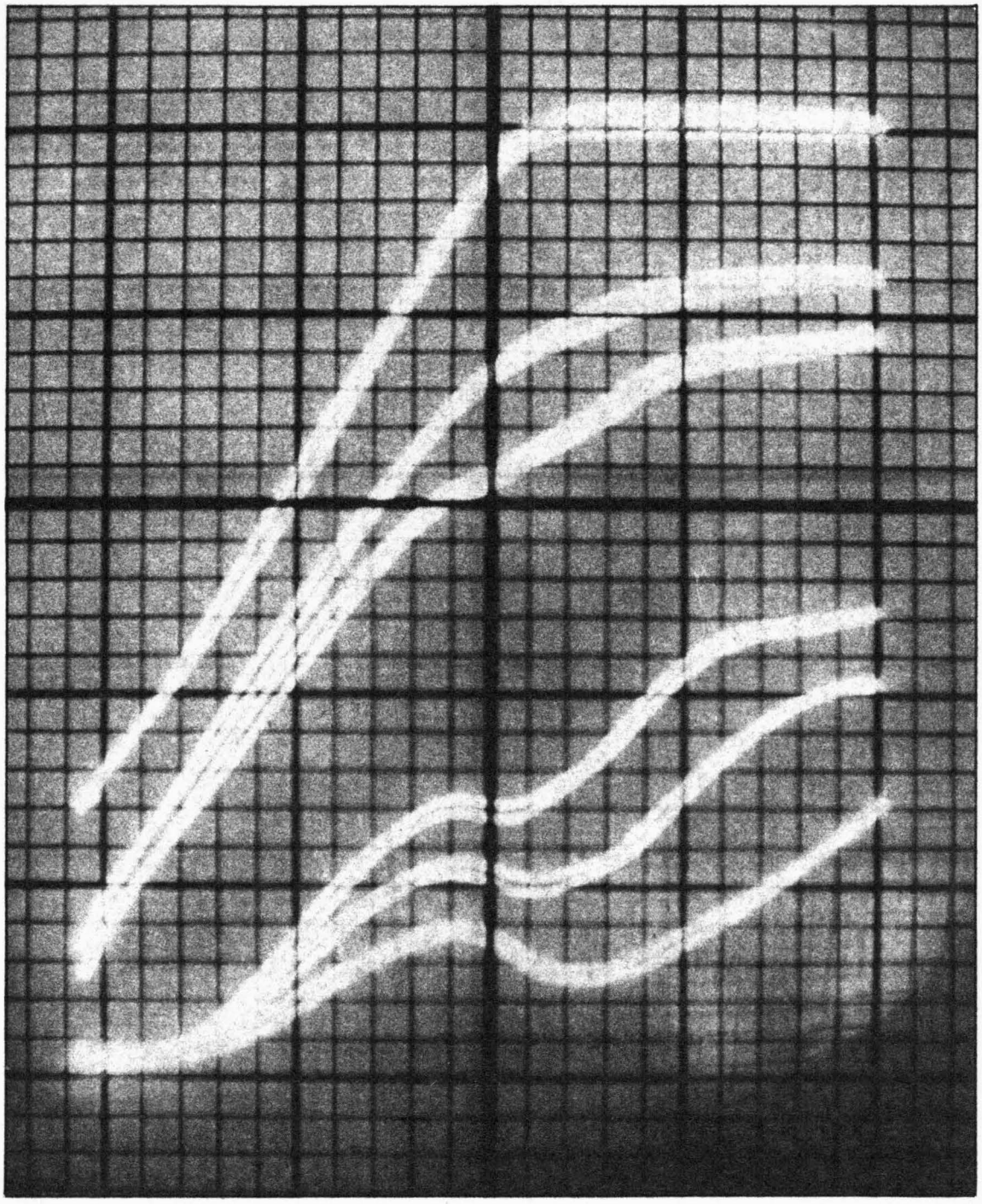

Figure 13.

OSCILLOGRAPH OF PLATE CURRENT-GRID VOLTAGE CHARACTERISTICS

FOR VARIOUS VALUES OF B

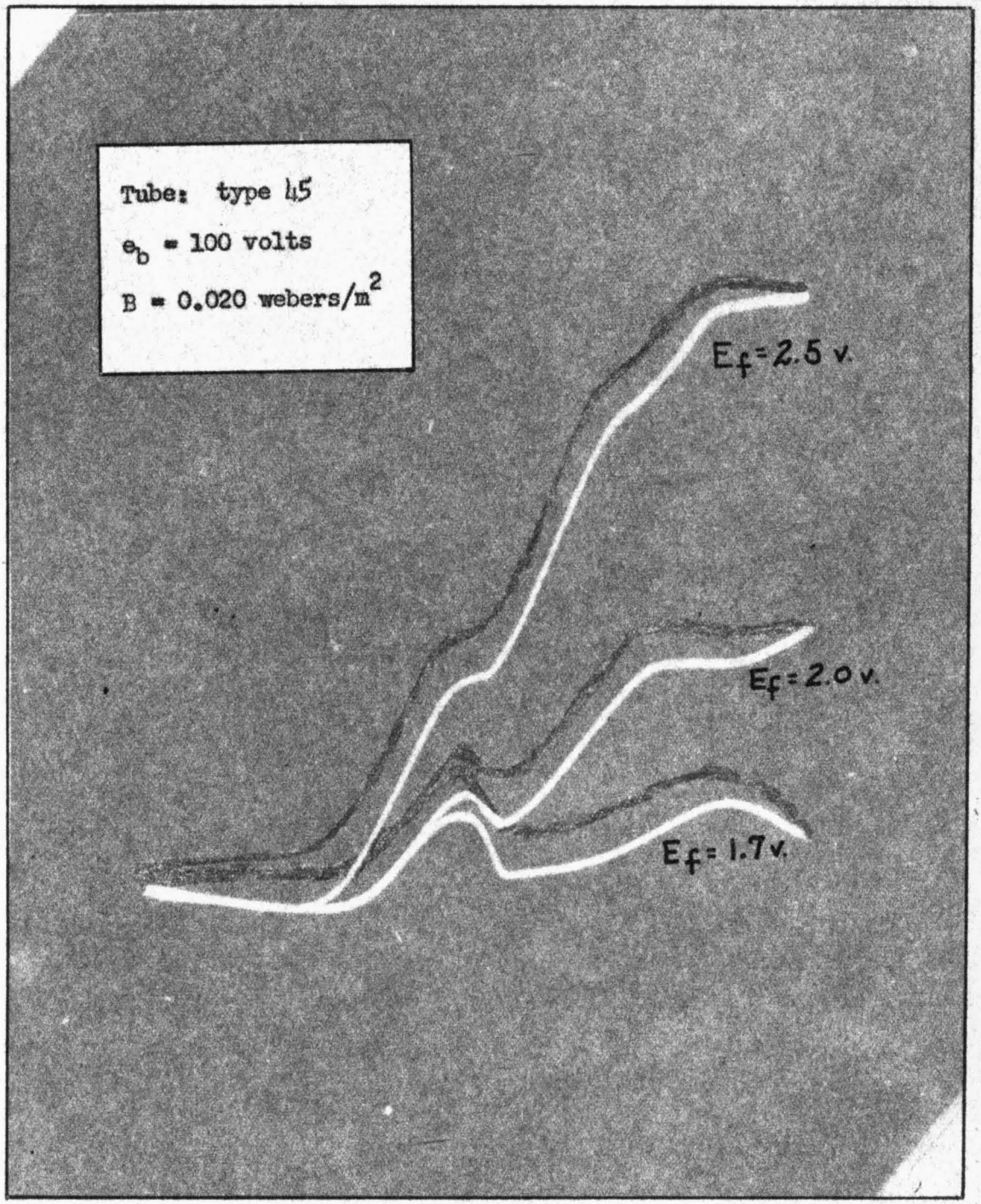

Figure 14.

OSCILLOGRAPH OF PLATE CURRENT-GRID VOLTAGE CHARACTERISTICS FOR VARIOUS VALUES OF FILAMENT POTENTIAL AND CONSTANT B

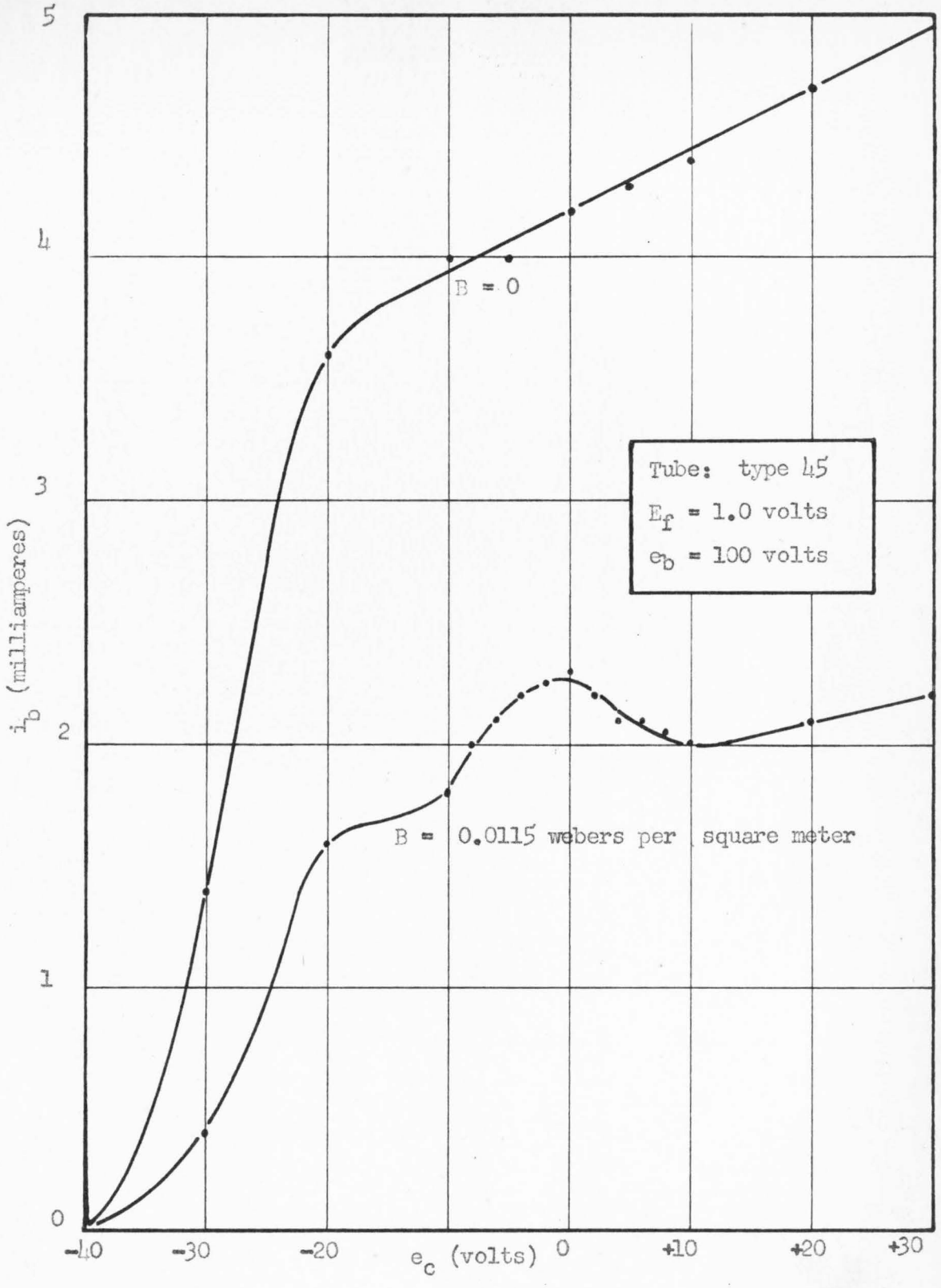

Figure 15.

PLATE CURRENT-GRID VOLTAGE CHARACTERISTICS WITH REDUCED FILAMENT POTENTIAL (BOTH WITH AND WITHOUT MAGNETIC FIELD)

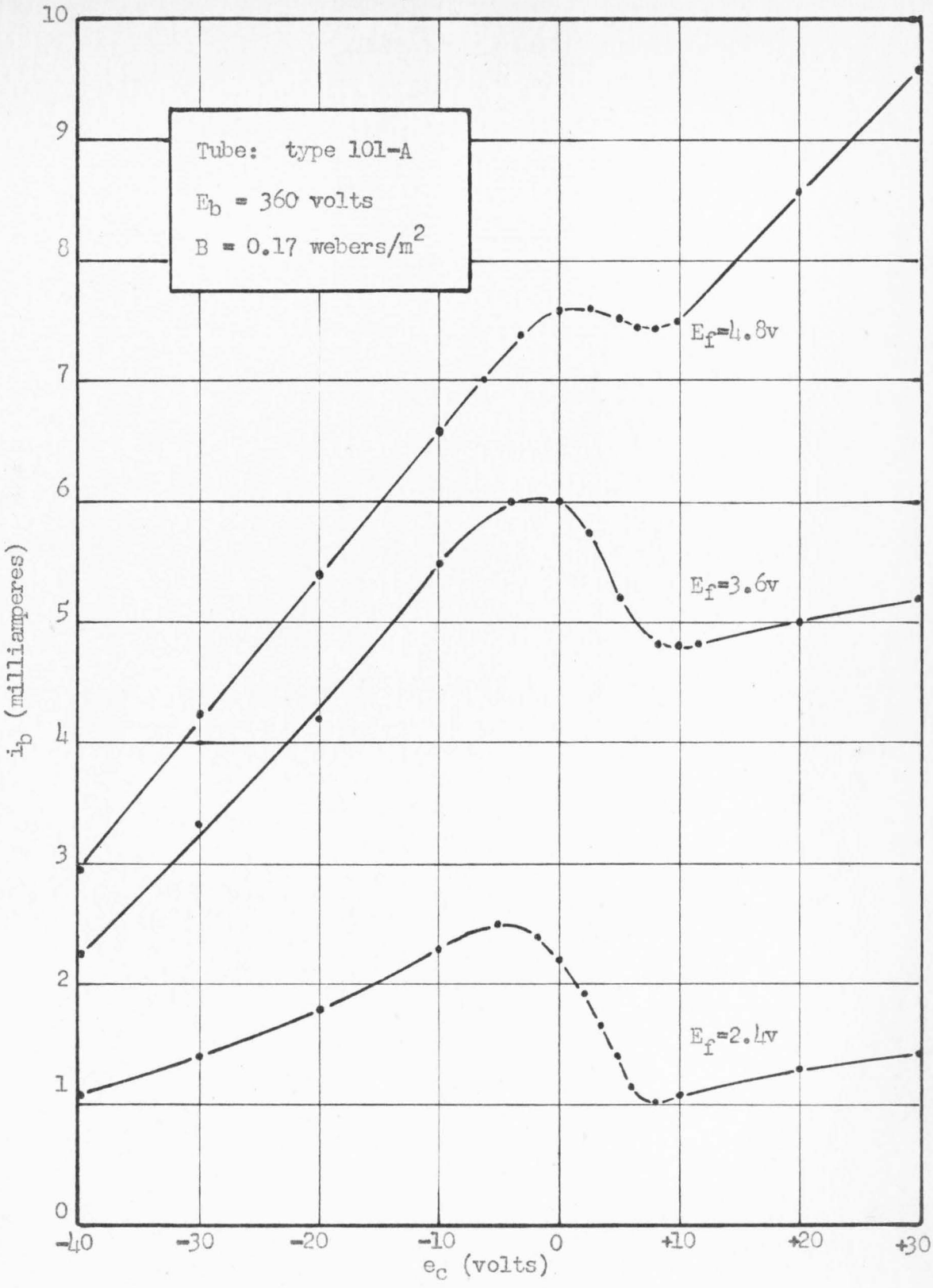

Figure 16.

PLATE CURRENT-GRID VOLTAGE CHARACTERISTICS OF TYPE 101-A ELECTRON TUBE FOR VARIOUS VALUES OF FILAMENT POTENTIAL

3. Distortion of the magnetic field due to the non-homogeneous permeability inside the tube is negligible.

4. Space-charge effects are negligible.

Since the average initial velocities of electrons leaving the heated filament are usually of the order of magnitude of one-half an electron volt,[8,9] and as the potentials used in this tube are much greater than this value, it is believed that the assumption of zero thermal electron velocities is justified. Figure 17 shows the distribution of initial electron velocities from an oxide coated filament for operating temperatures.[10] It may be seen that less than 0.1 per cent of the electrons emitted from a cathode of 1500 degrees K have velocities greater than one electron volt.

The ratio of the electrostatic mass to the static mass of a particle[11] may be expressed as

$$m_o/m = \sqrt{1 - (v/c)^2}.$$

The maximum velocities of electrons obtained in this study is about 5.9×10^6 meters per second. Therefore

$$m_o/m = \sqrt{1 - \left[\frac{5.9 \times 10^6}{3.0 \times 10^8}\right]^2} = 0.9997$$

an error of only 0.03 per cent if relativistic variation of mass is neglected.

The third assumption is that the distortion of the magnetic field is not severe even though the plates of the tube are constructed of magnetic material. Any distortion would be greatest near the plates themselves and therefore would produce no profound effect on the motion

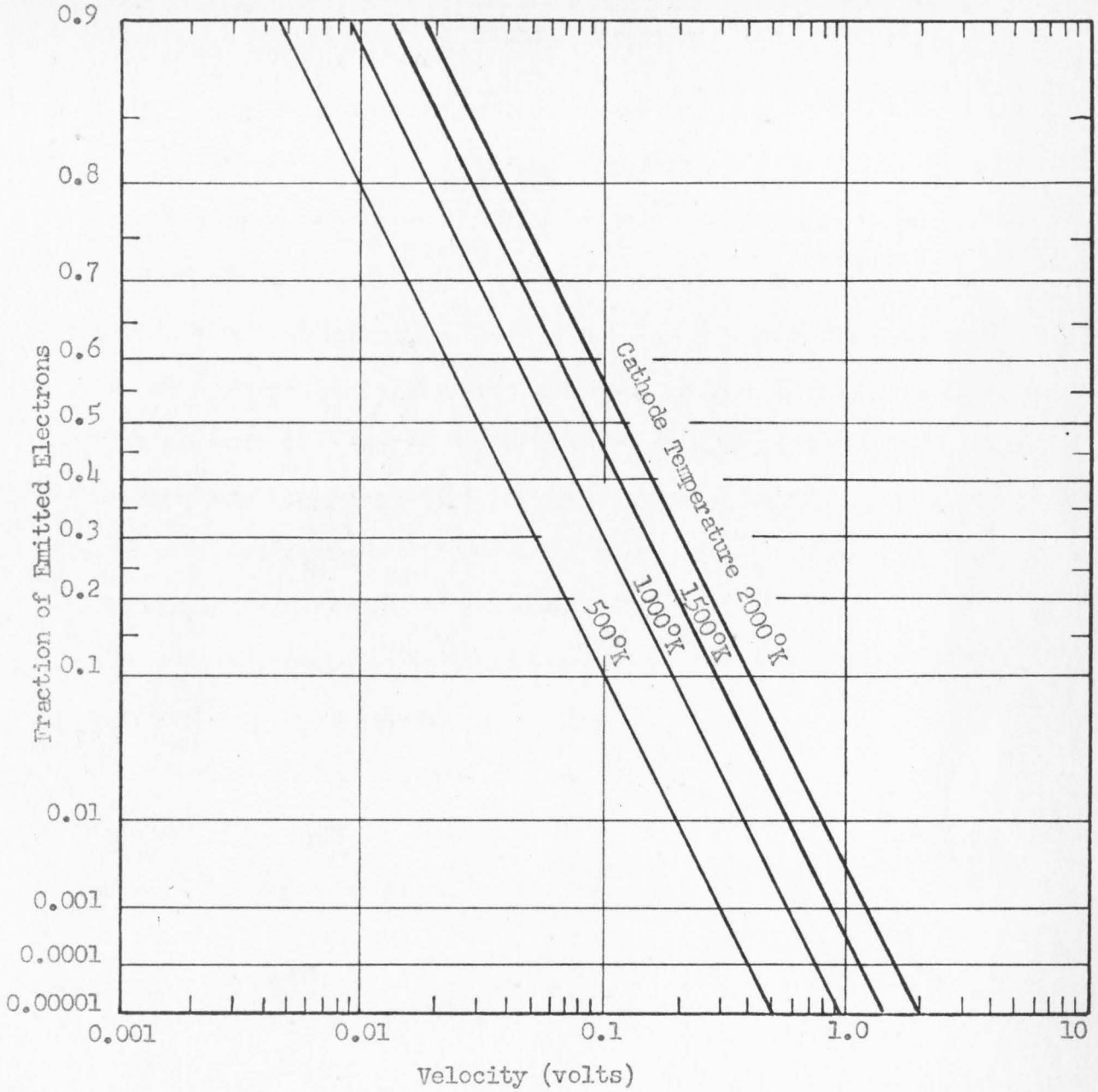

Figure 17.

VELOCITY DISTRIBUTION OF ELECTRONS RESULTING FROM THERMONIC EMISSION

of an electron until it reached this region. There would be some magnetic shielding of the space inside the plates, but a measurement of the flux density inside the plates failed to indicate any appreciable change in field strength.

The assumption that the effect of space-charge on the motion of the electrons is negligible might be questioned. It might even be expected that space-charge would modify the potential distribution in the tube under investigation more than it does in a tube without the magnetic field. This is because the transit time associated with the electron paths is relatively large and the electron will remain in the inter-electrode space much longer than if the magnetic field were not present. With the electrons traveling in their longest path, however, the probability of collision with and consequent ionization of gas molecules is greatest. This will result in partial neutralization of the existing space-charge. Proof of ionization is given in Figure 18. This is a photograph of a type 101-A electron tube with a magnetic field parallel to the plates. This tube was used instead of the type 45 because the plate did not completely surround the filament. From Figure 15, it may be seen that with a constant plate potential and magnetic field, the negative transconductance of the tube is increased when the filament temperature is lowered. When the filament temperature is lowered, there is a decrease in space-charge.[12] This is also shown by the characteristic curve of a type 101-A tube when operated at various filament voltages (Figure 16). As the effect under investigation increases with a decrease in space-charge, it can be assumed

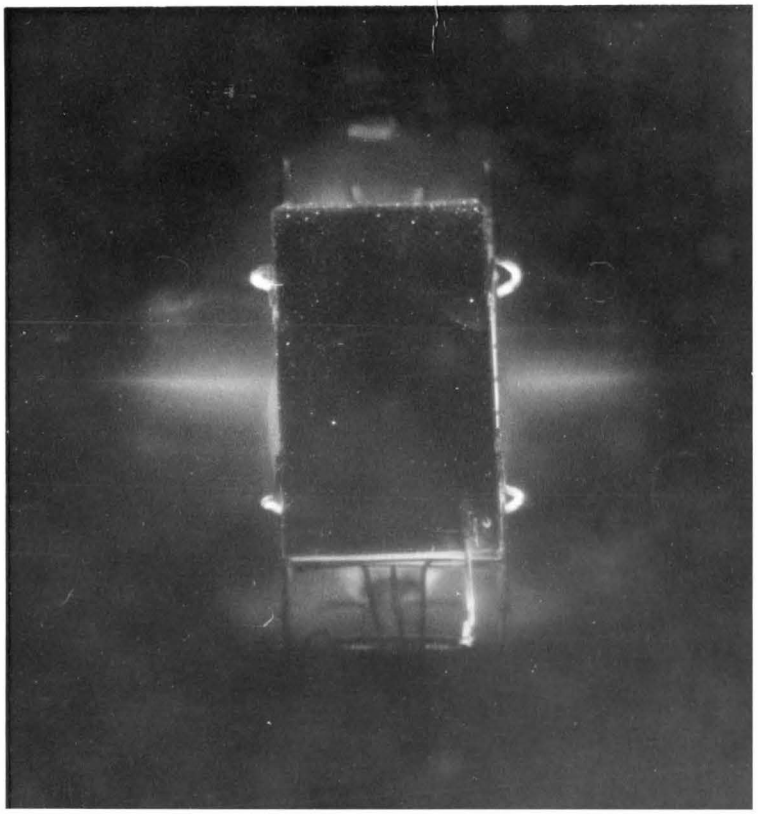

Figure 18.

PHOTOGRAPH SHOWING IONIZATION IN TYPE 101-A ELECTRON TUBE IN THE PRESENCE OF A MAGNETIC FIELD

that space-charge is not the cause of the effect and may be neglected as far as an explanation of the phenomenon is concerned. Space-charge probably will be a factor in determining quantitative results.[13]

Laws of Motion of Charged Particles

Electrostatic Fields. By definition, the electric field intensity ($\mathcal{E}$) at any point is the force (F) acting on a unit charge (q) at that point. Therefore

$$F = q\mathcal{E} . \tag{1}$$

If E is the potential at each point in the field taken with respect to any arbitrary zero of potential, the gradient of E is a vector oriented in the direction in which E changes most rapidly and whose magnitude is the rate of change of E with distance in this direction. Thus

$$\mathcal{E} = -\frac{dE}{ds} \tag{2}$$

the negative sign indicating that the force is exerted in a direction opposite to that of increasing potential. According to Newton's second law

$$F = m\frac{d^2s}{dt^2} . \tag{3}$$

Assuming that charged particles are present in small enough number so that their presence does not change the force field (zero space-charge), the only forces experienced by the particle moving in an evacuated tube are those caused by electric, magnetic, and gravitational fields. Supposing that only an electrostatic field is present

$$F = q\mathcal{E} = m\frac{d^2s}{dt^2}$$

or

$$d^2s/dt^2 = -(q/m)(dE/ds). \tag{4}$$

Specifying this motion mathematically with respect to the customary mutually perpendicular Cartesian axes

$$\begin{aligned} \ddot{x} &= (q/m)\mathcal{E}_x = -(q/m)(\partial E/\partial x) \\ \ddot{y} &= (q/m)\mathcal{E}_y = -(q/m)(\partial E/\partial y) \\ \ddot{z} &= (q/m)\mathcal{E}_z = -(q/m)(\partial E/\partial z). \end{aligned} \tag{5}$$

If the initial velocity, the position of a charged particle, and the potential distribution are known, the motion of the particle may be completely determined in electrostatic fields by use of the above differential equations.

If a charged particle travels from position s_1 to s_2, the kinetic energy acquired equals the work done on the particle by the field and may be expressed as

$$(1/2)m(v_2^2 - v_1^2) = \int_{s_1}^{s_2} F\,ds = q\int_{s_1}^{s_2} ds = -q(E_2 - E_1)$$

or

$$(1/2)mv_1^2 + qE_1 = (1/2)mv_2^2 + qE_2 \tag{6}$$

which is a statement of the conservation of energy. These equations are independent of the electron path and nature of the potential fields.

$$v_2 = \sqrt{v_1^2 - 2(q/m)(E_2 - E_1)} \tag{7}$$

If s_1 is the point from which the particle starts from rest and E_1 is zero potential

$$v = \sqrt{-2(q/m)E}\ . \tag{8}$$

If the charged particle is an electron,

$$q = -e = -1.602 \times 10^{-19} \text{ coulombs}$$

$$m = 9.106 \times 10^{-31} \text{ kilograms}$$

and $$v = 5.93 \times 10^{5} \sqrt{E} \text{ meters per second} \qquad (9)$$

where E is the potential in volts through which the electron has been accelerated.

Magnetostatic Fields. A charged particle in motion constitutes an electric current of magnitude qv, and as such experiences a force whose direction is perpendicular both to the direction of motion of the particle and to the direction of the field. The components of this force in terms of components of acceleration, velocity, and magnetic field are

$$\begin{aligned} F_x &= m\ddot{x} = q(B_y\dot{z} - B_z\dot{y}) \\ F_y &= m\ddot{y} = q(B_z\dot{x} - B_x\dot{z}) \\ F_z &= m\ddot{z} = q(B_x\dot{y} - B_y\dot{x}). \end{aligned} \qquad (10)$$

Since the force is always perpendicular to the direction of motion of the particle, the magnetic field can do no work on the particle nor can it change the speed or kinetic energy of the particle.

Only uniform magnetic fields will be considered in this study. If coordinate axes are chosen so that the z-axis is parallel to the direction of the magnetic field and the charged particle (an electron) starts at the origin with a velocity v_o in the y-z plane (Figure 19), the above equations may be written as

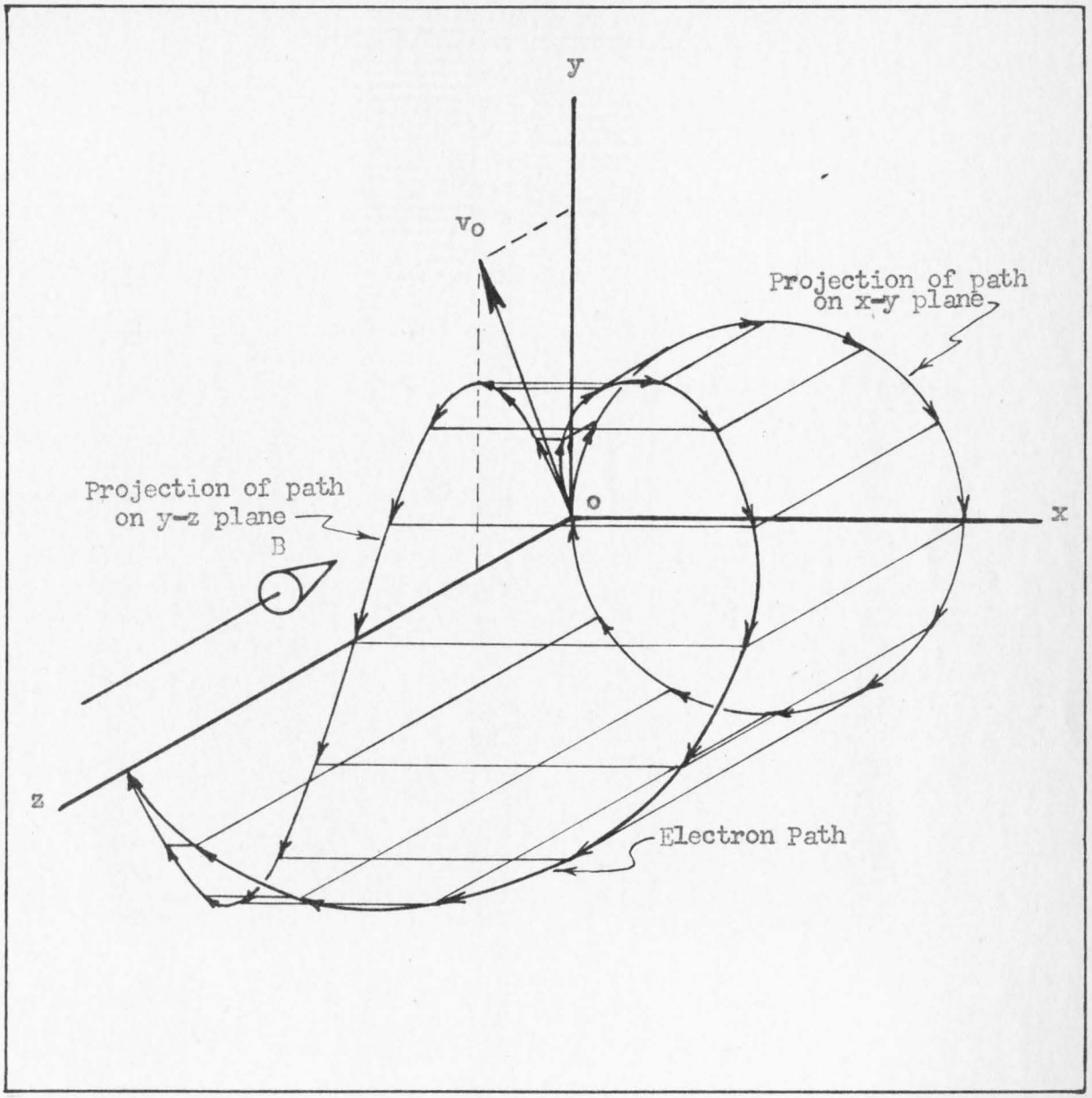

Figure 19.

HELICAL PATH OF ELECTRON IN MAGNETIC FIELD

$$F_x = eB\dot{y} = eBv_y \tag{11}$$

$$F_y = eB\dot{x} = -eBv_x \tag{12}$$

$$F_z = 0. \tag{13}$$

As $F_z = 0$, the component of velocity parallel to the magnetic field remains v_{oz} being unaltered by the presence of the field. A force normal to the velocity component v_{oy} will exist, resulting in a circular motion. This force may be considered as a centripetal force that must equal the centrifugal force developed by the circular motion of the electron. Therefore

$$Bev_{xy} = mv_{xy}^2/R. \tag{14}$$

Where R is the radius of the circle which is the projection of the path on the x-y plane and v_{xy} is the projection of the velocity vector on the x-y plane, the path itself being a helix whose axis is parallel to the z-axis and displaced from it a distance R along the x-axis.

$$R = mv_{xy}/eB. \tag{15}$$

If the velocity of the electron was caused by a potential of E volts and B is expressed in webers per square meter,

$$R = 3.37 \times 10^{-6} \sqrt{E}/B \text{ meters}. \tag{16}$$

The angular velocity of the electron,

$$\omega = v_{oy}/R = eB/m. \tag{17}$$

The time for one revolution is

$$t_1 = 2\Pi/\omega = 2\Pi m/eB. \tag{18}$$

The pitch of the helix is the z-distance covered in one revolution and is

$$t_1 v_{oz} = (2\pi m/eB)v_{oz}. \tag{19}$$

If the electron enters the magnetic field at right angles to it ($v_{oy} = v_o$), the resulting path of the particle is a circle which lies in the x-y plane.

Concurrent Electrostatic and Magnetostatic Fields. When electrostatic and magnetic fields simultaneously influence the motion of an electron, the net force is the sum of the electric and magnetic forces which would be exerted if each field acted independently. Therefore

$$\begin{aligned} F_x &= m\ddot{x} = e(\mathcal{E}_x - B_y\dot{z} + B_z\dot{y}) \\ F_y &= m\ddot{y} = e(\mathcal{E}_y - B_z\dot{x} + B_x\dot{z}) \\ F_z &= m\ddot{z} = e(\mathcal{E}_z - B_x\dot{y} + B_y\dot{x}). \end{aligned} \tag{20}$$

Since the coordinate axes are so chosen that the magnetic field is directed along the -z axis and the components of the electric field $\mathcal{E}_x$, $\mathcal{E}_y$, and $\mathcal{E}_z$ are directed along the -x, -y, and -z axes respectively, the above equations become

$$F_x = m\ddot{x} = e(\mathcal{E}_x + B\dot{y}) \tag{21}$$

$$F_y = m\ddot{y} = e(\mathcal{E}_y - B\dot{x}) \tag{22}$$

$$F_z = m\ddot{z} = e(\mathcal{E}_z). \tag{23}$$

If $\mathcal{E}_z = 0$

$$F_z = m\ddot{z} = 0 \tag{24}$$

and the electron will remain in the x-y plane.

If the electric field is non-uniform, as is the case in most three element electron tubes, it is very difficult to obtain an analytical solution of the above equations. If, however, the field is uniform (as is approximately true in the case of the plane electrode diode or a plane electrode triode when the grid is at its natural potential) and the field is such that $\mathcal{E}_x$ and $\mathcal{E}_z$ are zero, the force equation may be written as

$$F_x = m\ddot{x} = eB\dot{y} \tag{25}$$

$$F_y = m\ddot{y} = e(\mathcal{E} - B\dot{x}) \tag{26}$$

$$F_z = m\ddot{z} = 0. \tag{27}$$

Substituting $\omega = eB/m$

and $a = e\mathcal{E}/m$

we have

$$\ddot{x} = dv_x/dt = \omega v_y \tag{28}$$

$$\ddot{y} = dv_y/dt = a - \omega v_x \tag{29}$$

$$\ddot{z} = dv_z/dt = 0. \tag{30}$$

Differentiating (29) with respect to t gives

$$d^2v_y/dt^2 = -\omega(dv_x/dt). \tag{31}$$

If (28) and (31) are combined,

$$d^2v_y/dt^2 = -\omega^2 v_y. \tag{32}$$

Which is the differential equation of simple harmonic motion having the solution

$$v_y = A \cos \omega t + C \sin \omega t \qquad (33)$$

When $t = 0$, $v_y = v_{oy}$. Therefore $A = v_{oy}$.

Differentiating (33) with respect to t gives

$$dv_y/dt = -\omega A \sin \omega t + \omega C \cos \omega t. \qquad (34)$$

When $t = 0$, $v_x = v_{ox}$, and from (29)

$$dv_y/dt = a - \omega v_{ox} = \omega C \Big|_{t = 0} \qquad (35)$$

So,

$$C = (a/\omega) - v_{ox}$$

Therefore

$$v_y = v_{oy} \cos \omega t + (a/\omega - v_{ox}) \sin \omega t \qquad (36)$$

Integrating,

$$y = (v_{oy}/\omega) \sin \omega t + (v_{ox}/\omega - a/\omega^2) \cos \omega t + C_1$$

If $y = 0$ when $t = 0$, $C_1 = a/\omega^2 - v_{ox}/\omega$

Therefore,

$$y = (v_{oy}/\omega) \sin \omega t + (a/\omega^2 - v_{ox}/\omega)(1 - \cos \omega t) \qquad (37)$$

From (29)

$$v_x = (1/\omega)(a - dv_y/dt) \qquad (38)$$

Differentiating (36)

$$dv_y/dt = -\omega v_{oy} \sin \omega t + (a - \omega v_{ox}) \cos \omega t \qquad (39)$$

Substituting in (38)

$$v_x = (1/\omega) \left[a + \omega v_{oy} \sin \omega t - (a - \omega v_{ox}) \cos \omega t \right]$$

or

$$v_x = v_{oy} \sin \omega t + a/\omega + (v_{ox} - a/\omega) \cos \omega t. \qquad (40)$$

Integrating,

$$x = -(v_{oy}/\omega)\cos\omega t + at/\omega + (1/\omega)(v_{ox} - a/\omega)\sin\omega t + C_2 .$$

If $x = 0$ when $t = 0$, $C_2 = v_{oy}/\omega$.

Therefore,

$$x = (v_{oy}/\omega)(1 - \cos\omega t) + at/\omega + (v_{ox}/\omega - a/\omega^2)\sin\omega t . \qquad (41)$$

If it is assumed that the initial velocities are of negligible magnitude, equations (41) and (37) become

$$x = (a/\omega^2)(\omega t - \sin\omega t) \qquad (42)$$

$$y = (a/\omega^2)(1 - \cos\omega t) \qquad (43)$$

which are the parametric equations of an ordinary cycloid.

A Mechanical Analogy for Determining Electron Motion in Crossed Fields

The similarity between the motion of an electron in electric and magnetic fields and the motion of a gyroscope was suggested by William F. Osgood, of Harvard University.[14] A model for demonstrating this motion was devised by A. Rose of the R. C. A. Laboratories.[15] The model used in this investigation is similar to that used by Rose except that an electron tube consisting of three elements is being studied instead of a two-element magnetron as was used by him.

The equations of motion of the end of the axis of a gyroscope acted upon by a force normal to the axis will now be determined. Figure 20 shows a gyroscope which spins with a high angular velocity about its axis and is free to rotate about the fixed point O. Oxyz is a rectangular coordinate system fixed in space and OXYZ are rectangular

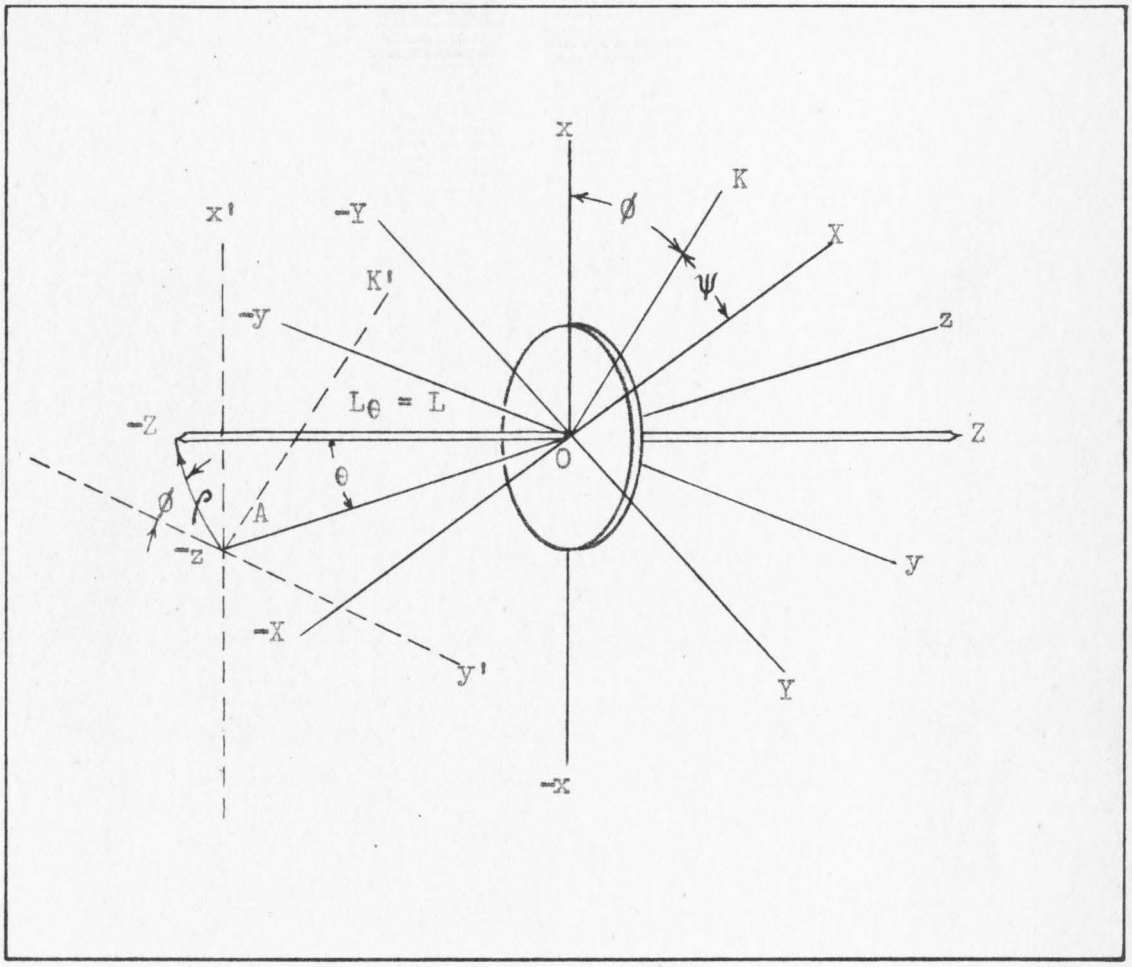

Figure 20.

COORDINATES USED IN GYROSCOPE ANALOGY

axes fixed relative to the body and moving with it and such that before displacement the two sets of axes are coincident. OK is perpendicular to the plane of zOZ and is the intersection of the planes of XOY and xOy. θ, ϕ, and ψ are the Eulerian angles[16] defined as follows:

$$\theta = zOZ,\ \phi = xOK,\ \text{and}\ \psi = XOK.$$

If ω_X, ω_Y, and ω_Z denote the components of angular velocity of the body about the axes OX, OY, and OZ respectively, Eulers geometrical relations[17] may be written

$$\begin{aligned} \omega_X &= \dot{\theta}\cos\psi + \dot{\phi}\sin\theta\sin\psi \\ \omega_Y &= \dot{\theta}\sin\psi - \dot{\phi}\sin\theta\cos\psi \\ \omega_Z &= \dot{\psi} + \dot{\phi}\cos\theta \end{aligned} \tag{43}$$

The kinetic energy of a dynamical system with one point fixed is

$$T = (1/2)(I_x\omega_x^2 + I_y\omega_y^2 + I_z\omega_z^2) \tag{44}$$

and since for the gyroscope, $I_x = I_y$, the energy equation may be written

$$T = (1/2)\left[I_x(\omega_x^2 + \omega_y^2) + I_z\omega_z^2 \right]. \tag{45}$$

Substituting Euler's relations

$$\begin{aligned} T = (1/2)\Big[& I_x(\dot{\theta}^2\cos^2\psi + 2\dot{\theta}\dot{\phi}\sin\theta\sin\psi\cos\psi + \dot{\phi}^2\sin^2\theta\sin^2\psi \\ & + \dot{\theta}^2\sin^2\psi - 2\dot{\theta}\dot{\phi}\sin\theta\sin\psi\cos\psi + \dot{\phi}^2\sin^2\theta\cos^2\psi) \\ & + I_z(\dot{\psi} + \dot{\phi}\cos\theta)^2\Big] \\ = (1/2)\Big[& I_x(\dot{\theta}^2 + \dot{\phi}^2\sin^2\theta) + I_z(\dot{\psi} + \dot{\phi}\cos\theta)^2\Big] \end{aligned} \tag{46}$$

Lagrange's equations[18] for the general case of a rotating rigid body fixed at its center of gravity are

$$\frac{d}{dt}\left(\frac{\partial T}{\partial \dot{\theta}}\right) - \frac{\partial T}{\partial \theta} = L_\theta F_\theta$$

$$\frac{d}{dt}\left(\frac{\partial T}{\partial \dot{\phi}}\right) - \frac{\partial T}{\partial \phi} = L_\phi F_\phi \qquad (47)$$

$$\frac{d}{dt}\left(\frac{\partial T}{\partial \dot{\psi}}\right) - \frac{\partial T}{\partial \psi} = L_\psi F_\psi$$

where F_θ, F_ϕ, and F_ψ are the forces and L_θ, L_ϕ, and L_ψ are the moment arms of the three torques.

Making the following substitutions in Lagrange's equations

$$\frac{\partial T}{\partial \dot{\theta}} = I_x \dot{\theta}$$

$$\frac{d}{dt}\left(\frac{\partial T}{\partial \dot{\theta}}\right) = I_x \ddot{\theta}$$

$$\frac{\partial T}{\partial \theta} = I_x(\dot{\phi}^2 \sin\theta \cos\theta) - I_z(\dot{\phi}\dot{\psi} \sin\theta + \dot{\phi}^2 \sin\theta \cos\theta)$$

$$\frac{\partial T}{\partial \dot{\phi}} = I_x(\dot{\phi} \sin^2\theta) + I_z(\dot{\psi} \cos\theta + \dot{\phi} \cos^2\theta)$$

$$\frac{d}{dt}\left(\frac{\partial T}{\partial \dot{\phi}}\right) = I_x(\ddot{\phi} \sin^2\theta + 2\dot{\theta}\dot{\phi} \sin\theta \cos\theta) - I_z(\dot{\theta}\dot{\psi} \sin\theta - \ddot{\psi} \cos\theta + 2\dot{\theta}\dot{\phi} \sin\theta \cos\theta - \ddot{\phi} \cos^2\theta)$$

$$= I_x\ddot{\phi} \sin^2\theta + 2(I_x - I_z)\dot{\theta}\dot{\phi} \sin\theta \cos\theta + I_z(\ddot{\phi} \cos^2\theta - \dot{\phi}\dot{\psi} \sin\theta + \ddot{\psi} \cos\theta)$$

$$\frac{\partial T}{\partial \phi} = 0$$

$$\frac{\partial T}{\partial \dot{\psi}} = I_z(\dot{\psi} + \dot{\phi}\cos\theta)$$

$$\frac{d}{dt}\left(\frac{\partial T}{\partial \dot{\psi}}\right) = I_z(\ddot{\psi} - \dot{\theta}\dot{\phi}\sin\theta + \ddot{\phi}\cos\theta)$$

$$\frac{\partial T}{\partial \psi} = 0$$

Gives:

$$\frac{d}{dt}\left(\frac{\partial T}{\partial \dot{\theta}}\right) - \frac{\partial T}{\partial \theta} = I_x\ddot{\theta} - I_x(\dot{\phi}^2\sin\theta\cos\theta) + I_z(\dot{\phi}\dot{\psi}\sin\theta + \dot{\phi}^2\sin\theta\cos\theta)$$

$$= I_x\ddot{\theta} + I_z\dot{\phi}\dot{\psi}\sin\theta - (I_x - I_z)\dot{\phi}^2\sin\theta\cos\theta = L_\theta F_\theta \qquad (48)$$

$$\frac{d}{dt}\left(\frac{\partial T}{\partial \dot{\phi}}\right) - \frac{\partial T}{\partial \phi} = I_x\ddot{\phi}\sin^2\theta + 2(I_x - I_z)\dot{\theta}\dot{\phi}\sin\theta\cos\theta$$

$$+ I_z(\ddot{\phi}\cos^2\theta - \dot{\theta}\dot{\psi}\sin\theta + \dot{\psi}\cos\theta) = L_\phi F_\phi \qquad (49)$$

$$\frac{d}{dt}\left(\frac{\partial T}{\partial \dot{\psi}}\right) - \frac{\partial T}{\partial \psi} = I_z(\ddot{\psi} - \dot{\theta}\dot{\phi}\sin\theta + \ddot{\phi}\cos\theta) = L_\psi F_\psi \qquad (50)$$

Neglecting the frictional force F_ψ, this last equation may be written as

$$\ddot{\psi} - \dot{\theta}\dot{\phi}\sin\theta + \ddot{\phi}\cos\theta = 0 \qquad (51)$$

Integration gives

$$\dot{\psi} + \dot{\phi}\cos\theta = \text{a constant} \qquad (52)$$

and from Euler's third geometrical relation, $\dot{\psi} + \dot{\phi}\cos\theta = \omega_z$

this constant must be ω_z

and $$\dot{\omega}_z = 0. \qquad (53)$$

If θ be restricted to very small angles and ρ is the distance that the end of the gyroscope axis moves, the following substitutions may be made:

$$L_\theta = L,\ L_\phi = L \sin\theta = \rho,\ \sin\theta = \rho/L,$$
$$\cos\theta = 1,\ L\dot{\theta} = \dot{\rho},\ L\ddot{\theta} = \ddot{\rho} \tag{54}$$

So:

$$I_x\ddot{\theta} + I_z\dot{\phi}\dot{\psi}\,(\rho/L) - (I_x - I_z)\,\dot{\phi}^2\,(\rho/L) = LF_\theta$$

$$I_x\ddot{\phi}\,(\rho/L)^2 + 2(I_x - I_z)\,\dot{\theta}\,\dot{\phi}\,(\rho/L) + I_z\left[\ddot{\phi} - \dot{\theta}\dot{\psi}\,(\rho/L) + \ddot{\psi}\right] = \rho F_\phi$$

or

$$I_x\left[\ddot{\theta} - \dot{\phi}^2(\rho/L)\right] + I_z\dot{\phi}\,(\rho/L)(\dot{\phi} + \dot{\psi}) = LF_\theta \tag{55}$$

$$I_x(\rho/L)\left[\ddot{\phi}\,(\rho/L) + 2\dot{\theta}\dot{\phi}\right] - I_z\left[2\dot{\theta}\dot{\phi}\,(\rho/L) - \ddot{\phi} - \dot{\theta}\dot{\psi}(\rho/L) + \ddot{\psi}\right] = \rho F_\phi \tag{56}$$

also substituting

$$\ddot{\psi} - \dot{\theta}\,\dot{\phi}\,(\rho/L) + \ddot{\phi} = 0$$

and

$$\omega_z = \dot{\psi} + \dot{\phi}$$

$$I_x\left[\ddot{\theta} - \dot{\phi}^2(\rho/L)\right] + I_z(\rho/L)\,\dot{\phi}\,\omega_z = LF_\theta$$
$$I_x(\rho/L)\left[\ddot{\phi}\,(\rho/L) + 2\dot{\theta}\dot{\phi}\right] - I_z(\rho/L)\,\dot{\theta}\,\omega_z = \rho F_\phi$$

$$L\ddot{\theta} - \rho\dot{\phi}^2 + (I_z/I_x)\rho\dot{\phi}\omega_z = (L^2F_\theta/I_x)$$
$$L\left[\ddot{\phi}\,(\rho/L) + 2\dot{\theta}\dot{\phi}\right] - (I_z/I_x)\,L\,\dot{\theta}\,\omega_z = (L^2F_\phi/I_x)$$

$$\ddot{\rho} - \rho\dot{\phi}^2 + (I_z/I_x)\rho\dot{\phi}\,\omega_z = (L^2F_\theta/I_x) \tag{57}$$

$$\rho\ddot{\phi} + 2\dot{\rho}\dot{\phi} - (I_z/I_x)\dot{\rho}\,\omega_z = (L^2F_\phi/I_x) \tag{58}$$

Which completely describe the motion of the end of the gyroscope axis for small values of θ.

Changing to rectangular coordinates by making use of the relations[19]

$$\dot{x} = -\dot{\rho}\cos\phi + \rho\dot{\phi}\sin\phi \tag{59}$$

$$\dot{y} = \dot{\rho}\sin\phi + \rho\dot{\phi}\cos\phi \tag{60}$$

$$\ddot{x} = -(\ddot{\rho} - \rho\dot{\phi}^2)\cos\phi + (\rho\ddot{\phi} + 2\dot{\rho}\dot{\phi})\sin\phi \tag{61}$$

$$\ddot{y} = (\ddot{\rho} - \rho\dot{\phi}^2)\sin\phi + (\rho\ddot{\phi} + 2\dot{\rho}\dot{\phi})\cos\phi \tag{62}$$

Multiplying equation (57) by cos ϕ,

$$(\ddot{\rho} - \rho\dot{\phi}^2)\cos\phi + (I_z/I_x)\dot{\rho}\phi\omega_z\cos\phi = \frac{L^2 F_\theta \cos\phi}{I_x} \tag{63}$$

and multiplying equation (58) by sin ϕ,

$$(\rho\ddot{\phi} + 2\dot{\rho}\dot{\phi})\sin\phi - (I_z/I_x)\dot{\rho}\omega_z\sin\phi = \frac{L^2 F\phi \sin\phi}{I_x} \tag{64}$$

Subtracting (63) from (64),

$$\ddot{x} - (I_z/I_x)\omega_z\dot{y} = \frac{L^2 F_x}{I_x} \tag{65}$$

Similarly:

$$\ddot{y} + (I_z/I_x)\omega_z\dot{x} = \frac{L^2 F_y}{I_x} \tag{66}$$

If point A is one end of a long permanent magnet having pole strength ν, and is subjected to a magnetic field B, these equations may be written as:

$$\ddot{x} = \frac{L^2 B_x \nu}{I_x} + (I_z/I_x)\,\omega_z\dot{y} \tag{67}$$

$$\ddot{y} = \frac{L^2 B_y \nu}{I_x} - (I_z/I_x)\,\omega_z \dot{x} \tag{68}$$

$$\ddot{z} = 0 \tag{69}$$

The equations of motion of an electron have already been found. From equations (21), (22), and (24) we may write:

$$\ddot{x} = (e/m)\,\mathcal{E}_x + (e/m)B\dot{y} \tag{70}$$

$$\ddot{y} = (e/m)\,\mathcal{E}_y - (e/m)B\dot{x} \tag{71}$$

$$\ddot{z} = 0 \tag{72}$$

It may be seen that these two sets of equations are identical in form. The following gives the correspondence which exists between the parameters.

Electron Motion	Gyroscope Motion
$(e/m)\,\mathcal{E}_x$	$L^2 B_x \nu / I_x$
$(e/m)\,\mathcal{E}_y$	$L^2 B_y \nu / I_x$
$(e/m)B$	$(I_z/I_x)\,\omega_z$

Application of the Gyroscope Analogy

A model of the electrode configuration of a type 45 tube was constructed by substituting the poles of an electromagnet for the cathode and annode of the tube, as shown in Figure 21. The negative ends of long, thin alnico magnets were placed between the poles of the electromagnet in the proper positions to represent the grids of the tube.

A long permanent magnet was fastened to one end of a gyroscope axis and a small incandescent lamp was fastened to the other end so that the path of the light would be similar to the path of the end of the magnet. As the position of the gyroscope changed, the path of the end of the magnet was determined by photographing the motion of the light. The speed of the gyroscope was determined by the use of a stroboscope.

The negative pole of the small magnet on the end of the gyroscope axis was inserted between the poles of the electromagnet near the negative pole and then released. The path of this negative pole, and hence the path of an electron, could be determined as described above. The effect of a change in plate voltage of the tube could be determined by varying the strength of the electromagnet. The effect of strength of the crossed magnetic field could be determined by varying the speed of the gyroscope.

The small magnets which represent the grids of the electron tube were removed. The model was then that of the tube with grid at natural potential, which would be at a positive voltage equal to one-third that of the plate voltage. The gyroscope was given a spin of 3000 r.p.m. and released. The ends of the axis described a path

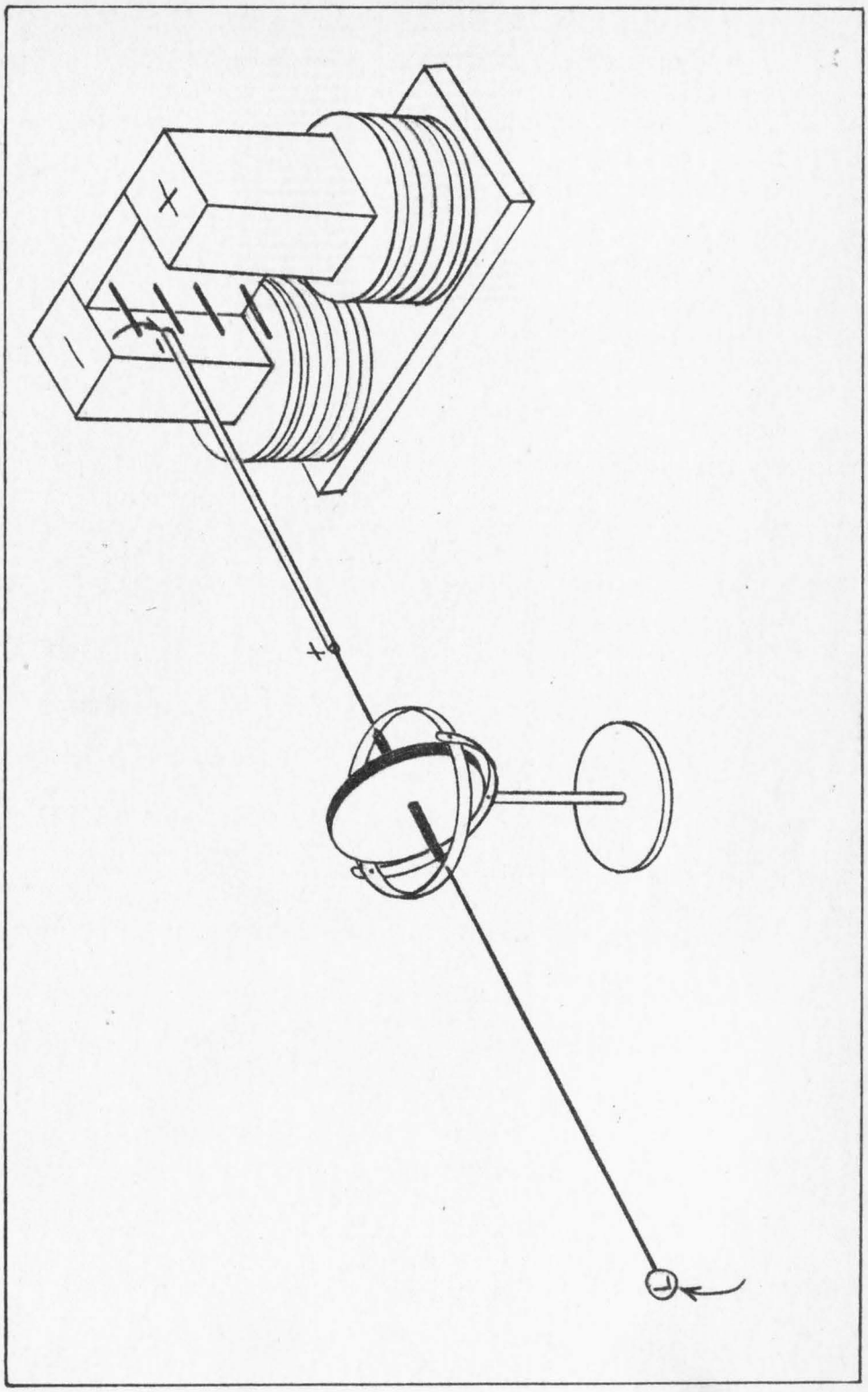

Figure 21.

GYROSCOPE AND MODEL OF ELECTRON TUBE

approximately cycloidal in shape. This was repeated with decreasing speeds of the gyroscope. At a speed of 1400 r.p.m., the magnet attached to the gyroscope axis reached the positive pole of the electromagnet. Figure 22a shows the path for speeds of the gyroscope varying from 3000 to 600 r.p.m. At a speed of 1550 r.p.m., the end of the axis missed the positive pole and returned to the negative pole. This was repeated several times and at that speed the positive pole was never reached. These conditions then represented a crossed magnetic field of sufficient strength to keep all electrons from reaching the plate of the tube. Figure 22b shows a single photograph at this speed.

It may be seen that this path is not exactly cycloidal. The reasons may be any of the following: Friction in the bearings of the gyroscope support, difficulty in releasing the gyroscope without an initial velocity, non-uniformity of the magnetic field, and failure to have the gyroscope, light, and small magnet in perfect balance. For these reasons, together with the fact that it was impossible to determine accurately the pole strength of the magnets used for the grid and the electron, no attempt was made to make a qualitative analysis by use of the gyroscope analogy. The gyroscope is sufficiently accurate, however, to demonstrate the fact that transfer characteristic curves as were obtained for crossed magnetic and electric fields is that which might be expected under such conditions.

For operation of the tube under the conditions previously described, that is, with grid at one-third of plate voltage and the magnet strength represented by a speed of 1550 r.p.m. of the gyroscope,

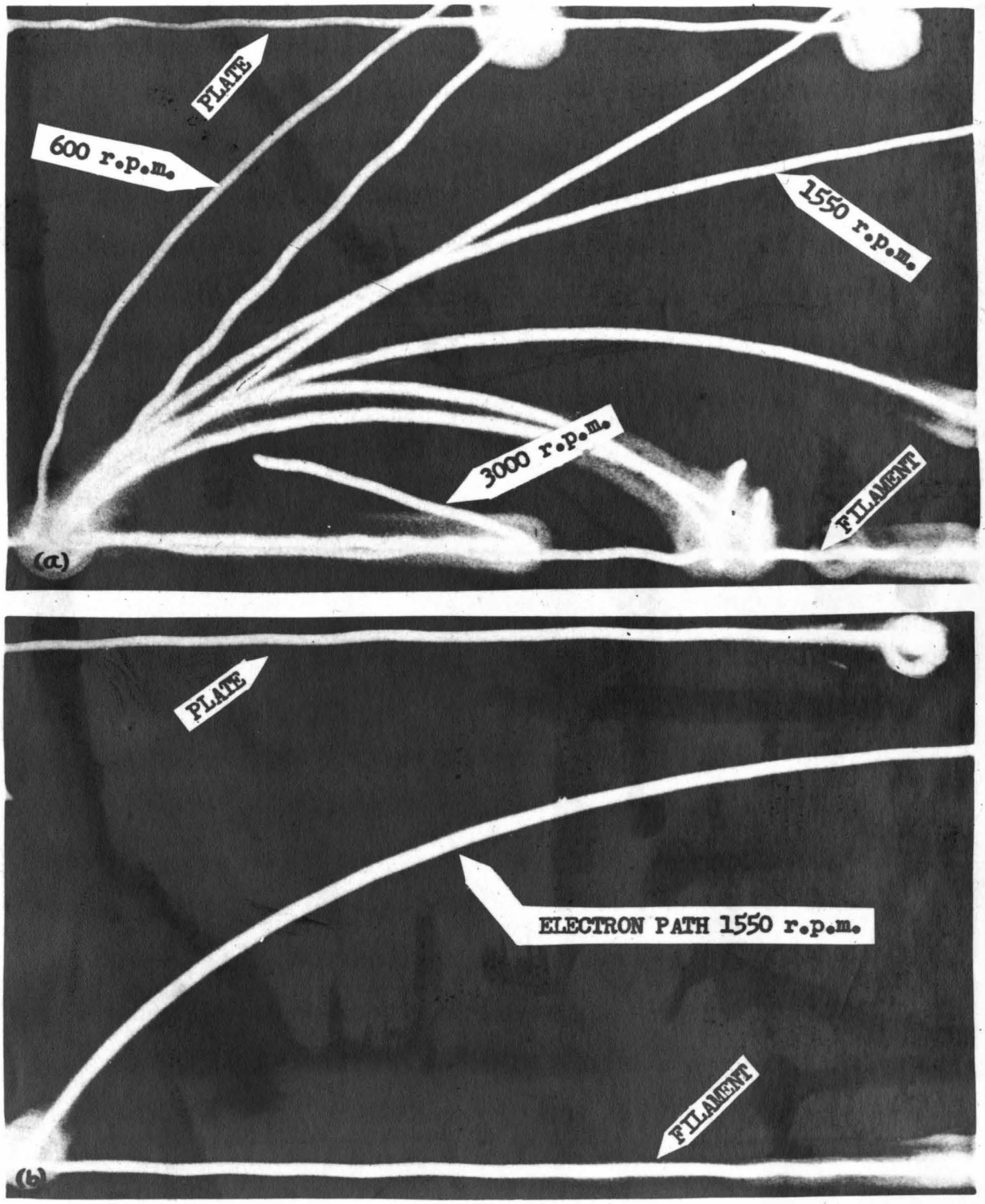

Figure 22.

PHOTOGRAPHS SHOWING VARIOUS SPEEDS OF GYROSCOPE

point A may be located for the theoretical transfer characteristic curve of the tube. (Figure 23)

Next, the small magnets representing the grid of the tube were inserted. These were of such strength as to represent a grid voltage of approximately zero. With a gyroscope speed of 1550 r.p.m., the end of the axis was released at various positions along the negative pole of the electromagnet. Figure 24 shows the resulting paths. This shows clearly that many of the electrons would reach the plate of the tube if the grid was at this potential. Therefore, point B should be placed at some point on the vertical axis of Figure 23.

If it were possible to make the magnets which represent the grid sufficiently negative, the magnet on the end of the gyroscope axis would be repelled with sufficient force so that it would never get past the grid, and hence never reach the plate. Point C may then be placed at some point on the negative end of the horizontal axis, giving a curve which must have the general shape CBA as shown.

There are electrons which would go from the filament of the tube to the ends of the plate whose path would not be affected by the presence of the magnetic field because the direction of the electron path is parallel to the magnetic lines of force. A more detailed study of this part of the plate current will be made later, but at this point it is sufficient to indicate that this portion of current must have a characteristic curve approximately as shown by DEF.

The curve representing the total plate current will be the sum of curves CBA and DEF or curve DGF. It will be seen that this

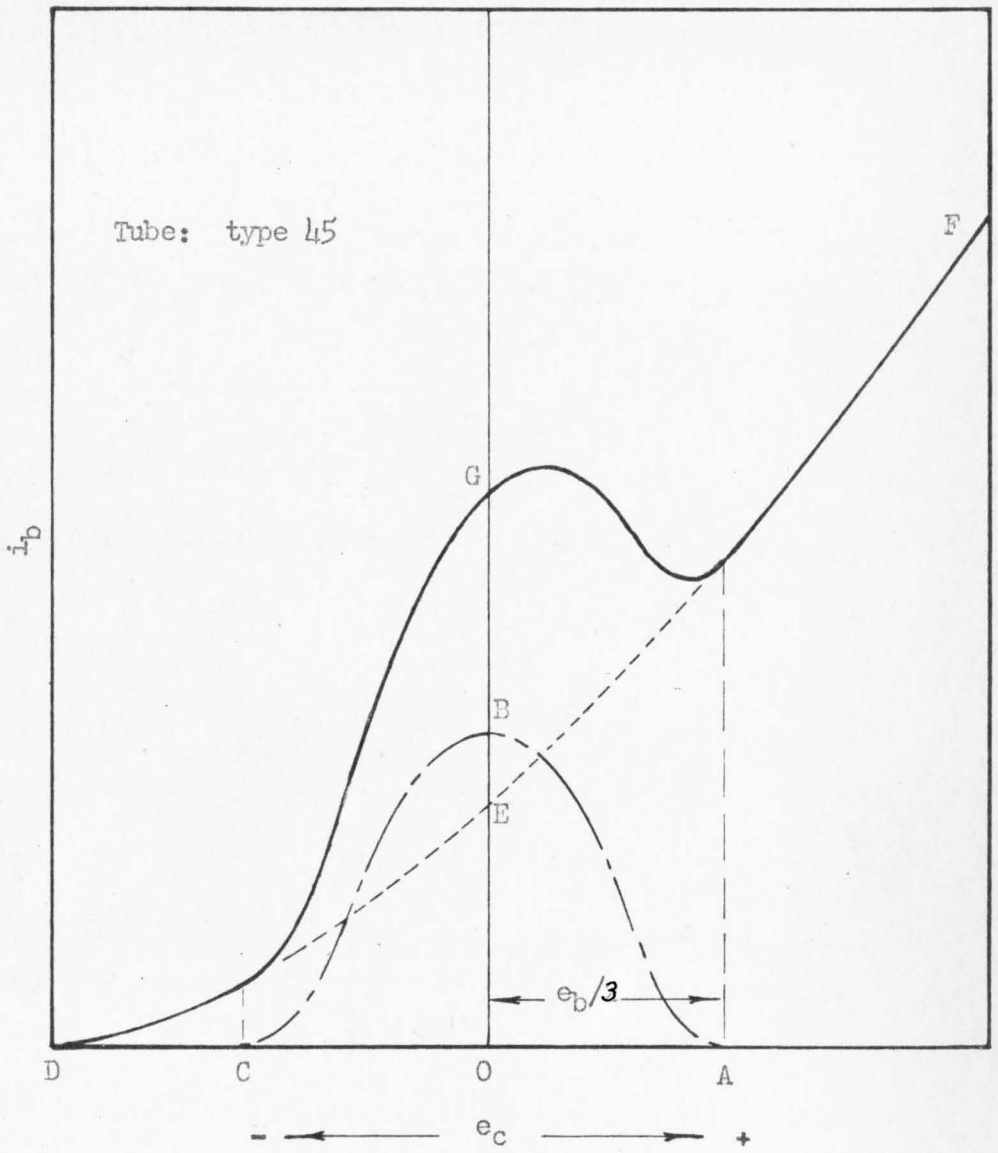

Figure 23.

THEORETICAL CHARACTERISTIC CURVE
BASED ON GYROSCOPE ANALOGY

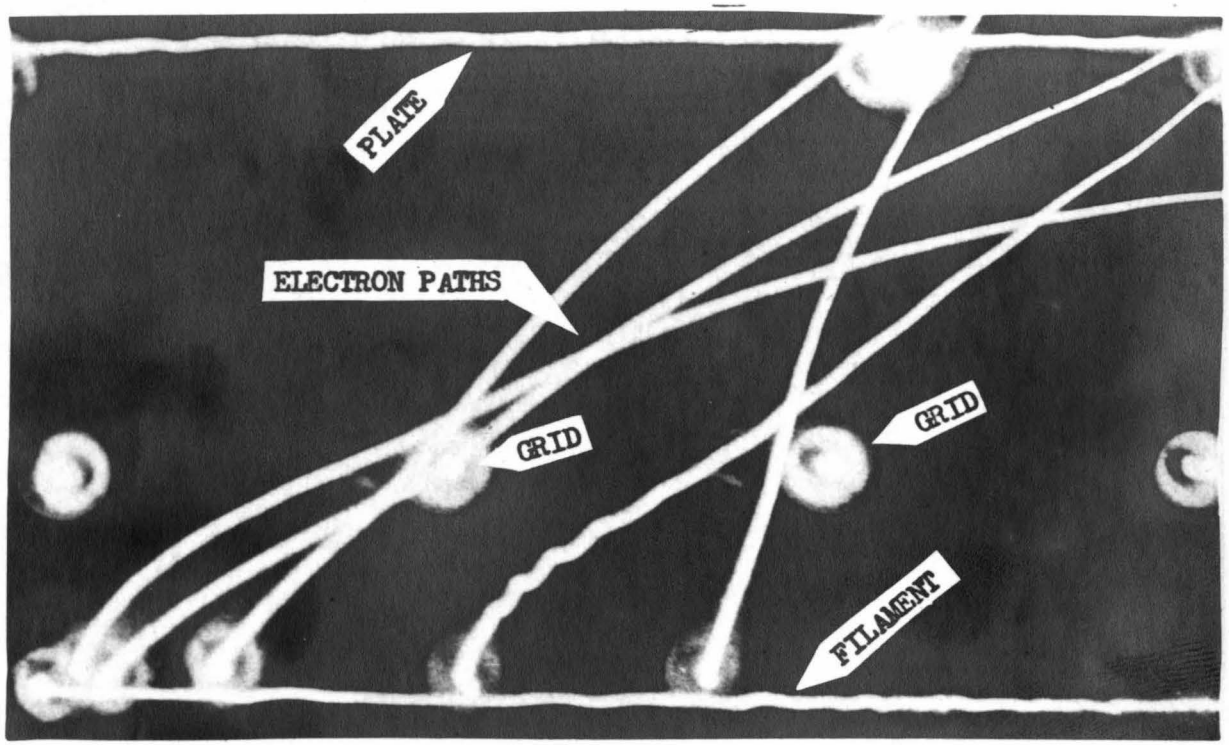

Figure 24.

PHOTOGRAPH SHOWING GYROSCOPE MOTION AT 1550 REVOLUTIONS PER MINUTE

curve has the same general shape of the actual characteristic curve of the tube under these conditions. (Figure 13)

A Graphical Method for Determining Electron Trajectories

As previously stated, it is very difficult to obtain analytical solutions for electron motion in non-uniform electric fields. If the field is not mathematically defined, such a solution is impossible. Hence there is a need for a graphical method by which the electron paths may be approximated. The method used in this study consists of computing the instantaneous radii of curvature of the path and plotting the trajectories as a series of joined circular segments.

It has been shown that the force due to an electrostatic field acting on an electron is $e\,\mathcal{E}$. The component of this force perpendicular to the instantaneous path is due to the component of the gradient of potential in that direction and may be expressed as

$$F_{NE} = e\,\mathcal{E}_N. \tag{73}$$

If the electron is moving in a curved path, this normal component of force must equal the centrifugal force, (mv^2/R_E), acting on the particle. Therefore

$$e\,\mathcal{E}_N = mv^2/R_E. \tag{74}$$

Assuming a negligible initial velocity, the kinetic energy of the electron, $(mv^2/2)$, must equal the potential energy lost (eE). Then,

$$e\,\mathcal{E}_N = 2eE/R_E$$

$$R_E = 2E/\mathcal{E}_N. \tag{75}$$

It has also been shown that the force due to a magnetic field acting on an electron is B_{ev} and that the instantaneous radius of curvature due to the magnetic field is (Equation 15)

$$R_M = (m/e)(v/B) = 3.37 \times 10^{-6} \sqrt{E}/B \text{ meters.}$$

The total normal force acting on the moving electron is

$$F_N = e \mathcal{E}_N \pm Bev = mv^2/R. \tag{76}$$

Therefore, the instantaneous radius of curvature due to the combined fields is

$$R = \frac{mv^2}{e \mathcal{E}_N \pm Bev} \tag{77}$$

This relation may be written as

$$R = \frac{2(v^2/2)(m/e)mv}{mv \mathcal{E}_N \pm 2(v^2/2)(m/e)Be}.$$

But since, from Equation 8, $E = (v^2/2)(m/e)$,

$$R = \frac{2\ Emv}{mv \mathcal{E}_N \pm 2\ EBe}. \tag{78}$$

The instantaneous curvature of the path may be expressed as

$$K = \frac{mv \mathcal{E}_N \pm 2EBe}{2Emv} = \mathcal{E}_N /2E \pm (e/m)(B/v) \tag{79}$$

$$K = \frac{1}{R_E} \pm \frac{1}{R_M} = K_E \pm K_M \tag{80}$$

When the potential distribution is known, the curvature of the electron path due to the presence of a crossed electrostatic and

magnetic field may be determined from the above relations. Figure 25 is a nomograph for Equation 78. The following examples illustrate the use of this chart:

Example I. Given: $1/\mathcal{E}_N = 2.5 \times 10^{-5}$ meters per volt.

$E = 50$ volts.

$B = 10^{-2}$ webers per square meter.

The fields are such that either the electric or magnetic field would produce clockwise rotation.

From point A on the $1/\mathcal{E}_N$-scale, a line is extended vertically to the 50-volt line at C and then horizontally to point D. Point F is located on E-scale, a line is extended horizontally to the curve representing the proper magnetic field strength, and then upward to point H. A line connecting points D and H intercepts the R-scale at 0.0012 giving the instantaneous radius of curvature of the electron path in meters.

Example II. Given: $1/\mathcal{E}_N = 4.3 \times 10^{-5}$ meters per volt.

$E = 20$ volts.

$B = 1.25 \times 10^{-2}$ webers per square meter.

The fields are such that the electric field would produce counterclockwise rotation and magnetic field would produce clockwise rotation.

Procedure is similar to Example 1. Points K, L, and M are located, corresponding to the given values of $1/\mathcal{E}_N$ and E. By use of dividers, the point N is located below O so that ON = OM since the curvature due to the electric field is negative (counterclockwise). Points O, P, and Q are located corresponding to the given values of E and B. A line through points N and Q intercepts the R-scale at S, giving an instantaneous radius of curvature of 0.0041 meters. The center of curvature would be located so as to produce

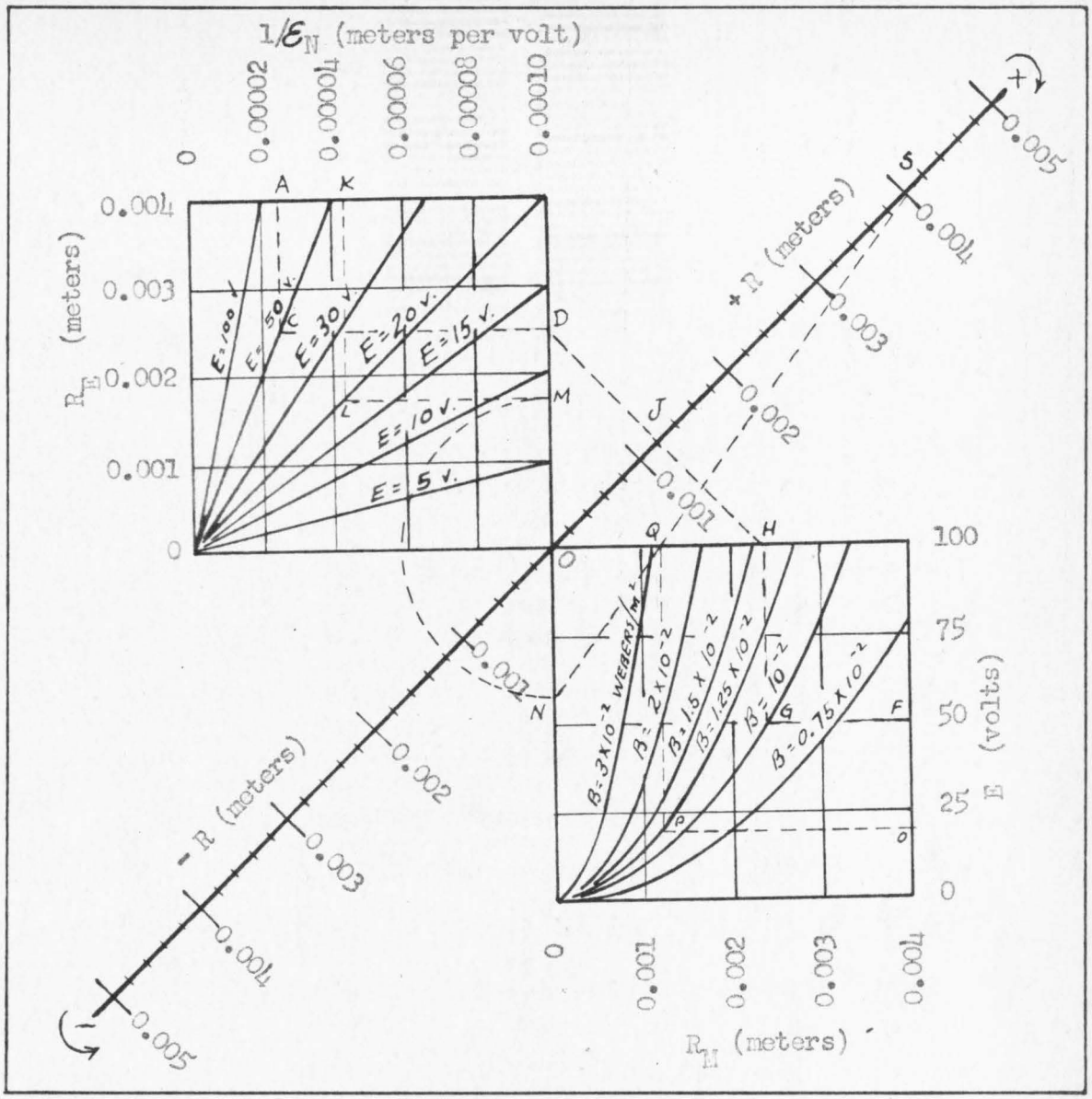

Figure 25.

NOMOGRAPH FOR FINDING INSTANTANEOUS RADIUS OF CURVATURE OF ELECTRON PATH

clockwise rotation of the electron. If the line were to intercept the negative end of the R-scale, the center would be so located as to give counter-clockwise rotation.

The values of $1/\mathcal{E}_N$ may easily be determined by using a transparent templet marked so as to give this value directly when placed over a plot of the potential field. This templet is shown in Figure 26. It is not necessary that there be any values marked on the templet if the $1/\mathcal{E}_N$-scale on Figure 25 corresponds to the scale of the potential field. Values of $1/\mathcal{E}_N$ may be transferred from the templet to the graph by the use of dividers. The graph may also be drawn so that the R-scale is the same as that of the potential field, eliminating the necessity of reading the values of the radius of curvature but enabling one to set his compass at the proper radius directly from the graph.

Since the graphical construction is only approximate, it was first used to plot the path of an electron in a uniform field so that this path could be compared with the path determined by analytical means. Figure 27 shows the construction and results.

Maximum Displacement in Uniform Fields

As the process of determining electron paths by the graphical method is rather long and tedious and also subject to some cumulative error, a shorter method will be derived for use in the regions where the potential field is uniform. In this study, it is only necessary to know if an electron reaches the plate of the electron tube in order to know whether or not it contributes to the plate current. The method described here will enable one to determine the maximum y-component of displacement in uniform fields thereby determining if an electron will reach the plate.

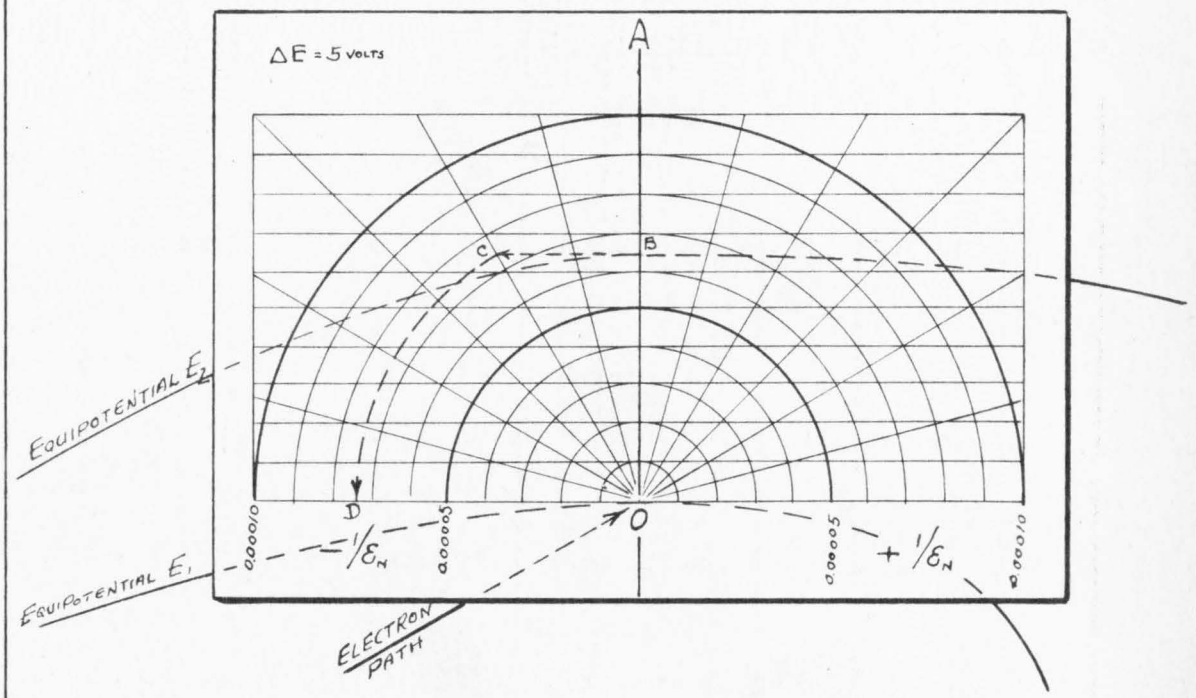

Directions: Place templet on plot of potential distribution with point O at position of electron and OA normal to equipotential line. Note point B where next equipotential line intersects OA. Follow horizontal line to point of intersection with line which is normal to electron path (C). The distance OC is the value of $1/\mathcal{E}$ and may be transferred by dividers to the nonograph (Figure 25). To determine values of $1/\mathcal{E}_N$, follow circle to point D and read value in meters per volt.

Figure 26.

TEMPLET FOR DETERMINING $1/\mathcal{E}_N$

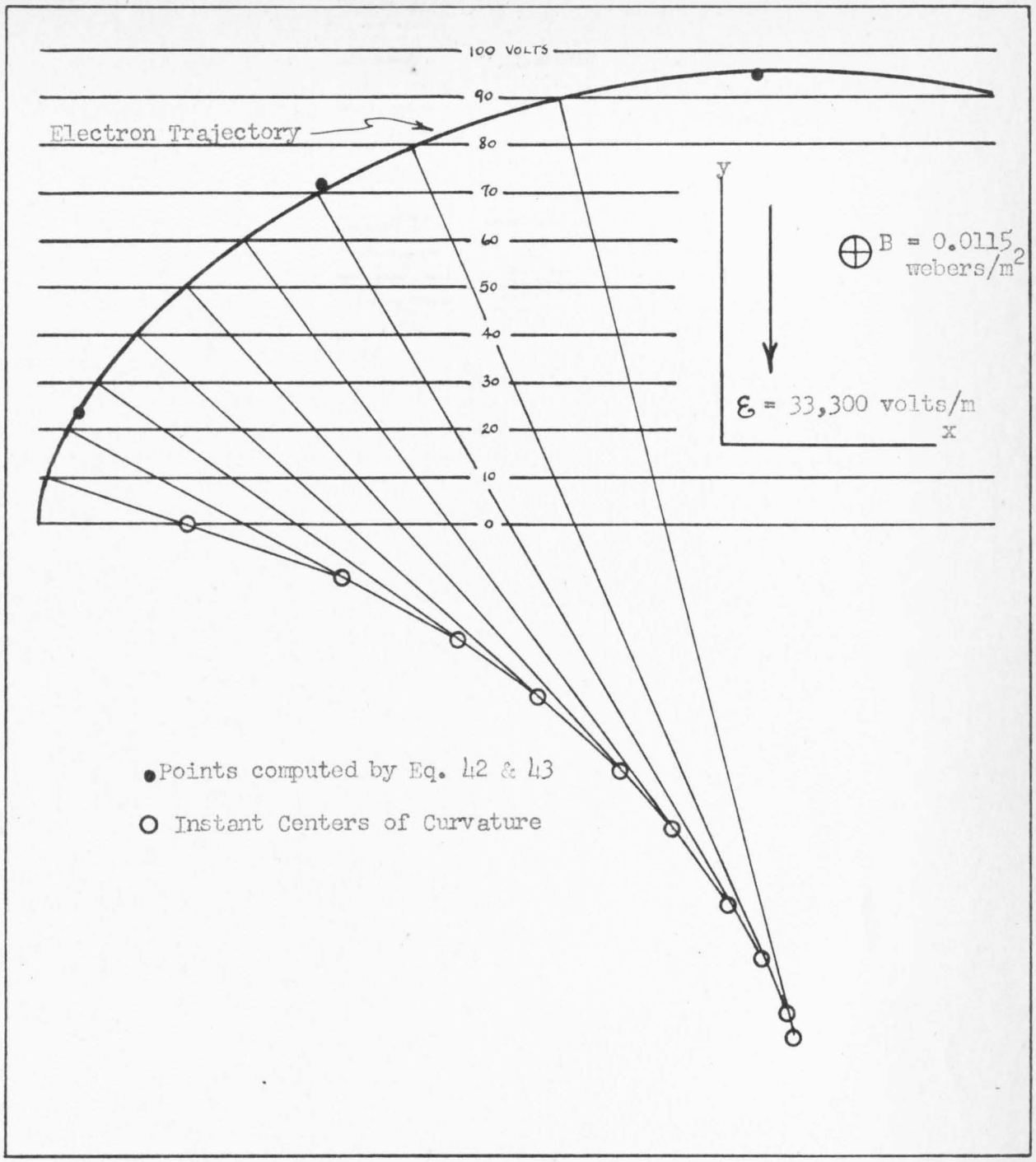

Figure 27.

GRAPHICAL METHOD OF DETERMINING ELECTRON PATH

For the condition of zero initial velocity, the maximum y-value of a trajectory may be determined from Equation 43 which gives

$$y_{max} = 2a/\omega^2 = 2(m/e)(\mathcal{E}/B^2)$$

$$= -11.38 \times 10^{-12} \ \mathcal{E}/B^2 \text{ meters.} \qquad (81)$$

Figure 28 shows this relation.

If the initial velocity of an electron is not zero or if the y-distance traveled beyond a certain point after the electron gains a velocity v and is moving in the direction α is desired, the solution of Equation 37 is not so simple. For such conditions, the electron reaches the maximum distance when

$$v_y = v_{oy} \cos \omega t + (a/\omega - v_{ox}) \sin \omega t = 0$$

or when

$$\tan \omega t = \frac{v_{oy}}{v_{ox} - (a/\omega)} = \frac{v_o \sin \alpha}{v_o \cos \alpha - (a/\omega)}$$

$$y_{max} = (1/\omega) \left[(a/\omega) - v_o^2 \cos \alpha + \sqrt{v_o^2 - (2a/\omega) v_o \cos \alpha + (a/\omega)^2} \right] \qquad (82)$$

A graphical solution of this equation will be given. Utilizing the fact that Equations 37 and 41 are the parametric equations of trochoidal motion, the rolling surfaces may be constructed providing that v and α are known. From Equation 40, it is seen that there is a constant x-component of velocity equal to (a/ω) which represents the translational velocity (v_T) of the circles that generate the trochoidal motion. The radius of the rolling circle must therefore be $(v_T/\omega) = (a/\omega^2) = (m/e)(\mathcal{E}/B^2)$ (see Figure 29). The radius of the tracing circle is v_R/ω, and

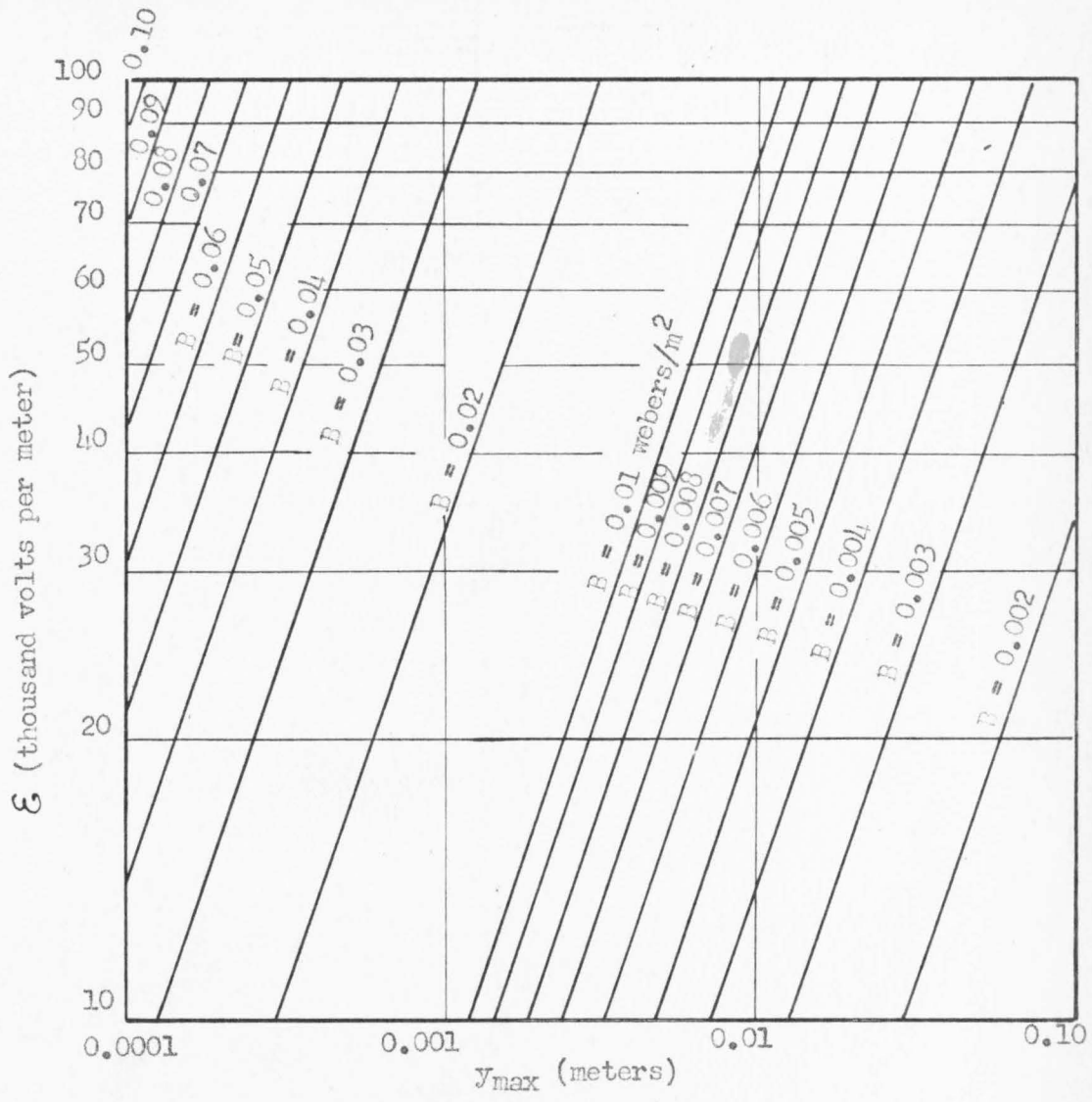

Figure 28.

MAXIMUM DISPLACEMENT OF ELECTRON IN y-DIRECTION

WHEN INITIAL VELOCITY IS ZERO

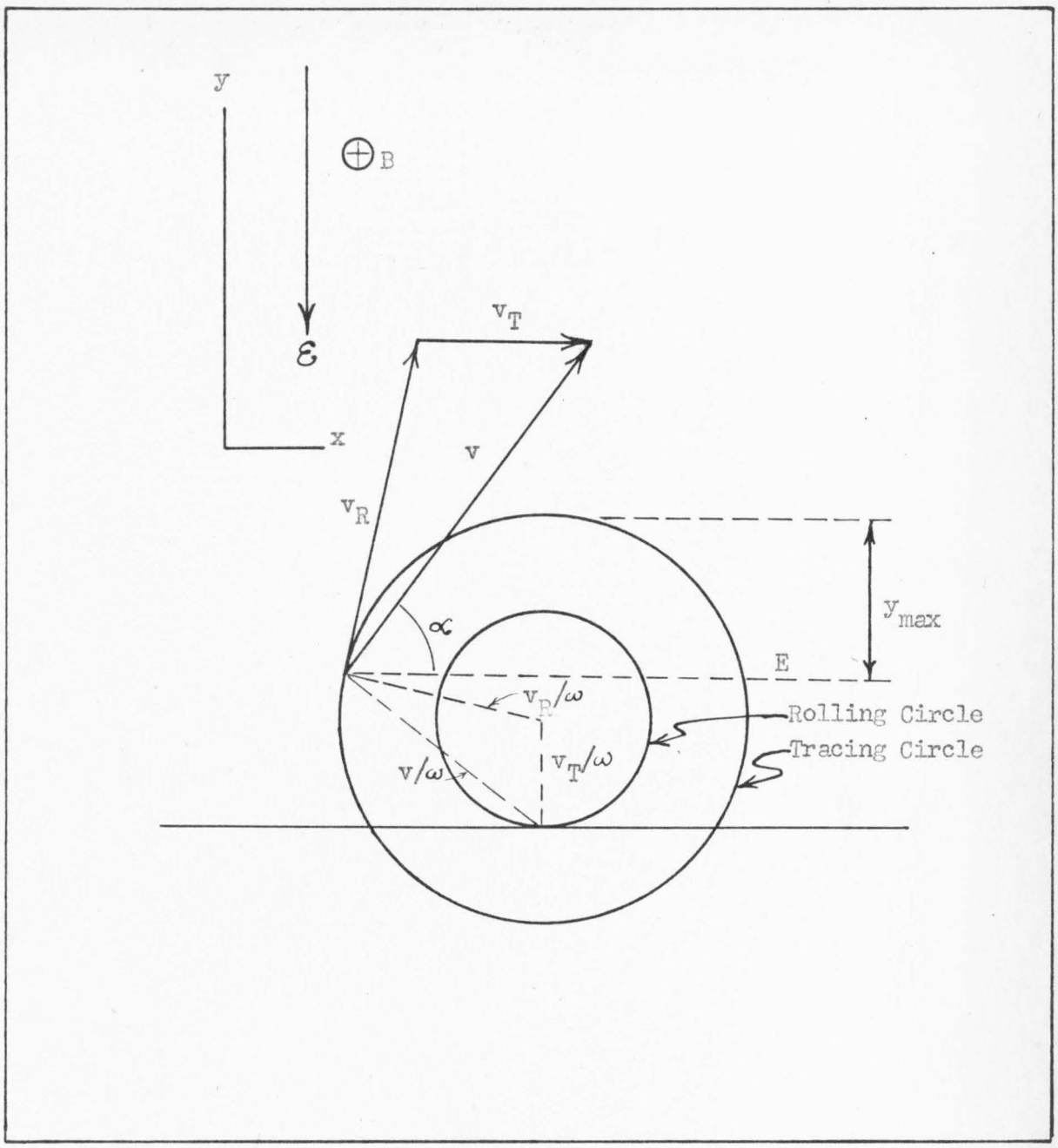

Figure 29.

ROLLING SURFACES WHICH GENERATE TROCHOIDAL MOTION

$v_R = v \longrightarrow v_T$. When $v_R > v_T$, the path of the electron is a prolate cycloid. When $v_R < v_T$, the path is a curtate cycloid and when $v_R = v_T$, the path is an ordinary cycloid.

In determining y_{max} graphically, all velocity vectors are divided by ω in order that they will have the same scale as the radii of the rolling and tracing circles. (Figure 30). The vector representing the velocity is drawn $v/\omega = (0.0337/B)\sqrt{E}$ meters long in the direction α. The translational velocity vector is drawn $v_T/\omega = a/\omega^2 = 0.0569\ \mathcal{E}/B^2$ meters long. The rotational velocity vector is now determined. A line drawn from the origin of this vector perpendicular to the vector and equal to it in length locates the center of the circles and radius of the generating circle. By swinging the radius around in the y-direction, the value of y_{max} is determined.

Potential Distribution in Electron Tube

Analytically, the potential distribution in space due to a system of electrodes is specified by Laplace's equation[20]

$$(\partial^2 E/\partial x^2) + (\partial^2 E/\partial y^2) + (\partial^2 E/\partial z^2) = 0 \qquad (83)$$

In order to determine the potential distribution in the type 45 electron tube, it will be assumed that the wires of the filament extend in the x-direction and the grid wires in the z-direction. It will be assumed, also, that all points in the plane of the filament (x-z plane) has the potential E= 0. Therefore $\mathcal{E}_z = -(\partial E/\partial z) = 0$, and the above equation may be expressed as

$$(\partial^2 E/\partial x^2) + (\partial^2 E/\partial y^2) = 0 \qquad (84)$$

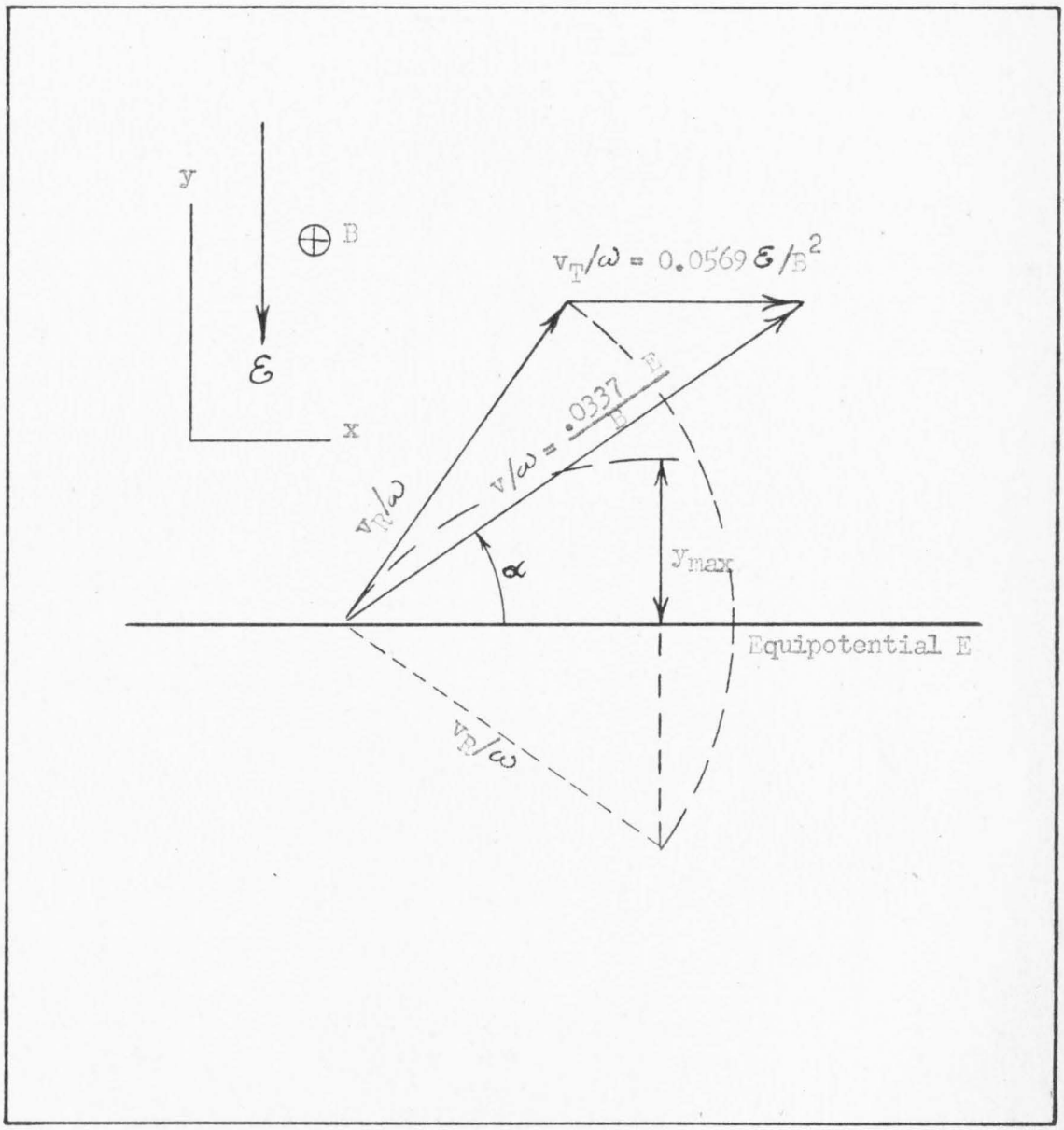

Figure 30.

GRAPHICAL DETERMINATION OF MAXIMUM DISPLACEMENT

OF ELECTRON IN y-DIRECTION

This may be expressed as a difference equation of which the differential equation is the limiting form.

Figure 31 represents a two dimensional configuration enclosing the region for which E is defined. A rectangular coordinate net having a mesh width Δ is drawn over the area.[21] At points 0, 1, 2, 3, and 4 the potential, E, will have the values denoted by E_0, E_1, E_2, E_3, and E_4 respectively. It is evident that at point 0

$$\frac{\partial^2 E}{\partial x^2} = \frac{1}{\Delta}\left[\frac{E_1 - E_0}{\Delta} - \frac{E_0 - E_3}{\Delta}\right]$$

and

$$\frac{\partial^2 E}{\partial y^2} = \frac{1}{\Delta}\left[\frac{E_2 - E_0}{\Delta} - \frac{E_0 - E_4}{\Delta}\right]$$

Substituting in Laplace's Equation

$$(\partial^2 E/\partial x^2) + (\partial^2 E/\partial y^2) = (1/\Delta^2)\left[E_1 + E_2 + E_3 + E_4 - 4E_0\right] = 0 \quad (85)$$

or

$$E_0 = (1/4)\left[E_1 + E_2 + E_3 + E_4\right] \quad (86)$$

which states that the potential at any point, 0, is the average of the potential at the four surrounding points. The finite difference equation is written

$$R_0 = E_1 + E_2 + E_3 + E_4 - 4E_0. \quad (87)$$

$R_0 = 0$ when E_1, E_2, . . . E_0 are the correct values. Conversely, if the values are not correct, $R_0 \neq 0$. The quantity, R_0, is called the residual at point 0. The numerical solution of the equation consists of adjustments in the initial values (assumed values) such as will make the residual vanish.

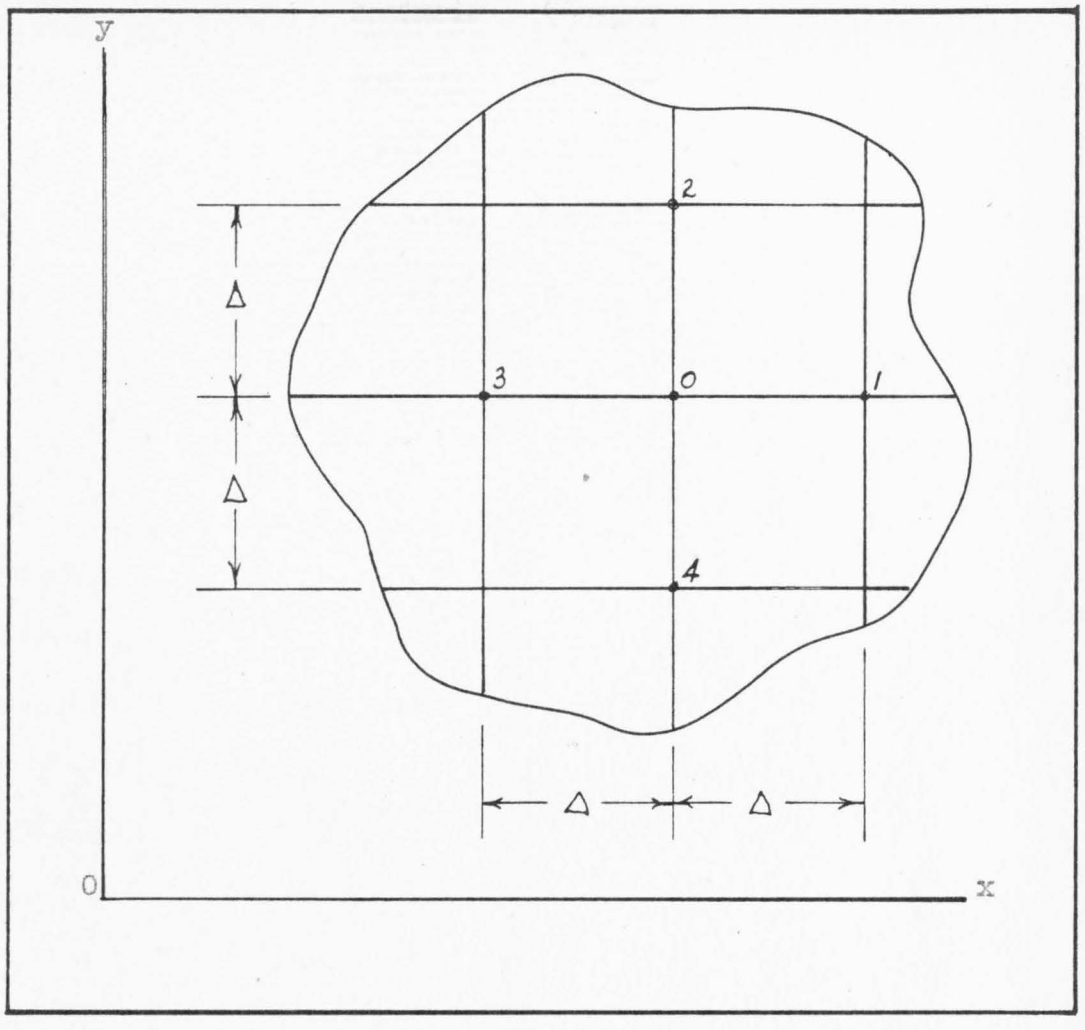

Figure 31

GRID FOR DETERMINING POTENTIAL DISTRIBUTION

BY RELAXATION METHOD

In this manner, the potential distribution in the type 45 tube for various grid voltages and a plate potential of 100 volts as shown in Figures 32 to 41 was obtained.

Theoretical Tube Characteristics

The first step in determining the characteristics of the type 45 tube in the presence of a magnetic field is to plot the paths of the electrons leaving the filament under various conditions. With a plate potential of 100 volts and the grid at its natural potential of +33 volts, the field, $\mathcal{E}_y = -(\partial E/\partial y)$, is constant and the electron path has been determined by both the analytical and the graphical methods (Figure 27). In this case, none of the electrons reached the plate when a magnetic field of 1.15×10^{-2} webers per square meter was applied. No attempt was made to determine the number of electrons intercepted by the grid.

It will be noticed that for all values of grid potential the electric field is almost uniform in that region of the tube having a potential of about 50 volts or greater. As the process of determining the electron paths by the graphical method is rather long and also subject to some cumulated error, and as it is only necessary to know whether or not electrons reach the annode, the graphical method of determining y_{max} will be used for the region beyond the 50 volt potential line. The electron trajectories beyond this point were not plotted accurately in the following instances but only the approximate path is indicated.

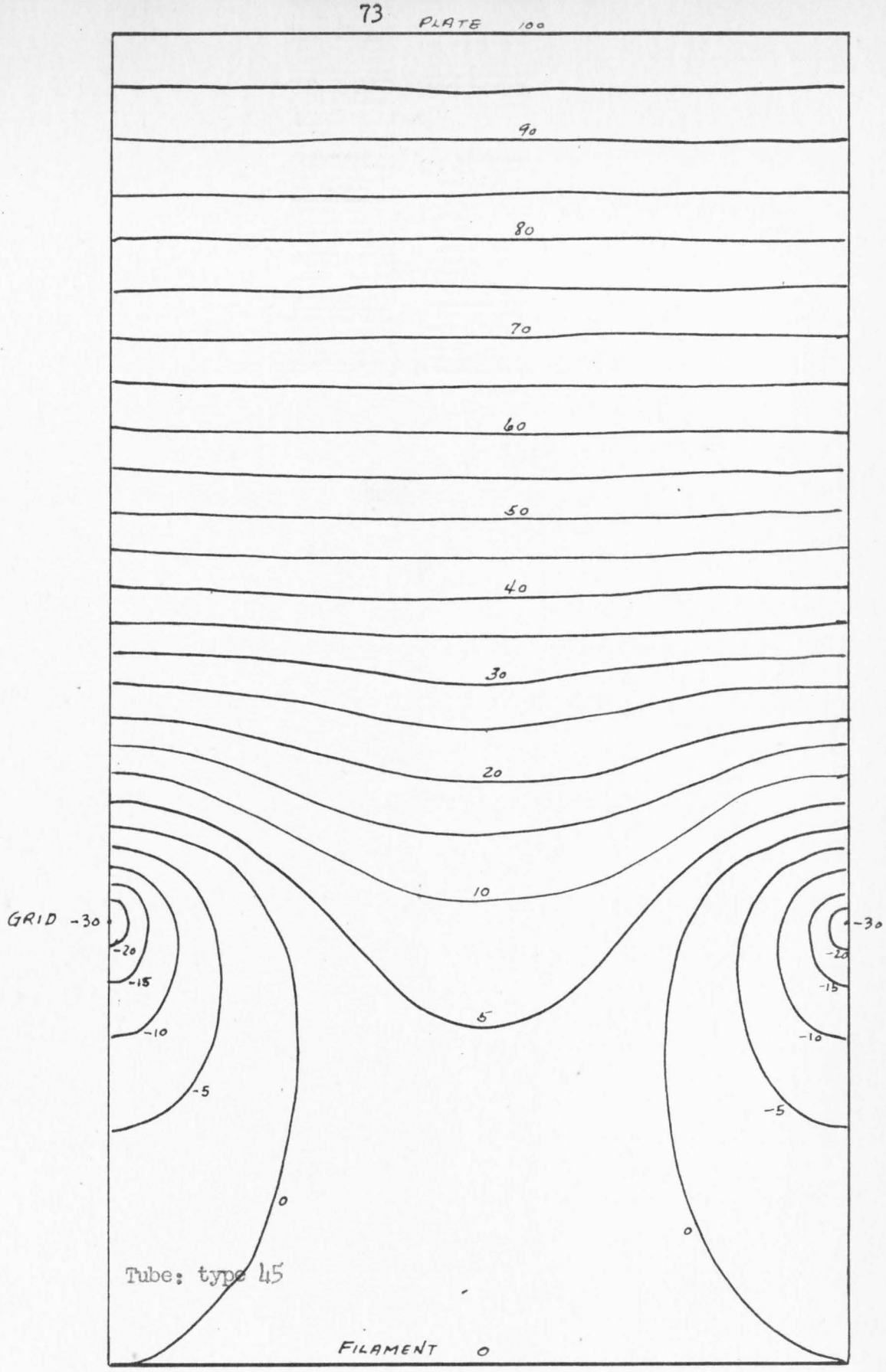

Figure 32.

POTENTIAL DISTRIBUTION IN ELECTRON TUBE
WITH GRID POTENTIAL OF -30 VOLTS

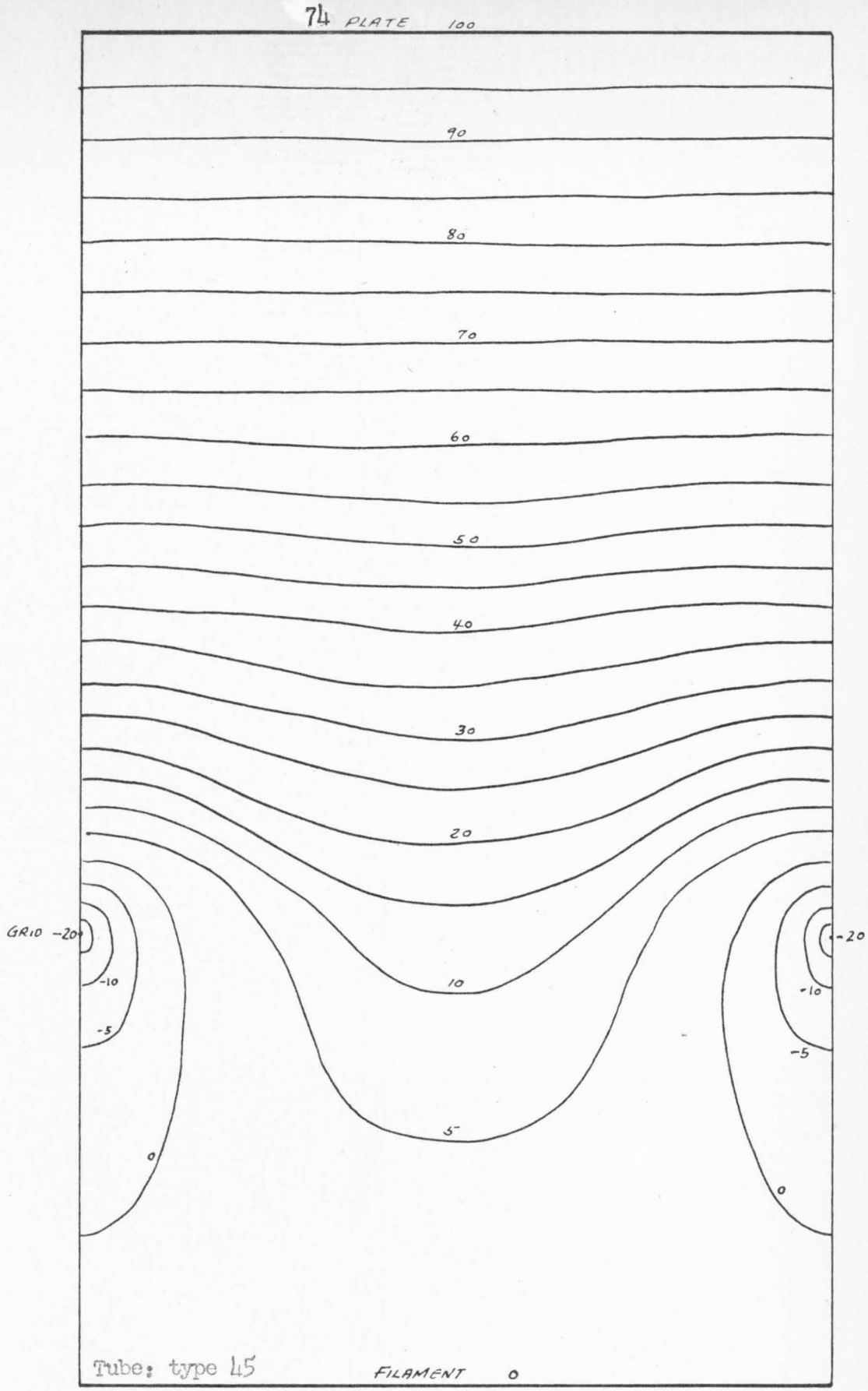

Figure 33.

POTENTIAL DISTRIBUTION IN ELECTRON TUBE
WITH GRID POTENTIAL OF -20 VOLTS

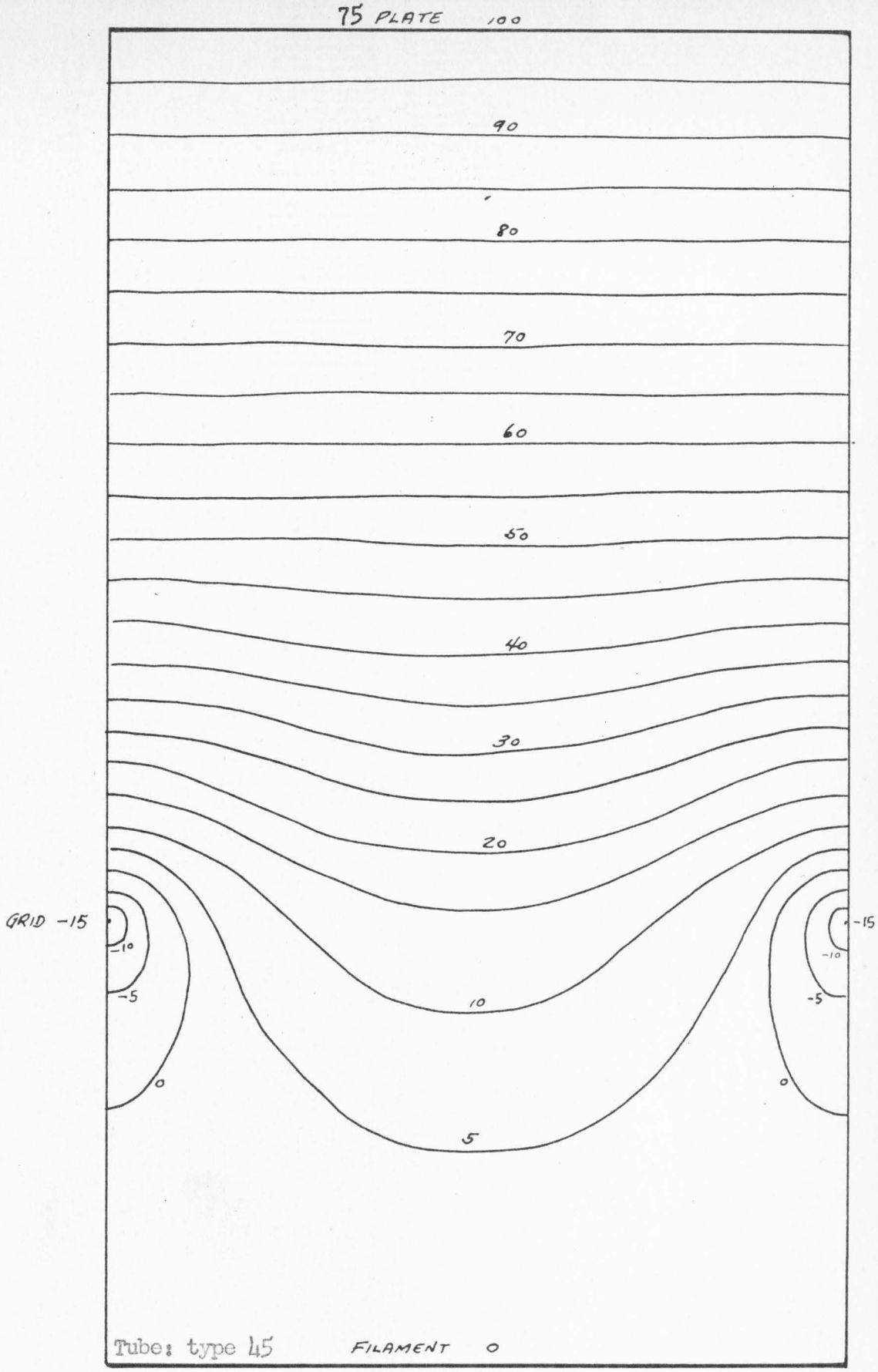

Figure 34.

POTENTIAL DISTRIBUTION IN ELECTRON TUBE
WITH GRID POTENTIAL OF -15 VOLTS

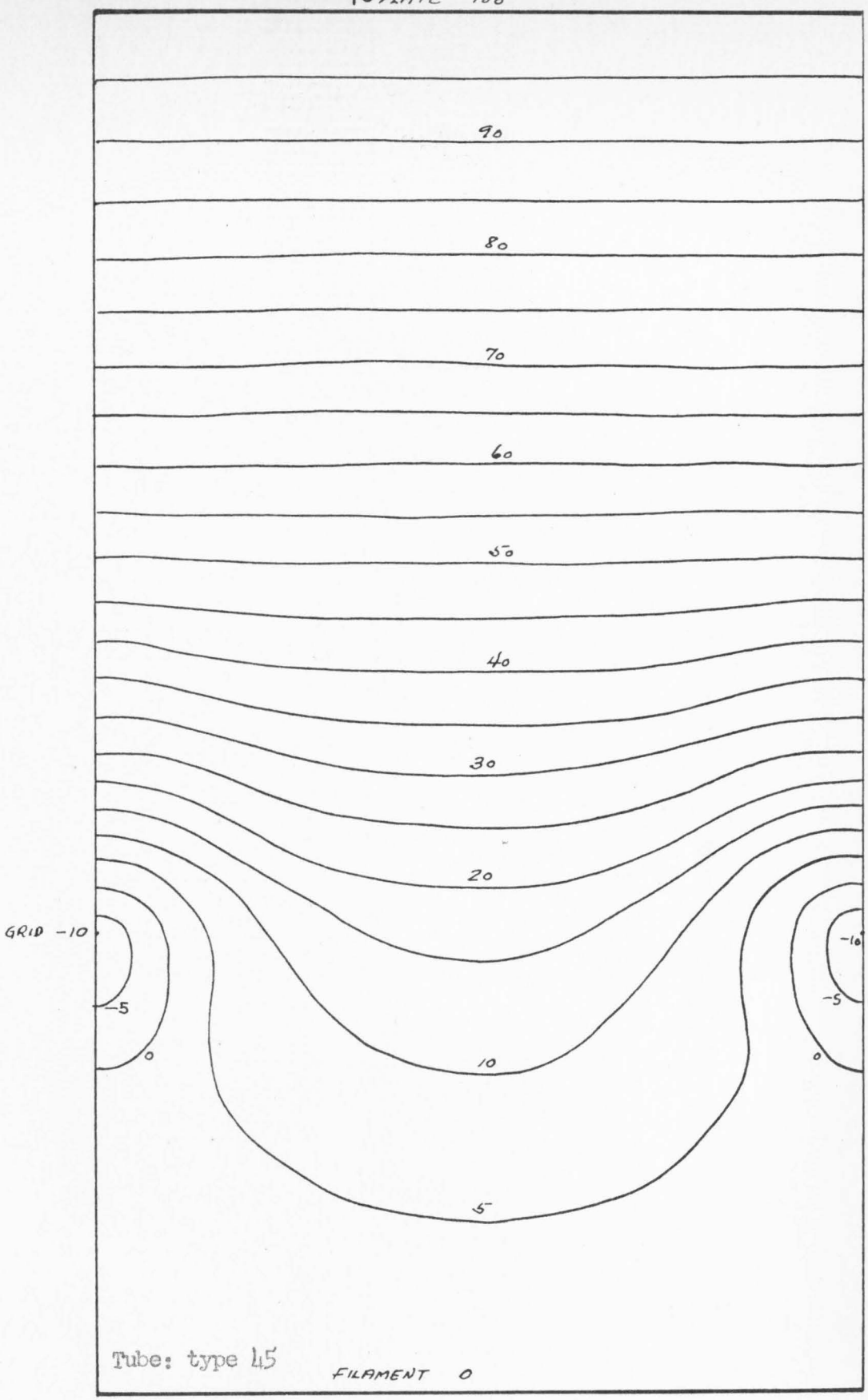

Figure 35.

POTENTIAL DISTRIBUTION IN ELECTRON TUBE
WITH GRID POTENTIAL OF -10 VOLTS

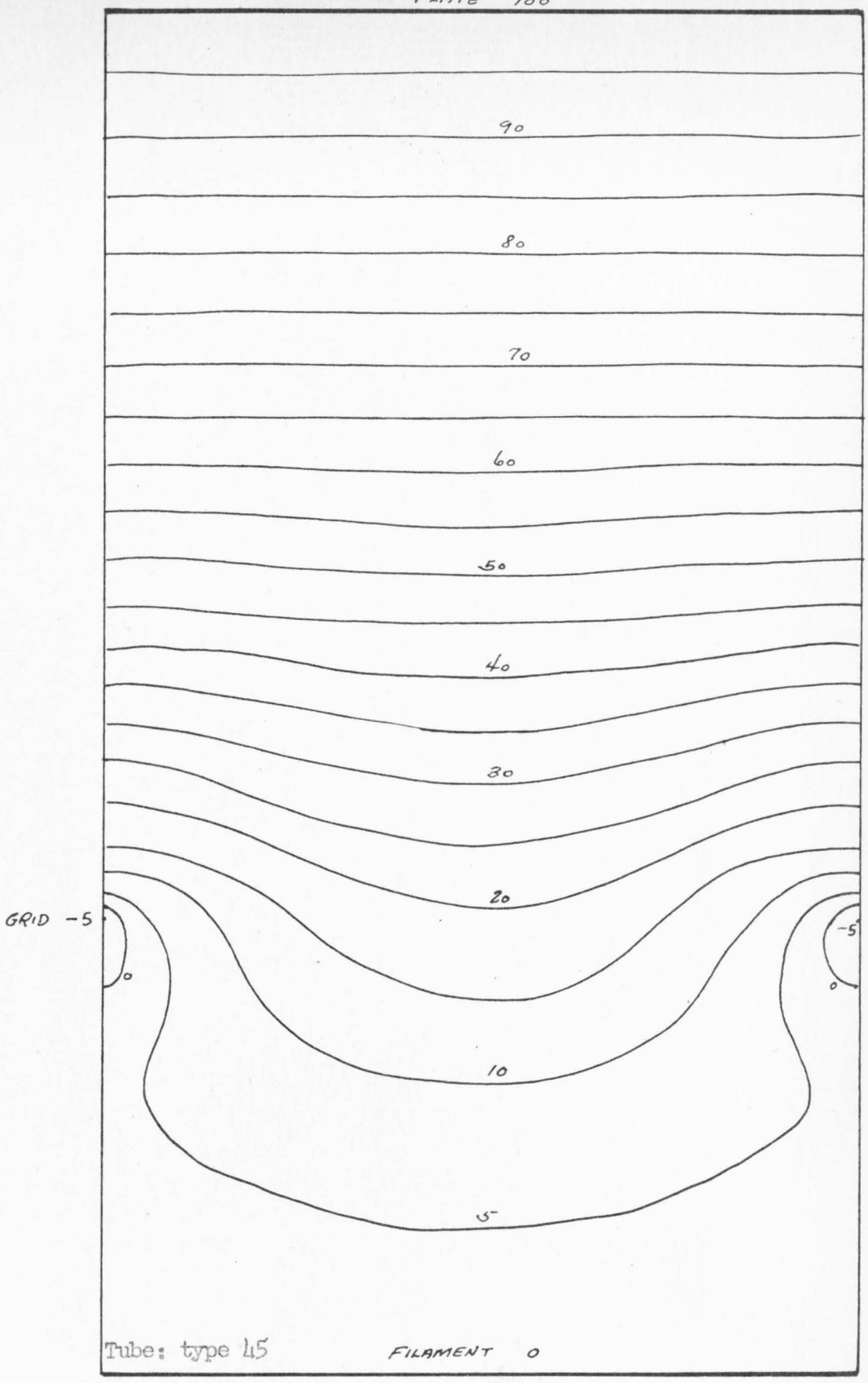

Figure 36.

POTENTIAL DISTRIBUTION IN ELECTRON TUBE
WITH GRID POTENTIAL OF -5 VOLTS

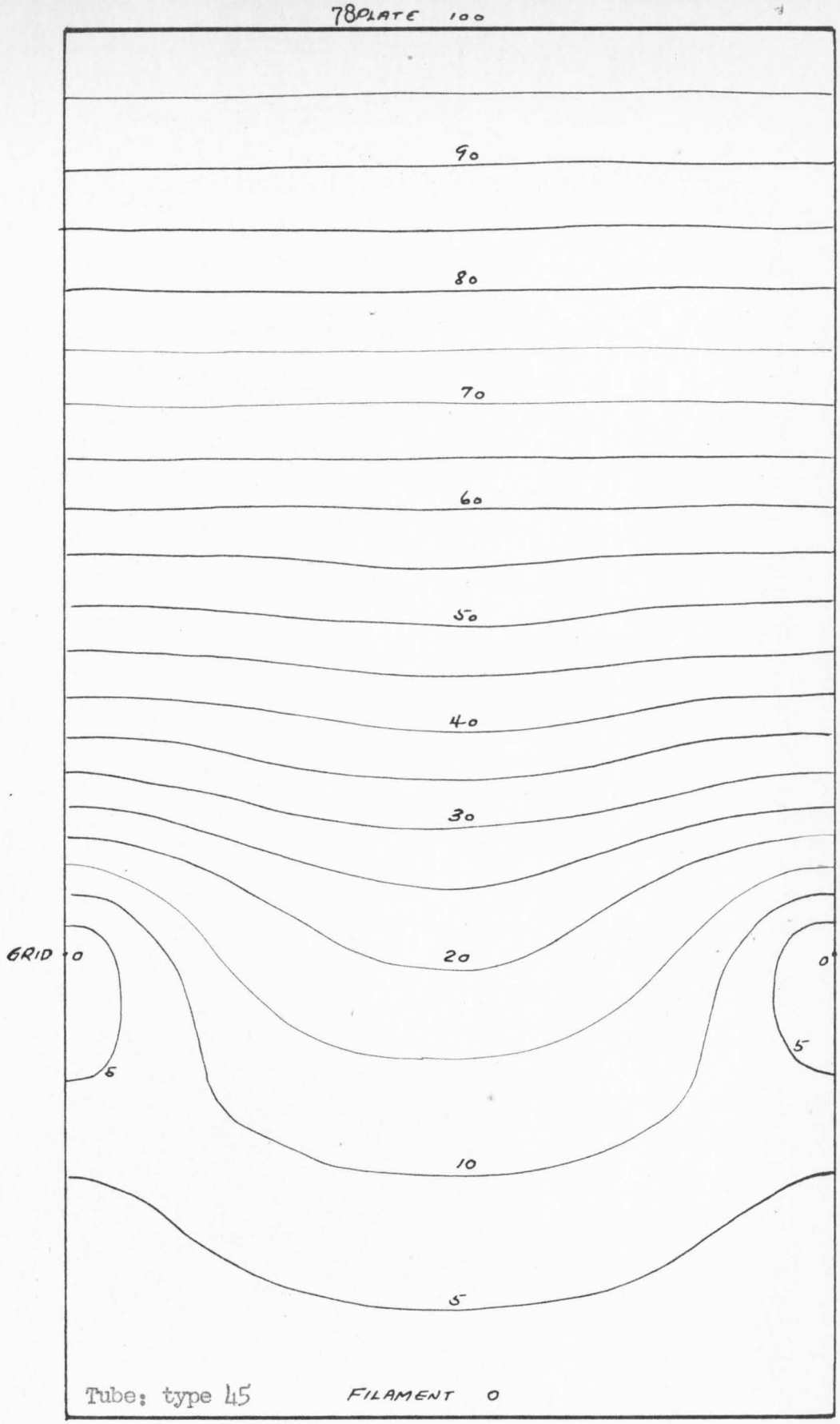

Figure 37.

POTENTIAL DISTRIBUTION IN ELECTRON TUBE
WITH GRID POTENTIAL OF 0 VOLTS

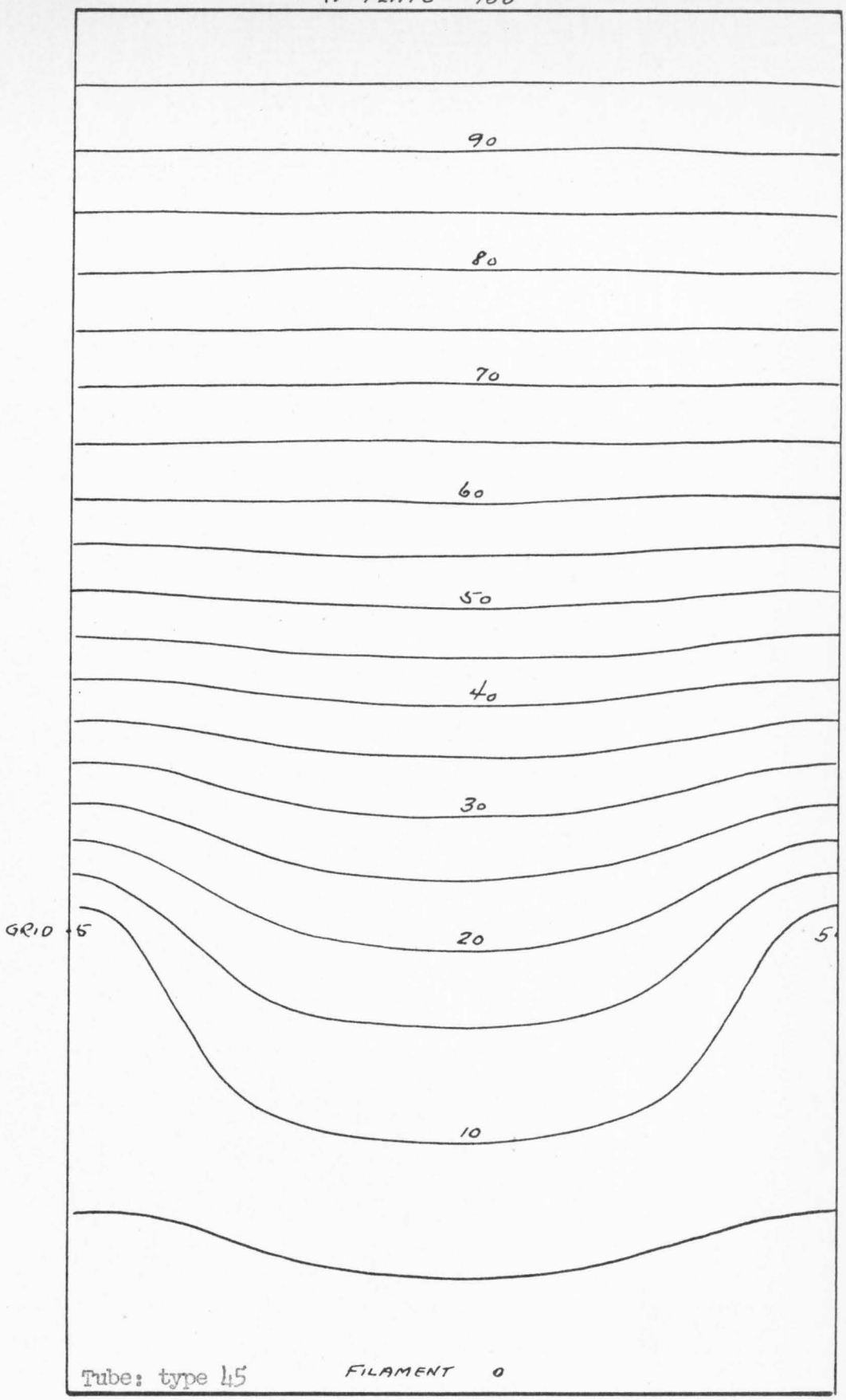

Figure 38.
POTENTIAL DISTRIBUTION IN ELECTRON TUBE
WITH GRID POTENTIAL OF +5 VOLTS

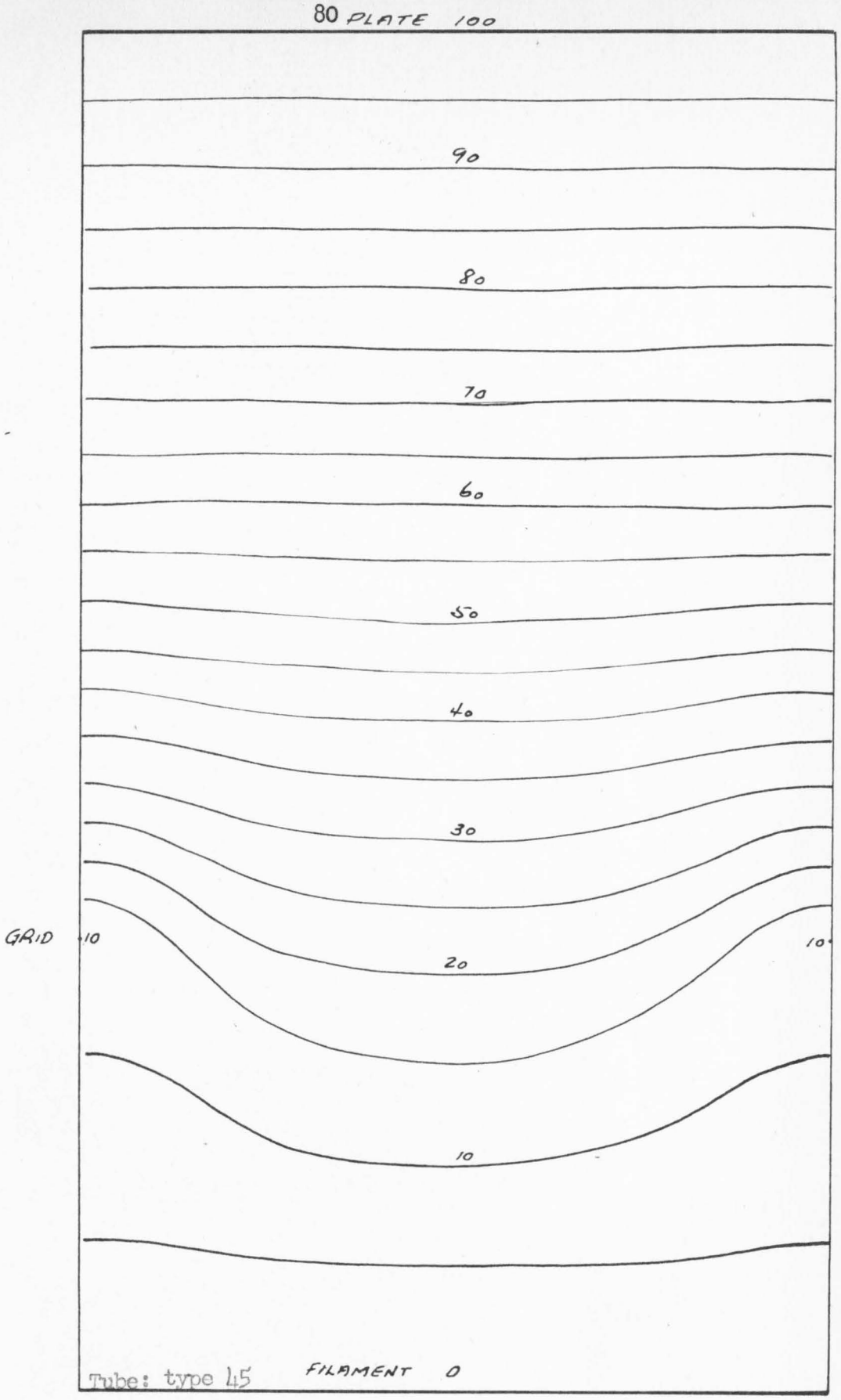

Figure 39.

POTENTIAL DISTRIBUTION IN ELECTRON TUBE
WITH GRID POTENTIAL OF + 10 VOLTS

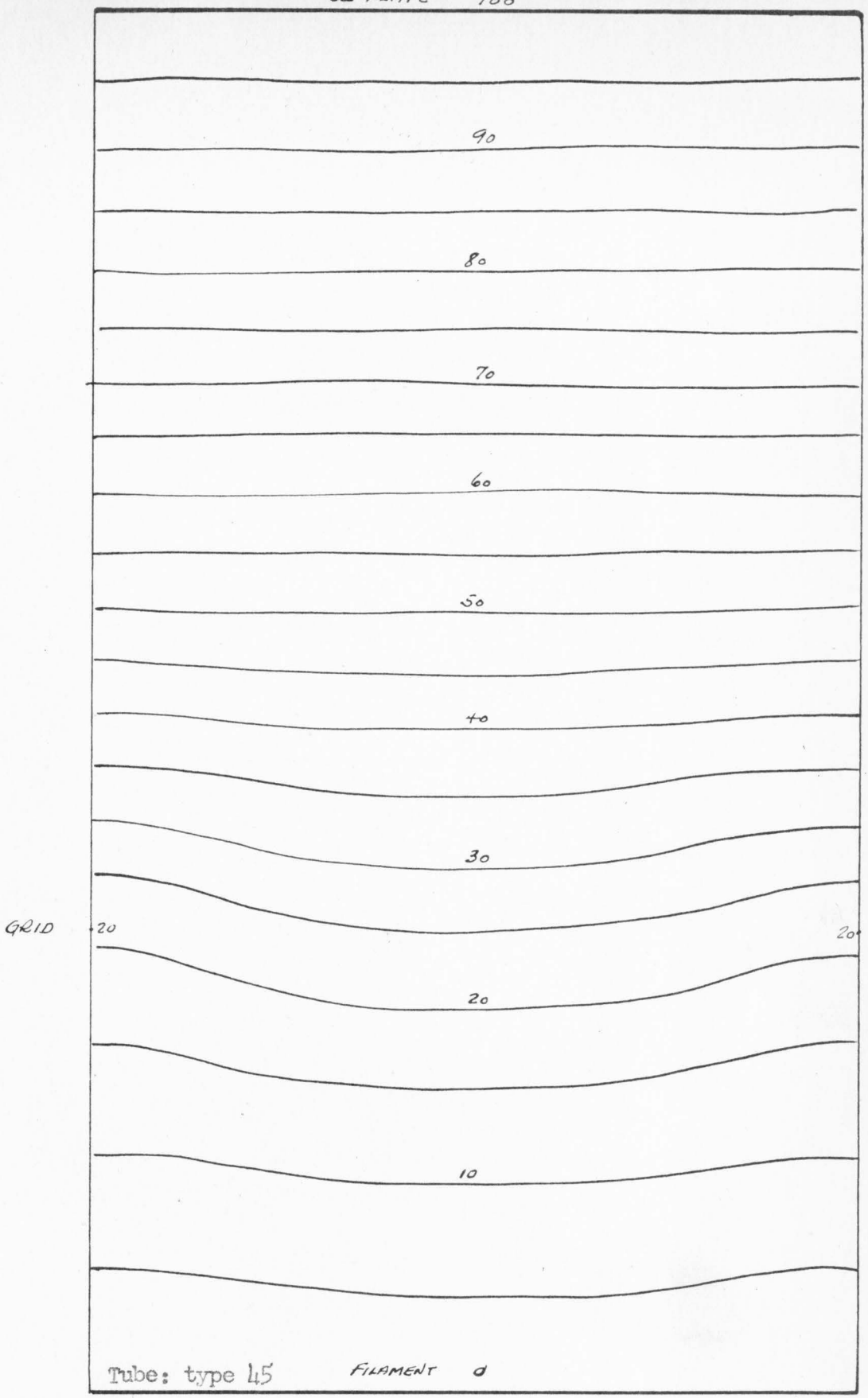

Figure 40

POTENTIAL DISTRIBUTION IN ELECTRON TUBE
WITH GRID POTENTIAL OF + 20 VOLTS

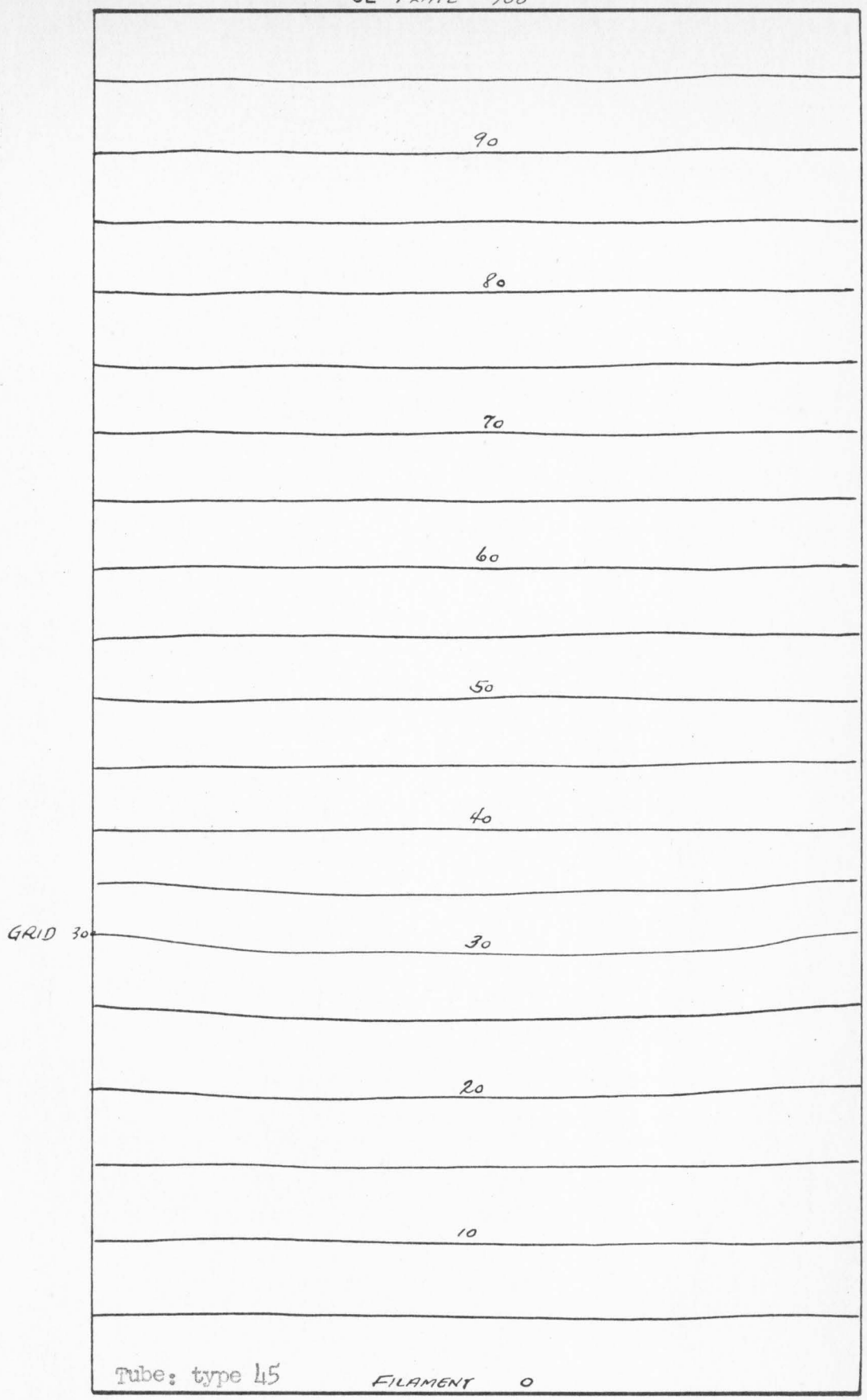

Figure 41.

POTENTIAL DISTRIBUTION IN ELECTRON TUBE
WITH GRID POTENTIAL OF +30 VOLTS

Next, the electron paths in a tube having a grid potential of +10 volts were determined. The electrons did not follow cycloidal paths, but still none of them reached the plate of the tubes although some came very close to it. When the potential of the grid was reduced still more, some of the electrons began to reach the plate. Figure 42 shows the electron paths for a grid of 0-volts. In this case, approximately 60% of the electrons which left the filament reached the plate. It can be seen that the gradient of potential is greatest just beyond the grid and if an electron reaches that point in the tube, there is sufficient force due to electric field to change the direction considerably. Of course, it is impossible to say definitely whether or not certain electrons will reach the plate. For example, an electron that leaves point A on the filament goes so near the grid that it might be intercepted by the grid. Likewise, an electron leaving point G might be deflected past the grid and reach the plate.

Figure 43 shows the electron paths in the tube when the grid potential is -10 volts. Here also, about 60% of the electrons leaving the filament reached the plate. If the assumption of zero initial velocities were strictly true, it would be impossible for any electron to enter the shaded area since all points in this area have a negative potential. This would mean that all electrons reaching this area would come to rest and would then start anew.

At a grid potential of -5 volts approximately 75% of the electrons reached the plate. When the grid was -20 volts, none of the electrons traversed the total distance from filament to plate. Figure 44

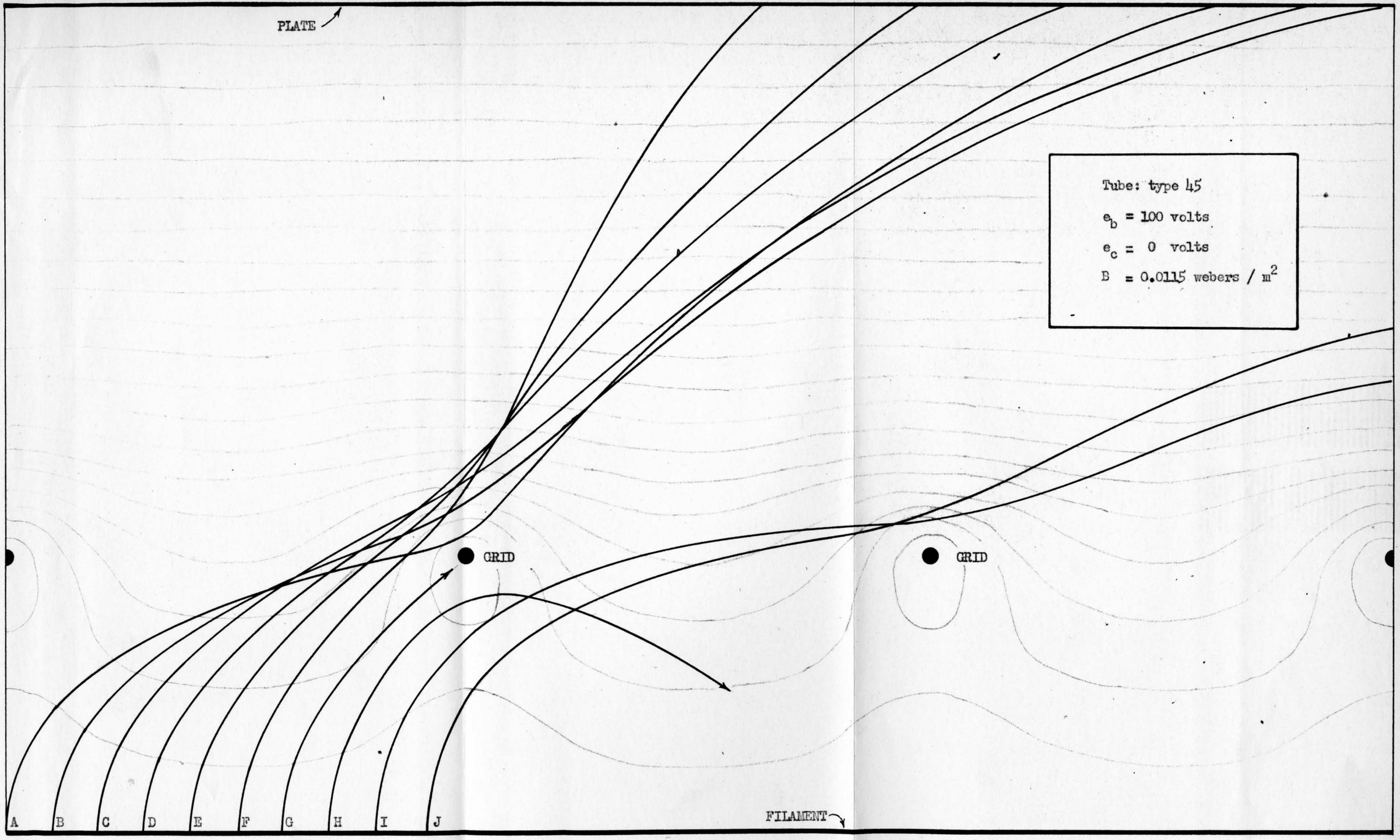

Figure 42

ELECTRON TRAJECTORIES WITH GRID POTENTIAL ZERO

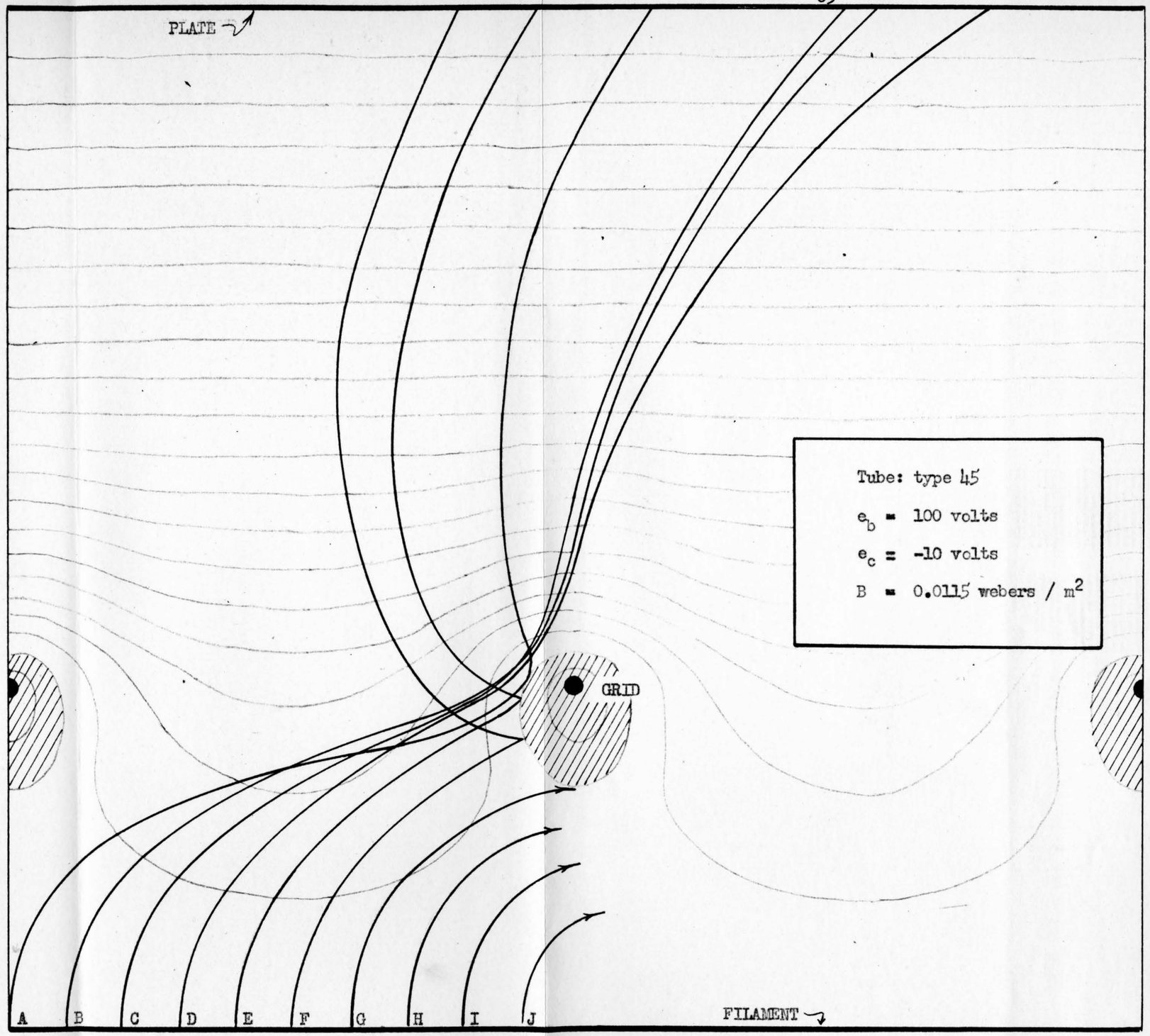

Figure 43

ELECTRON TRAJECTORIES WITH GRID POTENTIAL OF -10 VOLTS

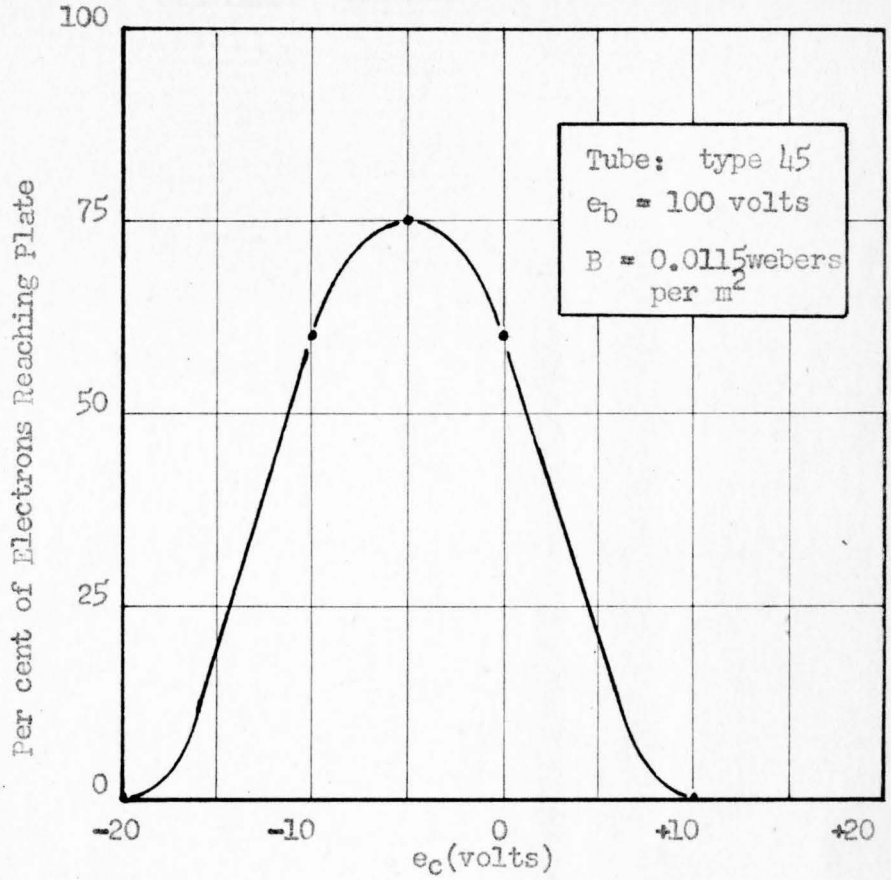

Figure 44

PERCENTAGE OF ELECTRONS REACHING PLATE OF TUBE

shows the percentage of the electrons leaving the filament which were found to reach the plate at various grid potentials.

It has been assumed that the plates of the tube were infinite planes and that the potential gradient in the z-direction is zero. This is a valid assumption as long as the electrons are free to go to the plates. Referring, however, to Figure 4, it will be seen that the plate of the type 45 tube completely surrounds the other elements of the tube. There is, therefore, a slight potential gradient from the outside wires of the filament to the ends of the plate. It is then reasonable to believe that approximately half of those electrons which miss the plate of the tube will be accelerated toward the ends of the plate and also contribute to the plate current. The fact that some of the electrons reached the ends of the plate could actually be seen in the tube. The filament voltage was decreased until it gave off very little light and, in a dark room, the plate of the tube could be seen glowing with a blue color where electrons were striking it. When a magnetic field was applied perpendicular to the plates of the tube, the image of the filament could be seen. As the magnetic field was rotated, the image would move along the plate and when the magnetic field was parallel to the plates of the tube, the ends of the plate would glow. It was impossible to photograph this in the type 45 tube, but when a type 101-A tube having plates open at the end was used, a sufficient number of electrons went to the wires which supported the plates that they glowed brightly and may be seen in Figure 17.

Theoretical characteristic curves may now be determined for the type 45 tube having a plate potential of 100 volts and subjected to a magnetic field parallel to the plates of the tube. In Figure 45, curve (a) shows the plate current-grid potential relation when no magnetic field is present. Applying the percentages shown in Figure 44 for a magnetic field of 1.15×10^{-2} webers per square meter, curve (b) is obtained, which would be the theoretical transfer characteristic curve if none of the electrons found their way to the ends of the plates. It has been decided, however, that approximately 50% of those not reaching the plate proper will go to the ends. The total plate current may then be determined by plotting the curve (c) whose ordinates are equal to one-half the sum of the corresponding ordinates of curves (a) and (b). The same procedure was followed in Figure 46 for determining the theoretical characteristic curve for the tube when operated at a reduced filament voltage.

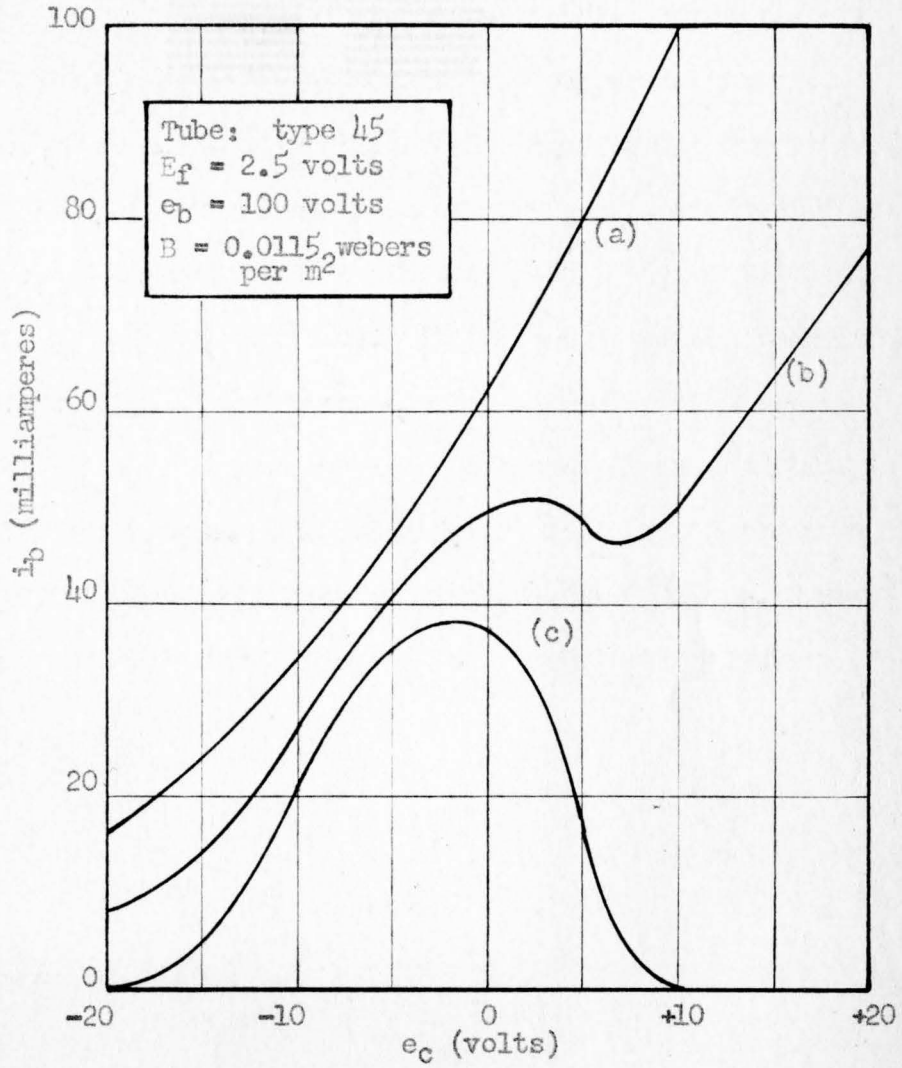

Figure 45.

THEORETICAL CHARACTERISTIC CURVE WITH NORMAL FILAMENT POTENTIAL

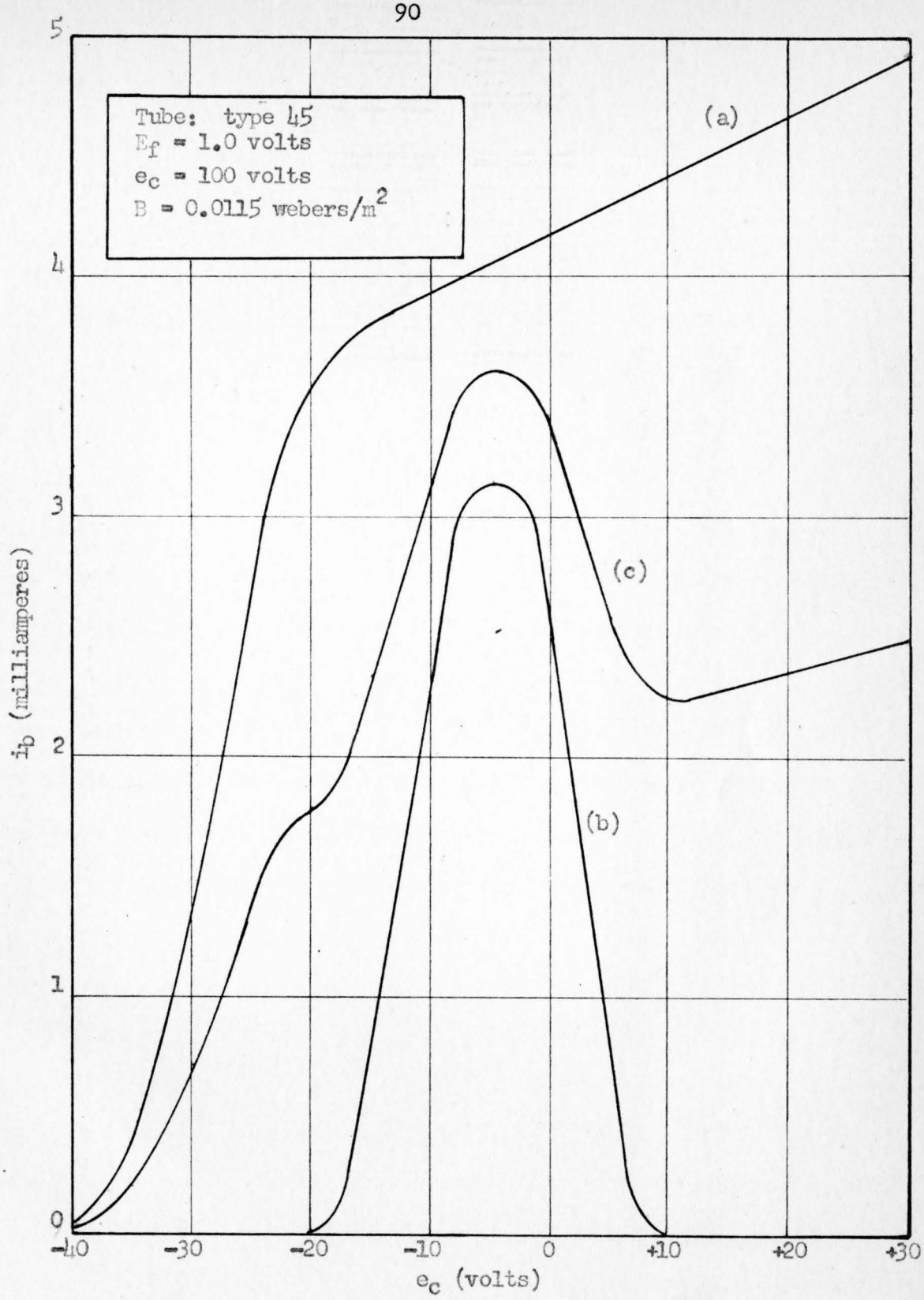

Figure 46.

THEORETICAL CHARACTERISTIC CURVE WITH REDUCED FILAMENT POTENTIAL

V

CONCLUSIONS

The general shape of the theoretical characteristic curves obtained by both the mechanical analogy (Figure 24) and the graphical analysis (Figure 45) agrees with that of the actual characteristic curves of the tube in the presence of a magnetic field (Figures 11, 12, and 13). A qualitative analysis of the gyroscope analogy was not attempted, and there was very little agreement between the values of the theoretical curves and the actual characteristic curves when the tube was operating at normal filament temperature. If a magnetic field of 1.15×10^{-2} webers per square meter had been applied to the tube in actual operation, there would have been very little change in its characteristics and there would have been no region of negative slope. If a much stronger magnetic field (say 5.0×10^{-2} webers per square meter) had been considered in the graphical analysis, the results would have been zero plate current for all values of grid potential although there was actually a definite region of negative transconductance in the actual operation of the tube in the presence of such a magnetic field. These results are not surprising in view of the original assumptions, principally that of negligible space charge. It was pointed out, however, that space charge would probably affect the qualitative results and cause a wide discrepancy between the actual and theoretical values.

If this is the principal reason for a lack of agreement between the actual and theoretical values, it would be expected that there might be some agreement when the tube is operated at a reduced

filament temperature, thereby reducing space charge in the tube. Figure 46 shows the theoretical characteristic curve at this reduced filament temperature.

Figure 47 shows a comparison of the actual and theoretical characteristic curves of the type 45 tube when operated at a plate potential of 100 volts and at a filament potential of 1.0 volt instead of the normal 2.5 volts. The similarity of the shapes of these curves may be seen. The differences in the values of the theoretical and actual plate current may be largely accounted for as follows:

1. It had been assumed that the plates of the tube were infinite planes, but in reality they are open at the top and bottom permitting electrons to escape, which, in the graphical analysis, were assumed to reach the plate either by traversing the region between filament and the plate, or by being attracted to the ends of the plate. From the dimension of the plate of the tube (Figure 4), it may be seen that if the electrons were traveling in cycloidal paths and just reaching the plate of the tube, that between 15% and 20% will not reach the plate but will go out either the top or bottom of the plates without contributing to the plate current.
2. Some of the electrons will be intercepted by the grid wires of the tube, thereby causing the plate current to be less than that indicated by the theoretical values.

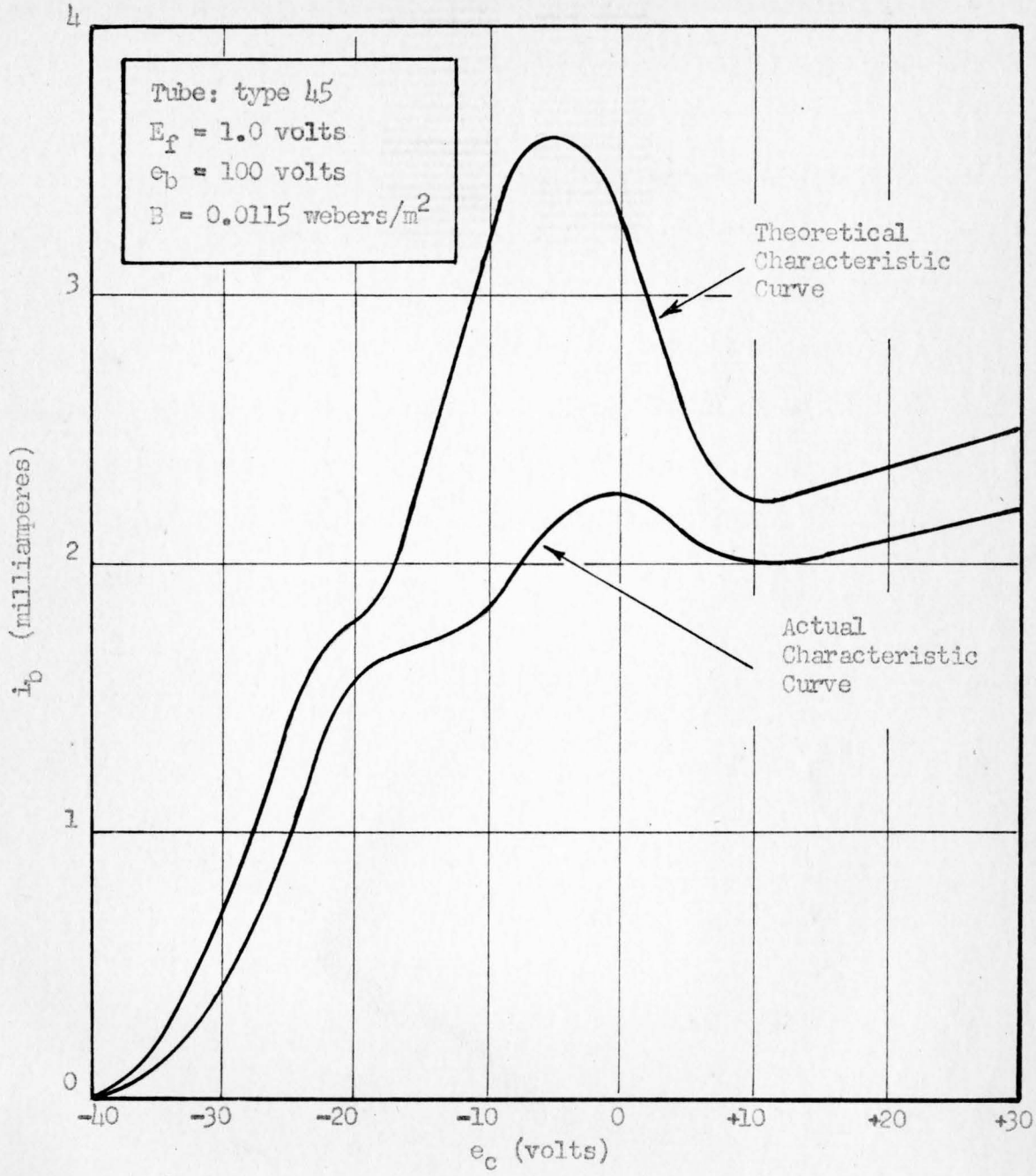

Figure 47.

COMPARISON OF ACTUAL AND THEORETICAL CHARACTERISTIC CURVES

3. The initial velocities of the electrons are not zero, although the assumption was made that they were of negligible value.

4. Space charge is still present to some extent even at a reduced filament temperature.

In view of the assumptions which have been made, and the close agreement between the theoretical and actual values obtained when the tube was operated as nearly as possible in agreement with these assumptions, it is believed that the explanation of the negative transconductance effect in crossed electrostatic and magnetic fields is a correct explanation of the phenomenon.

VI

ACKNOWLEDGMENTS

The author is indebted to Professor D. H. Pletta for his guidance and supervision; to William C. Meecham, as codiscoverer of the negative transconductance effect; to the Atomic Energy Commission for permission to perform this research; to the Tennessee Academy of Science and the American Association for the Advancement of Science for their financial aid; and to his graduate committee, Professors Ralph R. Wright, E. Q. Smith, Jr., and Daniel Frederick for their helpful suggestions throughout this investigation.

VII

BIBLIOGRAPHY

1. Spangenberg, Karl R. VACUUM TUBES. New York: McGraw-Hill Book Company, Inc., 1948, p. 723.

2. Kinslow, Ray, "Vacuum Tube Flux Meter," Patent, 2,509,394. Washington, D. C.: United States Patent Office, May 30, 1950.

3. Kinslow, Ray and Meecham, William C. "A Negative Transconductance Vacuum Tube," (abstract only) PHYSICAL REVIEW, July 15, 1951, Vol. 83, No. 2, p. 487.

4. Arguimbau, Lawrence Baker. VACUUM TUBE CIRCUITS. New York: John Wiley & Sons, Inc., 1948, p. 303.

5. Hill, W. R., Jr. "Analysis of Voltage Regulator Operation," PROCEEDINGS OF IRE, 38-45, January, 1945, p. 33.

6. Müller, Ralph H., Garman, R. L. and Droz, M. E. EXPERIMENTAL ELECTRONICS. New York: Prentice-Hall, Inc., 1945, p. 39.

7. RCA RECEIVING TUBE MANUAL. Harrison, New Jersey: R. C. A. Manufacturing Co., Inc., 1947, p. 179.

8. Millman, Jacob and Seely, Samuel. ELECTRONICS. New York: McGraw-Hill Book Company, Inc., 1941, p. 155.

9. Westinghouse Electric Corporation. INDUSTRIAL ELECTRONICS REFERENCE BOOK. New York: John Wiley & Sons, Inc., 1948, p. 13.

10. Spangenberg, Karl R. VACUUM TUBES. New York: McGraw-Hill Book Company, Inc., 1948, p. 723.

11. Hoag, J. Baron. ELECTRON AND NUCLEAR PHYSICS. New York: D. Van Nostrand Company, Inc., 1938, p. 37.

12. Wright, Ralph R. ELECTRONICS, PRINCIPLES AND APPLICATIONS. New York: The Ronald Press Company, 1950, p. 30.

13. Reverdin, D. L. "Optical Mapping of the Space Charge in the Magnetron," ELECTRONIC ENGINEERING, November, 1950, Vol. 22, p. 476.

14. Osgood, W. F. MECHANICS. New York: The Macmillan Company, 1949, p. 235.

15. Rose, A. "A Mechanical Model for the Motion of Electrons in a Magnetic Field," JOURNAL OF APPLIED PHYSICS, November, 1940, Vol. 11, pp. 711-717.

16. Whitaker, E. T. A TREATISE ON THE ANALYTICAL DYNAMICS OF PARTICLES AND RIGID BODIES. New York: Dover Publications, 1936, p. 9.

17. Whitaker, E. T. A TREATISE ON THE ANALYTICAL DYNAMICS OF PARTICLES AND RIGID BODIES. New York: Dover Publications, 1936, p. 16.

18. Whitaker, E. T. A TREATISE ON THE ANALYTICAL DYNAMICS OF PARTICLES AND RIGID BODIES. New York: Dover Publications, 1936, p. 37.

19. Sherwood, G. E. F. and Taylor, A. E. CALCULUS. New York: Prentice-Hall, Inc., 1946, p. 206.

20. Weber, Ernst. ELECTROMAGNETIC FIELDS, THEORY AND APPLICATIONS. New York: John Wiley & Sons, Inc., 1950, Vol. I, p. 7.

21. Southwell, R. V. RELAXATION METHODS IN THEORETICAL PHYSICS. Oxford: The Clarendon Press, 1946, pp. 38-60.

The vita has been removed from the scanned document